

Review of the Natural Circulation Effect in the Vermont Yankee Spent-Fuel Pool

Prepared by C. L. Wheeler

Pacific Northwest Laboratory
Operated by
Battelle Memorial Institute

Prepared for
U.S. Nuclear Regulatory
Commission

BB01250223 BB0131
PDR ADOCK 05000271
PDR
P

NOTICE

This report was prepared as an account of work sponsored by an agency of the United States Government. Neither the United States Government nor any agency thereof, or any of their employees, makes any warranty, expressed or implied, or assumes any legal liability or responsibility for any third party's use, or the results of such use, of any information, apparatus, product or process disclosed in this report, or represents that its use by such third party would not infringe privately owned rights.

NOTICE

Availability of Reference Materials Cited in NRC Publications

Most documents cited in NRC publications will be available from one of the following sources:

1. The NRC Public Document Room, 1717 H Street, N.W.
Washington, DC 20555
2. The Superintendent of Documents, U.S. Government Printing Office, Post Office Box 37082,
Washington, DC 20013-7082
3. The National Technical Information Service, Springfield, VA 22161

Although the listing that follows represents the majority of documents cited in NRC publications, it is not intended to be exhaustive.

Referenced documents available for inspection and copying for a fee from the NRC Public Document Room include NRC correspondence and internal NRC memoranda; NRC Office of Inspection and Enforcement bulletins, circulars, information notices, inspection and investigation notices; Licensee Event Reports, vendor reports and correspondence; Commission papers; and applicant and licensee documents and correspondence.

The following documents in the NUREG series are available for purchase from the GPO Sales Program: formal NRC staff and contractor reports, NRC-sponsored conference proceedings, and NRC booklets and brochures. Also available are Regulatory Guides, NRC regulations in the *Code of Federal Regulations*, and *Nuclear Regulatory Commission Issuances*.

Documents available from the National Technical Information Service include NUREG series reports and technical reports prepared by other federal agencies and reports prepared by the Atomic Energy Commission, forerunner agency to the Nuclear Regulatory Commission.

Documents available from public and special technical libraries include all open literature items, such as books, journal and periodical articles, and transactions. *Federal Register* notices, federal and state legislation, and congressional reports can usually be obtained from these libraries.

Documents such as theses, dissertations, foreign reports and translations, and non-NRC conference proceedings are available for purchase from the organization sponsoring the publication cited.

Single copies of NRC draft reports are available free, to the extent of supply, upon written request to the Division of Information Support Services, Distribution Section, U.S. Nuclear Regulatory Commission, Washington, DC 20555.

Copies of industry codes and standards used in a substantive manner in the NRC regulatory process are maintained at the NRC Library, 7920 Norfolk Avenue, Bethesda, Maryland, and are available there for reference use by the public. Codes and standards are usually copyrighted and may be purchased from the originating organization or, if they are American National Standards, from the American National Standards Institute, 1430 Broadway, New York, NY 10018.

Review of the Natural Circulation Effect in the Vermont Yankee Spent-Fuel Pool

Manuscript Completed: December 1987
Date Published: January 1988

Prepared by
C. L. Wheeler

Pacific Northwest Laboratory
Richland, WA 99352

Prepared for
Division of Engineering and Systems Technology
Office of Nuclear Reactor Regulation
U.S. Nuclear Regulatory Commission
Washington, DC 20555
NRC FIN I2003

ABSTRACT

A 7,429-node, three-dimensional computer model of the Vermont Yankee spent-fuel pool was set up and run using the porous media model of the TEMPEST computer code. The results of this analysis show that natural circulation is sufficient to ensure adequate cooling, regardless of the loading pattern used or the orientation of the cooling system discharge nozzle.

EXECUTIVE SUMMARY

To ensure adequate cooling of the spent fuel in the Vermont Yankee fuel pool with the proposed modification to the spent-fuel pool cooling system, the U.S. Nuclear Regulatory Commission (NRC) requested the Pacific Northwest Laboratory to independently verify that the removal of the dispersion header and the dumping of water above the fuel will have no adverse affect on ability to provide adequate spent-fuel cooling.

To accomplish this, a 7,429-node, three-dimensional computer model of the pool was set up and run using the porous media model of the TEMPEST computer code. This model is shown in Figure S.1. The results of 10 separate simulations are given in this report. The simulations used inlet temperatures of 100°, 130°, and 150°F; pool heat generation rates of 17 MBtu/h and 10.11 MBtu/h; and recirculation flow rates of 450, 1048, and 4187 gpm. The parameter configuration for each of the 10 runs is summarized in Table S.1.

Typical temperature and velocity distributions are given in Figure S.2. Figure S.2a is a view of the heat generating region, and Figure S.2b is an elevation view for one of the planes that passes through the rack leveling pads (as identified in Figure S.2a).

The results presented in this report show that approximately 50 to 80% of the peak fluid temperature rise results from bulk pool heatup, which can be estimated from a simple pool energy balance. The remaining 20 to 50% results from three interdependent factors: 1) the local heat generation rate, 2) the proximity of the heat bundle to the inlet nozzle, and 3) the proximity of the peak powered bundles to the rack leveling pads.

Extrapolation of the results shows that, for the worst case of pool inlet temperature of 150°F, pool heating rate of 10.11 MBtu/h, and peak local bundle heating rate of 49,000 Btu/h, natural circulation provides adequate cooling to prevent local boiling, independent of the loading pattern or the orientation of the spent-fuel pool cooling system discharge nozzle.

The results also show that the pool above the fuel is well mixed, except for the region of the discharge nozzle where large temperature gradients exist. A hypothetical calculation demonstrates that the 2-in. gaps between the spent-fuel racks and the pool wall are sufficient by themselves to supply adequate cooling to the open flow area below the fuel so that natural circulation will maintain an acceptable coolant temperature.

Locating the pool inlet in the region above the fuel rather than using a sparger below the fuel storage racks does not significantly degrade the pool cooling performance. However, locating the cooling system return line above the fuel bundles does change the location of the maximum temperature rise because it does not necessarily occur in the bundle with the highest heat generation rate. In addition, the incoming cold fluid tends to place a flow resistance cap over the bundles in the vicinity of the inlet, which competes

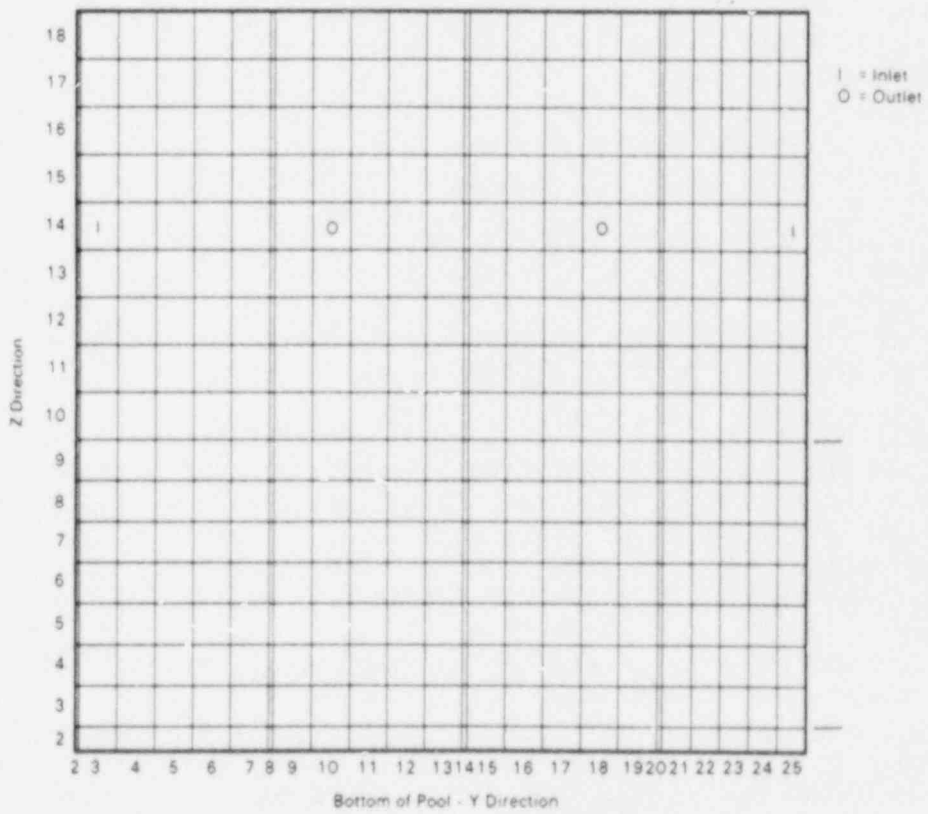
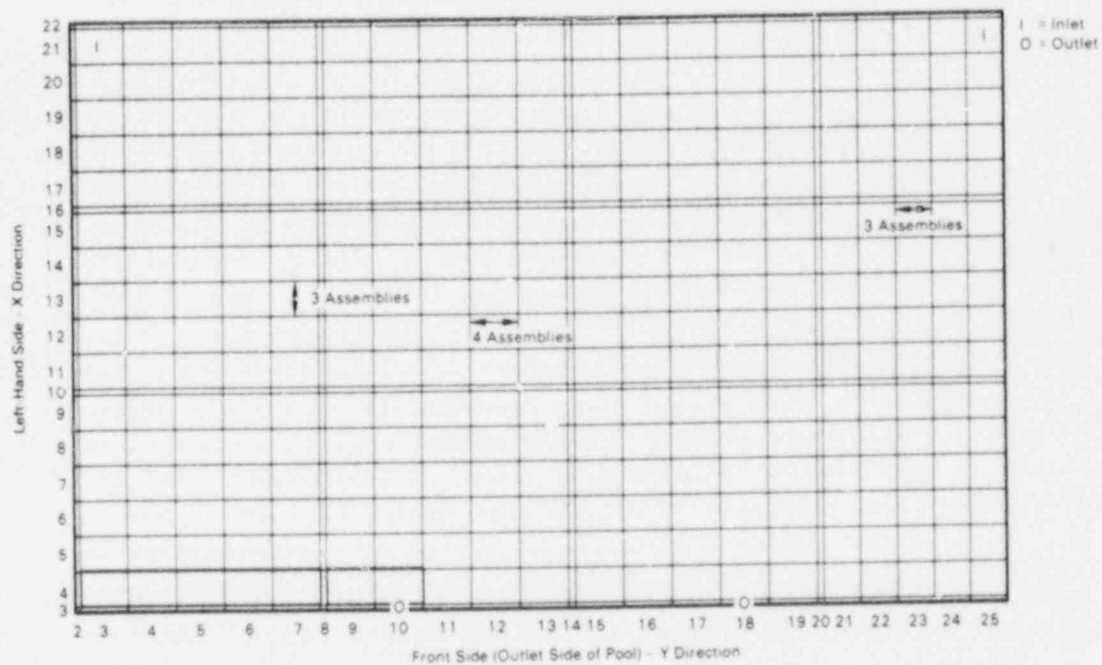
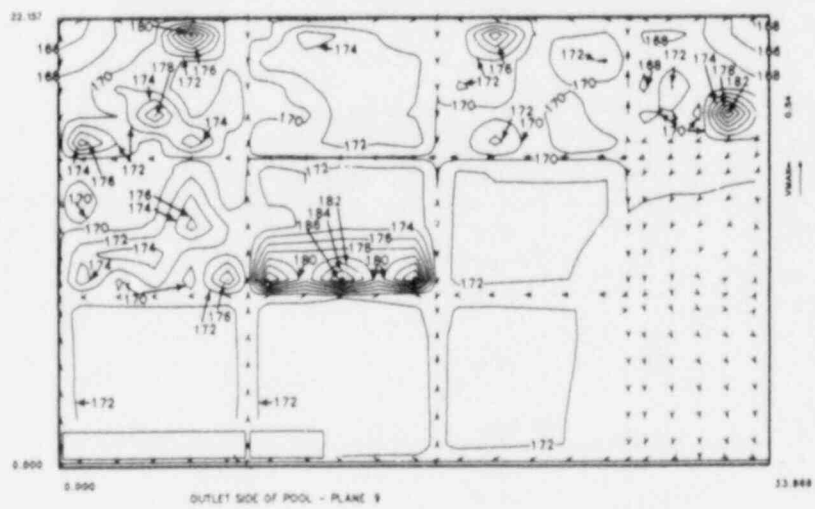
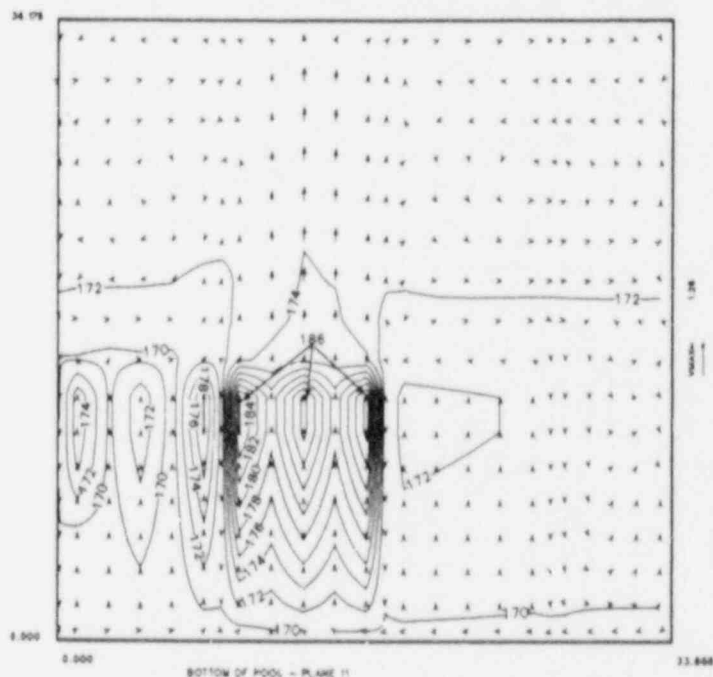


FIGURE S.1. TEMPEST Noding Model



a. XY Plane--Top of Fuel



b. YZ Plane Through Leveling Pads

FIGURE S.2. Typical Velocity and Temperature Distributions in the Pool for Case Number 17 ($Q = 450$ gpm, TINLET = 130°F , $P_t/P = 13.9$, inlet flow down, peak heat generation near center of pool)

TABLE S.1. Parameter Configuration for the Ten Reported Runs

Run Number	Total Heat Rate, MBtu/h	Pool Inlet Temperature, °F	Number of Bundles In Pool	Peak-Average Bundle Heat Ratio	Number and Location of Peak Bundles	Direction of Inlet Flow Rate	Pool Outlet Temperature, °F
5	4187	17.0	2878	1.4	368 Near Center	Down	159
9	1848	18.11	2878	1.4	368 Near Center	Down	169
10	1848	18.11	2878	1.4	368 Near Center	Down	149
11	1848	18.11	2878	1.4	368 Under Inlet	Down	169
12	1848	18.11	2878	13.9	132 Near Center	Down	169
14	1848	18.11	2878	13.9	132 Near Center	Horizontal	169
16	1848	18.11	2698	13.9	132 Near Edge	Down	169
17	458	18.11	2878	13.9	132 Near Center	Down	175
18	458	18.11	2878	13.9	132 Near Center	Down	145
19	458	18.11	2878	13.9	Near Center (cask area removed from calculation)	Down	175

with the buoyancy effects of the heated bundles below. This results in stable temperature oscillations of 8°F in some of the bundles near the return line discharge.

CONTENTS

ABSTRACT	iii
EXECUTIVE SUMMARY	v
INTRODUCTION	1
APPROACH	3
TEMPEST CODE	3
Limitations	3
Governing Equations	3
Solution Procedure	7
MODEL DESCRIPTION	9
RESULTS	15
CONCLUSIONS	93
REFERENCE	95
APPENDIX A - INPUT FOR CASES 5, 9, 10, 11, 12, 14, 16, 17, 18, 19 . . .	A.1

FIGURES

S.1	TEMPEST Noding Model	vi
S.2	Typical Velocity and Temperature Distributions in the Pool for Case Number 17	vii
1	Cross Section of Vermont Yankee Spent-Fuel Pool Showing Proposed Storage Rack Layout	20
2	Vertical Cross Section of Vermont Yankee Spent-Fuel Pool	21
3	TEMPEST Noding Model in X-Y Plane	22
4	TEMPEST Noding Model in X-Y Plane	23
5	Normalized Local Heat Generation Rate Distributions	24
6	Temperature Distribution at the Top of the Fuel Bundles for Case Number 5. (Q = 4187 GPM, TINLET = 150°F, PL/P = 1.4, inlet flow down, peak heat generation near center of pool)	25
7	Temperature Distribution at the Top of the Fuel Bundles for Case Number 9. (Q = 1048 GPM, TINLET = 150°F, PL/P = 1.4, inlet flow down, peak heat generation near center of pool)	26
8	Temperature Distribution at the Top of the Fuel Bundles for Case Number 10. (Q = 1048 GPM, TINLET = 130°F, PL/P = 1.4, inlet flow down, peak heat generation near center of pool)	27
9	Temperature Distribution at the Top of the Fuel Bundles for GPM, TINLET = 150°F, PL/P = 1.4, inlet flow down, peak heat generation under inlet)	28
10	Temperature Distribution at the Top of the Fuel Bundles for GPM, TINLET = 150°F, PL/P = 13.9, inlet flow down, peak heat generation near center of pool)	29
11	Temperature Distribution at the Top of the Fuel Bundles for Case Number 14. (Q = 1048 GPM, TINLET = 150°F, PL/P = 13.9, inlet flow horizontal, peak heat generation near center of pool)	30
12	Temperature Distribution at the Top of the Fuel Bundles for Case Number 16	31

13	Temperature Distribution at the Top of the Fuel Bundles for Case Number 17. (Q = 450 GPM, TINLET = 130°F, PL/P = 13.9, inlet flow down, peak heat generation near center of pool)	32
14	Temperature Distribution at the Top of the Fuel Bundles for Case Number 18. (Q = 450 GPM, TINLET = 100°F, PL/P = 13.9, inlet flow down, peak heat generation near center of pool)	33
15	Temperature Distribution at the Top of the Fuel Bundles for Case Number 19. (Q = 450 GPM, TINLET = 130°F, PL/P = 13.9, inlet flow down, peak heat generation near center of pool, large open flow region of cask area removed from model)	34
16	Temperature and Flow Distribution along the Back Wall of the Pool for Case Number 5. (Q = 4187 GPM, TINLET = 150°F, PL/P = 1.4, inlet flow down, peak heat generation near center of pool)	35
17	Temperature and Flow Distribution along the Back Wall of the Pool for Case Number 9. (Q = 1048 GPM, TINLET = 150°F, PL/P = 1.4, inlet flow down, peak heat generation near center of pool)	36
18	Temperature and Flow Distribution along the Back Wall of the Pool for Case Number 11. (Q = 1048 GPM, TINLET = 150°F, PL/P = 1.4, inlet flow down, peak heat generation under inlet)	37
19	Temperature and Flow Distribution along the Back Wall of the Pool for Case Number 12. (Q = 1048 GPM, TINLET = 150°F, PL/P = 13.9, inlet flow down, peak heat generation near center of pool)	38
20	Temperature and Flow Distribution along the Back Wall of the Pool for Case Number 14. (Q = 1048 GPM, TINLET = 150°F, PL/P = 13.9, inlet flow horizontal, peak heat generation near center of pool) .	39
21	Temperature and Flow Distribution along the Back Wall of the Pool for Case Number 16. (Q = 1048 GPM, TINLET = 150°F, PL/P = 13.9, inlet flow down, peak heat generation near edge of pool)	40
22	Temperature and Flow Distribution along the Back Wall of the Pool for Case Number 17. (Q = 450 GPM, TINLET = 130°F, PL/P = 13.9, inlet flow down, peak heat generation near center of pool)	41
23	Temperature and Flow Distribution along the Back Wall of the Pool for Case Number 18. (Q = 450 GPM, TINLET = 100°F, PL/P = 13.9, inlet flow down, peak heat generation near center of pool)	42
24	Temperature and Flow Distribution along the Back Wall of the Pool for Case Number 19. (Q = 450 GPM, TINLET = 130°F, PL/P = 13.9, inlet flow down, peak heat generation near center of pool, large open flow region of cask area removed from model)	43

25	Temperature and Flow Distribution in Bundles next to the Back Wall of the Pool for Case Number 5. (Q = 4187 GPM, TINLET = 150°F, PL/P = 1.4, inlet flow down, peak heat generation near center of pool)	44
26	Temperature and Flow Distribution in Bundles next to the Back Wall of the Pool for Case Number 9. (Q = 1048 GPM, TINLET = 150°F, PL/P = 1.4, inlet flow down, peak heat generation near center of pool)	45
27	Temperature and Flow Distribution in Bundles next to the Back Wall of the Pool for Case Number 11. (Q = 1048 GPM, TINLET = 150°F, PL/P = 1.4, inlet flow down, peak heat generation under inlet) . . .	46
28	Temperature and Flow Distribution in Bundles next to the Back Wall of the Pool for Case Number 12. (Q = 1048 GPM, TINLET = 150°F, PL/P = 13.9, inlet flow down, peak heat generation near center of pool)	47
29	Temperature and Flow Distribution in Bundles next to the Back Wall of the Pool for Case Number 14. (Q = 1048 GPM, TINLET = 150°F, PL/P = 13.9, inlet flow horizontal, peak heat generation near center of pool)	48
30	Temperature and Flow Distribution in Bundles next to the Back Wall of the Pool for Case Number 16. (Q = 1048 GPM, TINLET = 150°F, PL/P = 13.9, inlet flow down, peak heat generation near edge of pool)	49
31	Temperature and Flow Distribution in Bundles next to the Back Wall of the Pool for Case Number 17. (Q = 450 GPM, TINLET = 130°F, PL/P = 13.9, inlet flow down, peak heat generation near center of pool)	50
32	Temperature and Flow Distribution in Bundles next to the Back Wall of the Pool for Case Number 18. (Q = 450 GPM, TINLET = 100°F, PL/P = 13.9, inlet flow down, peak heat generation near center of pool)	51
33	Temperature and Flow Distribution in Bundles next to the Back Wall of the Pool for Case Number 19. (Q = 450 GPM, TINLET = 130°F, PL/P = 13.9, inlet flow down, peak heat generation near center of pool, large open flow region of cask area removed from model) . . .	52
34	Temperature and Flow Distribution below the Fuel Bundles for Case Number 5. (Q = 4187 GPM, TINLET = 150°F, PL/P = 1.4, inlet flow down, peak heat generation near center of pool)	53

35	Temperature and Flow Distribution below the Fuel Bundles for Case Number 9. (Q = 1048 GPM, TINLET = 150°F, PL/P = 1.4, inlet flow down, peak heat generation near center of pool)	54
36	Temperature and Flow Distribution below the Fuel Bundles for Case Number 10. (Q = 1048 GPM, TINLET = 130°F, PL/P = 1.4, inlet flow down, peak heat generation near center of pool)	55
37	Temperature and Flow Distribution below the Fuel Bundles for Case Number 11. (Q = 1048 GPM, TINLET = 150°F, PL/P = 1.4, inlet flow down, peak heat generation under inlet)	56
38	Temperature and Flow Distribution below the Fuel Bundles for Case Number 12. (Q = 1048 GPM, TINLET = 150°F, PL/P = 13.9, inlet flow down, peak heat generation near center of pool)	57
39	Temperature and Flow Distribution below the Fuel Bundles for Case Number 14. (Q = 1048 GPM, TINLET = 150°F, PL/P = 13.9, inlet flow horizontal, peak heat generation near center of pool)	58
40	Temperature and Flow Distribution below the Fuel Bundles for Case Number 16. (Q = 1048 GPM, TINLET = 150°F, PL/P = 13.9, inlet flow down, peak heat generation near edge of pool)	59
41	Temperature and Flow Distribution below the Fuel Bundles for Case Number 17. (Q = 450 GPM, TINLET = 130°F, PL/P = 13.9, inlet flow down, peak heat generation near center of pool)	60
42	Temperature and Flow Distribution below the Fuel Bundles for Case Number 18. (Q = 450 GPM, TINLET = 100°F, PL/P = 13.9, inlet flow down, peak heat generation near center of pool)	61
43	Temperature and Flow Distribution below the Fuel Bundles for Case Number 19. (Q = 450 GPM, TINLET = 130°F, PL/P = 13.9, inlet flow down, peak heat generation near center of pool, large open flow region of cask area removed from model)	62
44	Temperature and Flow Distribution above the Fuel Bundles for Case Number 5. (Q = 4187 GPM, TINLET = 150°F, PL/P = 1.4, inlet flow down, peak heat generation near center of pool)	63
45	Temperature and Flow Distribution above the Fuel Bundles for Case Number 9. (Q = 1048 GPM, TINLET = 150°F, PL/P = 1.4, inlet flow down, peak heat generation near center of pool)	64
46	Temperature and Flow Distribution above the Fuel Bundles for Case Number 10. (Q = 1048 GPM, TINLET = 130°F, PL/P = 1.4, inlet flow down, peak heat generation near center of pool)	65

47	Temperature and Flow Distribution above the Fuel Bundles for Case Number 11. (Q = 1048 GPM, TINLET = 150°F, PL/P = 1.4, inlet flow down, peak heat generation under inlet)	66
48	Temperature and Flow Distribution above the Fuel Bundles for Case Number 12. (Q = 1048 GPM, TINLET = 150°F, PL/P = 13.9, inlet flow down, peak heat generation near center of pool)	67
49	Temperature and Flow Distribution above the Fuel Bundles for Case Number 14. (Q = 1048 GPM, TINLET = 150°F, PL/P = 13.9, inlet flow horizontal, peak heat generation near center of pool)	68
50	Temperature and Flow Distribution above the Fuel Bundles for Case Number 16. (Q = 1048 GPM, TINLET = 150°F, PL/P = 13.9, inlet flow down, peak heat generation near edge of pool)	69
51	Temperature and Flow Distribution above the Fuel Bundles for Case Number 17. (Q = 450 GPM, TINLET = 130°F, PL/P = 13.9, inlet flow down, peak heat generation near center of pool)	70
52	Temperature and Flow Distribution above the Fuel Bundles for Case Number 18. (Q = 450 GPM, TINLET = 100°F, PL/P = 13.9, inlet flow down, peak heat generation near center of pool)	71
53	Temperature and Flow Distribution above the Fuel Bundles for Case Number 19. (Q = 450 GPM, TINLET = 130°F, PL/P = 13.9, inlet flow down, peak heat generation near center of pool, large open flow region of cask area removed from model)	72
54	Temperature and Flow Distribution along the Front Wall of the Pool for Case Number 5. (Q = 4187 GPM, TINLET = 150°F, PL/P = 1.4, inlet flow down, peak heat generation near center of pool)	73
55	Temperature and Flow Distribution along the Front Wall of the Pool for Case Number 11. (Q = 1048 GPM, TINLET = 150°F, PL/P = 1.4, inlet flow down, peak heat generation under inlet)	74
56	Temperature and Flow Distribution along the Front Wall of the Pool for Case Number 9. (Q = 1048 GPM, TINLET = 150°F, PL/P = 1.4, inlet flow down, peak heat generation near center of pool)	75
57	Temperature and Flow Distribution along the Front Wall of the Pool for Case Number 10. (Q = 1048 GPM, TINLET = 130°F, PL/P = 1.4, inlet flow down, peak heat generation near center of pool)	76

58	Temperature and Flow Distribution along the Front Wall of the Pool for Case Number 12. (Q = 1048 GPM, TINLET = 150°F, PL/P = 13.9, inlet flow down, peak heat generation near center of pool)	77
59	Temperature and Flow Distribution along the Front Wall of the Pool for Case Number 14. (Q = 1048 GPM, TINLET = 150°F, PL/P = 13.9, inlet flow horizontal, peak heat generation near center of pool)	78
60	Temperature and Flow Distribution along the Front Wall of the Pool for Case Number 16. (Q = 1048 GPM, TINLET = 150°F, PL/P = 13.9, inlet flow down, peak heat generation near edge of pool)	79
61	Temperature and Flow Distribution along the Front Wall of the Pool for Case Number 17. (Q = 450 GPM, TINLET = 130°F, PL/P = 13.9, inlet flow down, peak heat generation near center of pool)	80
62	Temperature and Flow Distribution along the Front Wall of the Pool for Case Number 18. (Q = 450 GPM, TINLET = 100°F, PL/P = 13.9, inlet flow down, peak heat generation near center of pool)	81
63	Temperature and Flow Distribution along the Front Wall of the Pool for Case Number 19. (Q = 450 GPM, TINLET = 130°F, PL/P = 13.9, inlet flow down, peak heat generation near center of pool, large open flow region of cask area removed from model) . . .	82
64	Temperature and Velocity Distribution in a Plane above the Leveling Pads for Case Number 5	83
65	Temperature and Velocity Distribution in a Plane above the Leveling Pads for Case Number 9. (Q = 1048 GPM, TINLET = 150°F, PL/P = 1.4, inlet flow down, peak heat generation near center of pool)	84
66	Temperature and Velocity Distribution in a Plane above the Leveling Pads for Case Number 10. (Q = 1048 GPM, TINLET = 130°F, PL/P = 1.4, inlet flow down, peak heat generation near center of pool)	85
67	Temperature and Velocity Distribution in a Plane above the Leveling Pads for Case Number 11. (Q = 1048 GPM, TINLET = 150°F, PL/P = 1.4, inlet flow down, peak heat generation under inlet)	86

68	Temperature and Velocity Distribution in a Plane above the Leveling Pads for Case Number 12. (Q = 1048 GPM, TINLET = 150°F, PL/P = 13.9, inlet flow down, peak heat generation near center of pool)	87
69	Temperature and Velocity Distribution in a Plane above the Leveling Pads for Case Number 14. (Q = 1048 GPM, TINLET = 150°F, PL/P = 13.9, inlet flow horizontal, peak heat generation near center of pool)	88
70	Temperature and Velocity Distribution in a Plane above the Leveling Pads for Case Number 16. (Q = 1048 GPM, TINLET = 150°F, PL/P = 13.9, inlet flow down, peak heat generation near edge of pool)	89
71	Temperature and Velocity Distribution in a Plane above the Leveling Pads for Case Number 17. (Q = 450 GPM, TINLET = 130°F, PL/P = 13.9, inlet flow down, peak heat generation near center of pool)	90
72	Temperature and Velocity Distribution in a Plane above the Leveling Pads for Case Number 18. (Q = 450 GPM, TINLET = 100°F, PL/P = 13.9, inlet flow down, peak heat generation near center of pool)	91
73	Temperature and Velocity Distribution in a Plane above the Leveling Pads for Case Number 19. (Q = 450 GPM, TINLET = 130°F, PL/P = 13.9, inlet flow down, peak heat generation near center of pool, large open flow region of cask area removed from model)	92

TABLES

S.1	Parameter Configuration for the Ten Reported Runs	viii
1	TEMPEST Code Capabilities	4
2	Local Pressure Loss Coefficient	11
3	Parameter Configuration for the 10 Reported Runs	13
4	Summary of Maximum Temperature Rise	16

ACKNOWLEDGMENTS

This project was funded by the U.S. Nuclear Regulatory Commission under NRC FIN I2003. Mr. John Ridgely was the NRC Project Manager. Appreciation is extended to N. C. Waugh, word processor, for assistance in preparing this document.

REVIEW OF THE NATURAL CIRCULATION EFFECT IN THE
VERMONT YANKEE SPENT-FUEL POOL

INTRODUCTION

Spent-fuel storage is becoming a major concern for many U.S. utilities. The onsite storage facilities were designed to store spent fuel from only two to four refueling operations because it was assumed that fuel would be stored for a short time before being shipped to a reprocessing facility. After the federal government removed the reprocessing option, the utilities were obliged to find or develop alternative methods of onsite storage of spent fuel. One method being considered is that of storing more fuel bundles in the spent-fuel pool by replacing existing low-density spent-fuel storage racks with new high-density storage racks.

Generally, the fuel within the spent-fuel pool is cooled by one or more fuel-pool cooling systems. The system removes the heated water from the top of the pool via scupper tanks, cools the water via heat exchangers, and returns the cooled water to the pool through dispersion headers on the pool floor. Because the cooled water is supplied at the bottom of the pool, adequate cooling is ensured. The integrity of the system has been demonstrated to be independent of the relative placement of hot or cool fuel bundles.

In 1977, the Vermont Yankee operating license was modified to allow installation of new racks that could accommodate 1,680 fuel bundles within the spent-fuel pool. However, it has become apparent that as delays mount and the proposed date for a federal waste repository slips further into the future, it is necessary to further increase onsite storage capacity. Unless the onsite capacity is increased, the Vermont Yankee reactor will lose its full core offload capability in 1990. One proposal for increasing the storage capacity is to further modify the fuel pool design to include 2870 storage spaces. To achieve this storage capability, it is necessary to modify the pool-cooling flow distribution system by removing the dispersion header from the bottom of the pool so that the cooling water is discharged directly into the pool above the stored fuel.

To ensure adequate cooling for the spent fuel with the proposed modification to the spent-fuel pool cooling system, the U. S. Nuclear Regulatory Commission (NRC) requested the Pacific Northwest Laboratory (PNL)(a) to independently verify that the removal of the dispersion header and the dumping of water above the fuel will have no adverse effect on ability to provide

(a) Operated for the U.S. Department of Energy by Battelle Memorial Institute under Contract DE-AC06-76RLO 1830.

adequate spent-fuel cooling by demonstrating that natural circulation is sufficient to remove the decay heat and prevent local boiling in the high density racks. A secondary objective is to verify that the fuel loading pattern in the spent-fuel pool and the orientation of the spent-fuel pool cooling-system discharge nozzle will not adversely affect the ability to provide adequate pool cooling. This report documents this independent analysis.

APPROACH

Because a realistic evaluation of the potential for natural circulation to adequately cool spent fuel in the spent-fuel pool, a full three-dimensional model of the pool was required. The TEMPEST computer code satisfies this requirement. Therefore, a pool model was developed for analysis using TEMPEST.

TEMPEST CODE

The TEMPEST code offers simulation capabilities over a wide range of hydrothermal problems that are definable by input instructions. Code capabilities, limitations, and conservation laws are described in this section. Capabilities of the base version of TEMPEST (Trent, Eyler, and Budden 1983) are summarized in Table 1.

Limitations

The TEMPEST porosity and turbulence models are not compatible, so they cannot be used at the same time.

Governing Equations

The equations governing momentum, heat, and mass transport solved by TEMPEST are based on three conservation laws:

- conservation of mass (continuity)
- conservation of momentum (Newton's Second Law)
- conservation of energy (First Law of Thermodynamics).

These laws are simulated subject to six assumptions and/or restrictions:

- The fluid is single phase and incompressible (insofar as sonic effects are not considered).
- The body forces other than gravity are not considered. Forces resulting from an accelerating reference frame are included.
- The fluid is Newtonian (for laminar situations, Navier-Stokes equations apply).
- The turbulent flow conservation equations are time-averaged, and Reynolds stresses are incorporated through appropriate eddy-viscosity models.
- The viscous dissipation is eliminated.
- The Boussinesq approximation holds.

TABLE 1. TEMPEST Code Capabilities

Modeling Capabilities

- full three-dimensional
- time-dependent with transient approach to steady state
- turbulence models ($k-\epsilon$ model) (mutually excludes porosity model)
- cartesian or cylindrical coordinates
- heat diffusion in solid regions
- full implicit solution to all scalar equations
- direct solution for thermal steady state
- multiple flow regions (may be connected through conduction heat transfer)
- arbitrary orientation of solution coordinate system (WRT gravity)
- variable grid spacing along all/any coordinate direction
- use of specified or precomputed flow regions
- internal heat generation (20 time-dependent tables possible)
- fifty different material types
- inflow/outflow boundaries specified or computed
- time-dependent flow and thermal boundary condition tables (20 tables possible)
- variable materials properties (thermal conductivity, density, specific heat, and viscosity)
- single-cell width or zero width wall logic
- drag coefficient correlations for each direction of each cell (98 different coefficient types available from input specification)
- film coefficient for each direction of each cell
- partial material-properties table built in
- wind shear
- planetary Coriolis effects
- porosity model (mutually excludes turbulence model).

Program Control

- hydrodynamics only
- solids heat transfer only
- decoupled hydrodynamics (no buoyancy effects)
- fully coupled hydrodynamics and heat transfer
- hydrodynamic solution explicit in time--no direct solution for steady state
- pressure boundary conditions not available
- curved boundaries (except circular) required to be stair-stepped.

Input/Output Control

- velocity and temperature array output
- postprocessing and restart file dumping
- graphics plotting of velocity and temperature distributions.

For low-speed flows that involve density variations (i.e., $|\Delta\rho/\rho_0| \ll 1$), the well-known Boussinesq approximation is valid. This approximation is commonly used in natural-convection simulations involving either liquids or gases. Although the approximation is consistent with the accuracy of other approximations required for numerical simulation, its validity is questionable if density changes considered are large compared to local fluid density. Most simulations involving liquid systems are within the valid range of this approximation.

The conservation equation solved in TEMPEST version NPOR mod 0 for this application is:

Continuity

The equation describing the conservation of mass is

$$\frac{\partial \alpha U}{\partial Y} + \frac{\partial \gamma W}{\partial X} + \frac{\partial \delta V}{\partial Z} = 0$$

Symbols U, W, and V refer to velocity components and α , γ , and δ refer to surface porosities in the X, Y, and Z directions, respectively.

Momentum

The equations describing the conservation of momentum in each of the three coordinate directions are:

- Y-direction component, U

$$\begin{aligned} & \xi \frac{\partial U}{\partial t} + \frac{\partial}{\partial Y} \left(\alpha U U \right) + \frac{\partial}{\partial X} (\gamma W U) + \frac{\partial}{\partial Z} (\delta V U) \\ &= \frac{1}{\rho_0} \left[- \frac{\partial P}{\partial Y} + \xi \rho g_Y + \frac{\partial}{\partial r} \left(\alpha \epsilon \frac{\partial U}{\partial Y} \right) + \frac{\partial}{\partial X} \left(\gamma \epsilon \frac{\partial U}{\partial X} \right) + \frac{\partial}{\partial Z} \left(\delta \epsilon \frac{\partial U}{\partial Z} \right) + S_Y \right] \end{aligned}$$

$$\text{where } S_Y = \frac{\partial \epsilon \alpha}{\partial Y} \frac{\partial U}{\partial Y} + \frac{\partial \epsilon \gamma}{\partial X} \frac{\partial W}{\partial Y} + \frac{\partial \epsilon \delta}{\partial Z} \frac{\partial V}{\partial Y} - F_Y(u)$$

ξ = volume porosity

ϵ = $\mu + \mu_T$

μ = dynamic viscosity

μ_T = turbulent (eddy) viscosity

$F_Y(U)$ = Y-direction flow drag

- X-direction component, W:

$$\xi \frac{\partial W}{\partial t} + \frac{\partial}{\partial Y} (\alpha UW) + \frac{\partial}{\partial X} (\gamma WW) + \frac{\partial}{\partial Z} (\delta VW)$$

$$= \frac{1}{\rho_0} \left[- \frac{\partial P}{\partial X} + \xi \rho g_X + \frac{\partial}{\partial Y} \left(\alpha \epsilon \frac{\partial W}{\partial Y} \right) + \frac{\partial}{\partial X} \left(\gamma \epsilon \frac{\partial W}{\partial X} \right) \right. \\ \left. + \frac{\partial}{\partial Z} \left(\delta \epsilon \frac{\partial W}{\partial Z} \right) + S_X \right]$$

where $S_X = \frac{\partial \epsilon}{\partial Y} \frac{\partial U}{\partial X} + \frac{\partial \epsilon \gamma}{\partial X} \frac{\partial W}{\partial X} + \frac{\partial \epsilon \delta}{\partial Z} \frac{\partial V}{\partial X} - F_X(W).$

- Z-direction component, V:

$$\xi \frac{\partial V}{\partial t} + \frac{\partial}{\partial Y} (\alpha UV) + (\gamma WV) + \frac{\partial}{\partial Z} (\delta VV)$$

$$= \frac{1}{\rho_0} \left[- \frac{\partial P}{\partial Z} + \xi \rho g_Z + \frac{\partial}{\partial Y} \left(\alpha \epsilon \frac{\partial V}{\partial Y} \right) + \frac{\partial}{\partial X} \left(\gamma \epsilon \frac{\partial V}{\partial X} \right) + \frac{\partial}{\partial Z} \left(\delta \epsilon \frac{\partial V}{\partial Z} \right) + S_Z \right]$$

where $S_Z = \frac{\partial \epsilon \alpha}{\partial Y} \frac{\partial U}{\partial Z} + \frac{\partial \epsilon \gamma}{\partial X} \frac{\partial W}{\partial Z} + \frac{\partial \epsilon \delta}{\partial Z} \frac{\partial V}{\partial Z} - F_Z(V).$

Thermal Energy

The equation describing the conservation of thermal energy is

$$\rho_0 c \xi \left[\frac{\partial T}{\partial t} + \frac{\partial}{\partial Y} (\alpha UT) + \frac{\partial}{\partial X} (\gamma TW) + \frac{\partial}{\partial Z} (\delta VT) \right]$$

$$= \frac{\partial}{\partial Y} \left(\alpha \sigma \frac{\partial T}{\partial Y} \right) + \frac{\partial}{\partial X} \left(\gamma \sigma \frac{\partial T}{\partial X} \right) + \frac{\partial}{\partial Z} \left(\delta \sigma \frac{\partial T}{\partial Z} \right) + Q$$

where $\sigma = \kappa + \kappa_T$
 κ = thermal conductivity
 κ_T = turbulent (eddy) thermal conductivity
 c = specific heat
 Q = volumetric heat generation rate.

Solution Procedure

The TEMPEST solution procedure is a semi-implicit, time-marching, finite-difference procedure that sequentially solves all governing equations. At each time step, the momentum equations are solved explicitly and the pressure equations implicitly. Temperature, turbulent kinetic energy dissipation, and other scalar transport equations are solved using an implicit continuation procedure. Thus, the solution proceeds in three phases:

- Phase I, tilde phase - The three momentum equations are advanced in time ($t + \Delta t$) to obtain approximate (tilde) velocities, \tilde{U} , \tilde{V} , and \tilde{W} , based on the previous time values of pressure and density, P and ρ . Although these values of the velocity components satisfy the momentum equations based on current values of P and ρ , continuity will usually not be satisfied.
- Phase II, implicit phase - The velocity component and pressure corrections (U' , V' , W' , and P') are obtained such that the equations $U^{n+1} = \tilde{U} + U'$, $V^{n+1} = \tilde{V} + V'$, $W^{n+1} = \tilde{W} + W'$, and $P^{n+1} = \tilde{P} + P'$ satisfy continuity.
- Phase III, scalar phase - Using the previously computed values of U^{n+1} , V^{n+1} , and W^{n+1} , the advanced time ($t + \Delta t$) values of temperature T^{n+1} and other scalar quantities are computed as required.

The solution is advanced step by step in time by continued application of the above three solution phases. New time-mixture properties are computed at the end of Phase III. The solution procedure is explained in more detail in the TEMPEST Users' Manual (Trent, Eyler, and Budden 1983).

MODEL DESCRIPTION

The proposed arrangement for the Vermont Yankee spent-fuel pool is shown in Figures 1 and 2. The spent fuel is to be stored in 10 racks that can contain from 180 to 360 fuel bundles, depending on rack location in the pool. Each rack is separated from adjacent racks or the wall by an approximate 2-in. gap. Within the racks, the fuel bundles are tightly packed; there is very little room for bypass flow outside the bundle flow area. However, a cask area on the right side of the pool contains a relatively large volume of water that is unobstructed with respect to flow between the upper and lower regions of the pool (Figure 1).

As shown in Figure 2, coolant enters the pool on the back side and exits the pool on the front side. The water enters the pool approximately 9 ft below the top water surface and exits approximately 5 ft below the surface. The racks are supported by rack-leveling pads (four to six per rack), which produce a relatively large open flow area (approximately 14 in. high) below the fuel bundles. However, the leveling pads act as flow obstructors to the fuel bundle located directly above them. The fuel-handling machines are located along the left front side of the pool.

As shown in Figures 3 and 4, the features specifically modeled in the TEMPEST nodalization are:

- the 2-in. gaps between racks and between the racks and the wall - These are represented by nodes 3, 10, 16, and 22 on the left-hand side, and by nodes 2, 8, 14, and 20 along the front side of the pool on Figure 3. These are open channels, and flow is allowed to flow through them in all three directions.
- the fuel machine area - This area is modeled by a solid nonparticipating material, represented by node 3 along the left-hand side and nodes 3 through 7 and nodes 9 through 10 along the front face.
- the cask area - This open flow area is represented by nodes 3 through 17 along the left-hand side and nodes 20 through 25 along the front side.
- the region below the racks, represented by node 2 on Figure 4
- the pool above the fuel, represented by nodes 10 through 18 on Figure 4.

Each TEMPEST node in the X-Y plane represents 12 bundles (three in the X direction and four in the Y direction), except for the nodes behind the cask area, which represent nine bundles (three in the Y direction and three in the X direction). The axial node length is 2 ft in the fuel region, 2.33 ft in the upper pool region, and 1.2 ft in the node between the floor and the fuel.

One row of boundary nodes surrounds the pool on all six sides. In this study, the boundary nodes are considered to be adiabatic. This assumption is conservative, as convection and evaporation from the pool surface will remove a significant amount of energy from the pool. An additional but substantially smaller amount will be removed by conduction through the pool floor and walls. To enable plotting these outflow vectors, an additional nonparticipating boundary node was added to the front side of the pool.

The pool inlet and outlet are designated by I and O, respectively, in Figures 3 and 4. [Note that the inlet to the pool (I) is the discharge from the spent-fuel cooling system (i.e., the discharge nozzle), and that the outlet from the pool (O) is the inlet to the spent-fuel pool cooling system.] The inlet flow rate is modeled by mass (divergence), momentum, and energy source terms. However, because of node size restrictions the model momentum is diffused. The relatively large TEMPEST node size necessitates specifying a smaller velocity in the simulation than would be exiting from the 8-in inlet pipe.

The fuel bundles are modeled using volume and surface porosities. The volume and surface porosity in the axial directions are set to 0.695. Flow is constrained in the axial direction only, by setting the porosity in the transverse direction (X and Y faces) to zero. The fuel bundles are represented by axial nodes 3 through 9. The structure in the region below the racks (axial node 2) is modeled using a volume porosity of 0.54, X and Y surface porosities of 0.54, and Z direction surface porosities of 0.695. These are applied uniformly to all nodes below the fuel racks. The 13.5-in. region containing no fuel at the back of the fuel pool is modeled by assigning a volume porosity of 0.602 to the nodes adjacent to the 13.5-in. region.

Friction pressure losses (within the fuel bundles and in the 2-in. gap region between the racks) are modeled using local loss coefficients defined by the pressure equation

$$\Delta P = K \left(\frac{\rho}{2g} \right) V^c$$

where ΔP = pressure loss

V = local velocity in fuel bundle region

ρ = coolant density

g = gravitational constant

K = local pressure loss coefficient (input)

c = exponent on velocity (input).

The input values for K and c are given in Table 2. Local expansion and contractions losses where the coolant enters and leaves the fuel bundles are also modeled using the local loss coefficients given in Table 2. These coefficients, supplied by the utility, appeared to be very conservative. Special loss coefficients representing the effect of the rack-leveling pads are also

TABLE 2. Local Pressure Loss Coefficient

<u>Location</u>	<u>K</u>	<u>C</u>	<u>Direction</u>	<u>Where Applied</u>
Fuel bundle	0.13	1	Z	Nodes 3 through 8 in fuel bundle nodes
Peripheral gaps	0.003	1	Z	All 2-in. gaps around edge
Peripheral gaps	0.003	1	Y or X	All 2-in. gaps around edge
Center gaps	0.002	1	Z	All interior gaps between racks
Center gaps	0.002	1	Y or X	All interior gaps between racks
Region below pool	1.04	2	Y	All nodes below fuel racks
Region below pool	0.78	2	X	All nodes below fuel racks
Fuel bundle inlet	23.77	2	Z	All fuel bundles at axial node 3
All 2-in. gaps between racks	1.6	2	Z	At level 2, simulates expansion and contraction losses between the bundles and the upper and lower plenums
Below 6 specific fuel nodes in center rack	283.0	2	Z	Axial node 2, simulates leveling pad losses

defined; however, they are not applied in the model at all locations where they occurred in the actual pool but only to one fuel rack near the pool center. The leveling pads are modeled in this manner so that the effect of the pad could be evaluated without additional computer runs.

The calculations presented in this report were made using one of the four different heat generation distributions shown in Figure 5. In the first configuration (Figure 5a), 368 bundles are operating at a local to average power ratio of 1.4. For the most part these bundles are located near the center of the pool. All other bundles have a local heat generation ratio of 0.939. In the second configuration, most of the higher power bundles ($P/P = 1.4$) are in the rack under the back left inlet as shown in Figure 5b. The third configuration (Figure 5c) represents a pool full of newly loaded spent fuel immediately after loading. In this case, 132 bundles have a local to average heat generation ratio of 13.9, 263 bundles have heat generation ratios of 0.52, and the remaining bundles have a heat generation ratio of 0.49. All the fuel bundles with the high heating rate are located near the center of the pool. The fourth configuration represents the same case as the third; however, the freshly discharged fuel is isolated in one corner in the front and surrounded by 84 empty bundle locations, which separate it from the older spent fuel.

A total of 19 simulations were performed. Of these 19, 10 simulations are represented as complete evaluations in this report. The simulations used inlet temperatures of 100°, 130°, and 150°F, pool heat generation rates of 17 MBtu/h and 10.11 MBtu/h, and recirculation flow rates of 450, 1048, and 4187 gpm. The pool geometry was changed for the final run to remove the cask area from the calculation. This was done to determine hypothetically if the 2-in. spacing around each rack is sufficient by itself to maintain sufficient cooling flow. The parameter configuration for each of the 10 runs is summarized in Table 3.

Because the desired output was the steady-state temperature distribution within the pool, and because the pool thermal capacitance is large, a hybrid solution procedure was used. This procedure consisted of solving the transient momentum and mass conservation equations to determine a time-dependent velocity distribution, but the steady-state energy equation was iteratively solved at each time step using a loose convergence criterion to advance the thermal solutions at a rapid rate. Each case was started from a previous run, which already had a developed velocity and temperature profile, and the run was continued for approximately a 2-min simulation time. The temperature at various locations was monitored. It was found that a true steady state could not be achieved, but that the maximum calculated temperatures at a given location varied by 8°F, and that the location of the pool peak temperature also changed between adjacent nodes. The peak pool temperature, however, remained relatively constant ($\pm 2^\circ\text{F}$) over the final 30 s of simulation time. The inability of the simulation to reach a true steady state is consistent with the results of pool temperature measurement where local measured temperatures fluctuate with time, but the average remains constant.

TABLE 3. Parameter Configuration for the 10 Reported Runs

Run Number	Total Heat Rate, Q,gpm	Pool Inlet Temperature, °F	Number and Bundles In Pool	Peak-Average Bundle Heat Ratio	Number on Location of Peak Bundles	Direction of Inlet Flow Rate	Pool Outlet Temperature, °F
6	4187	17.8	2878	1.4	368 Near Center Figure 5a	Down	159
9	1848	18.11	2878	1.4	368 Near Center Figure 5a	Down	169
10	1848	18.11	138	1.4	368 Near Center Figure 5a	Down	149
11	1848	18.11	158	1.4	368 Under Inlet Figure 5b	Down	169
12	1848	18.11	158	13.9	132 Near Center Figure 5c	Down	169
14	1848	18.11	158	13.9	132 Near Center Figure 5c	Horizontal	169
16	1848	18.11	158	13.9	132 Near Edge Figure 5d	Down	169
17	458	18.11	138	13.9	132 Near Center Figure 5c	Down	176
18	458	18.11	188	13.9	132 Near Center Figure 5c	Down	146
19	458	18.11	138	13.9	Near Center Figure 5c (cask area removed from calculation)	Down	175

RESULTS

The maximum calculated temperature rise (maximum calculated temperature minus pool inlet temperature) and the location at which it occurred are summarized in Table 4. As shown, 46 to 80% of the maximum temperature rise results from the pool average temperature rise, which is determined by the simple pool energy balance

$$\bar{\Delta T} = \frac{Q_{\text{total}}}{C_p M_{\text{total}}}$$

where $\bar{\Delta T}$ = pool average temperature rise
 Q_{total} = total pool heat generation rate
 M_{total} = total pool inlet flow rate
 C_p = coolant specific heat = 1 Btu/(lbm * °F).

The remaining 20 to 54% of the pool maximum temperature rise results from three competing factors: the local heat generation rate, the proximity of the hot bundle to the inlet piping, and the proximity of the peak powered bundles to the rack-leveling pads. It is difficult to generalize any specific rules for the location of the predicted peak temperatures, because these three factors are interdependent as well as dependent on the pool temperature and temperature rise. In general, however, the peak temperature rise tended to occur either above a leveling pad for high local heat generation rates at that location or near, but not directly under, the inlet piping if the local power ratio above the leveling pad was low. The difference in calculated temperature at these two locations is, however, relatively small (less than 10°F for all cases studied) when the maximum temperature rise is near the inlet.

The effect of increasing the ratio of pool heat generation rate to pool flow rate is demonstrated by comparing Figures 6 and 7. The heat-to-flow ratio shown in Figure 7 is 2.4 times greater than that of Figure 6. Comparison of Figures 10 and 13 also demonstrates this effect; the heat-to-flow ratio of Figure 10 is 2.3 times that of Figure 13. These comparisons show that increasing the pool heat-to-flow ratio has little effect on the shape of the temperature distribution within the central rack, which is the higher powered region of the pool for this comparison. It also has little effect on the shape of the local temperature increase caused by the rack-leveling pads. The leveling pad effect produces the six small regions of local temperature increase in the central rack of Figures 6 and 7, as well as the three regions of temperature increase in the central rack in Figures 10 and 13. The effect of the leveling pads is visible only in the central rack, primarily because this is the only location where they were set up in the model. The model was defined in this manner so that the leveling pad effect could be evaluated with a minimum number of computer runs. The magnitude of the leveling pad effect is further demonstrated by comparing Figures 10 and 12 where the leveling pads were under the hot zone in 10 but omitted under the high heat generation

TABLE 4. Summary of Maximum Temperature Rise

Run Number	Location of Maximum Temperature Rise	Pool Energy Balance Temperature Rise, °F	Inlet Temperature, °F	Maximum Local Temperature Rise, °F (ΔT_m)	$\frac{\Delta T}{\Delta T_m}$
5	above foot	6	150	9	0.67
9	near inlet	13	150	19	0.68
10	near inlet	13	130	28	0.46
11	near inlet	19	150	24	0.79
12	above foot	19	150	32	0.60
14	above foot	19	150	32	0.60
16	near inlet	19	150	26	0.73
17	above foot	45	130	56	0.80
18	above foot	45	100	60	0.75
19	above foot	45	130	58	0.78

zone in Figure 12. This shows that the leveling pad increased the local temperature by only 8°F for the largest possible relative heating rate distribution that can occur. This is a small increase in temperature; it is expected that the effect in the real pool will be even smaller because the loss coefficients used in this analysis to model the leveling pads are conservative. These results also demonstrate that, if the relative power of the bundles above the pads is small, the pad has little effect on the temperature distribution.

In Figures 6 through 15, it is apparent that the inlet flow affects the temperature distribution to some degree in the bundles near the inlet locations and that the effect is greater when the pool heat generation-to-flow ratio is increased. It is also greater if the local heating rate is increased somewhere in the pool. However, if the local heat generation rate is increased in the region of an inlet (Figure 9), the inlet effect on the flow distribution is somewhat negated, as demonstrated by comparing Figure 9 to Figure 7 where the only difference between the two cases is the location of the higher heat generating bundles.

Several factors combine to produce the observed temperature distribution near the inlets. The major factors are the transverse velocities above and below the fuel bundles, the slightly higher density of the coolant in the pool above the bundles near the inlet, and, to a lesser degree, the axial momentum of the fluid leaving the inlet piping. The general flow pattern is such that the inlet coolant tends to flow downward along the back and side walls of the pool and, the colder it is, the faster it falls. This is demonstrated in Figure 16 through 24, where the flow and temperature distribution are given along the back wall. The pattern of flow down the back wall is approximately the same in each of the 10 runs except that the region of higher velocities is slightly broadened when the inlet flow is horizontal and directed away from the back and side walls. This is shown in Figure 20. In all 10 cases the velocities are also downward through some of the bundles in the vicinity of the inlet as shown in Figures 25 through 33.

Another effect (which is visible in Figures 25 through 33) is a cooler fluid cap, which is carried out over the top of the spent fuel in the vicinity of the inlet. The water falls downward in the pool above the bundles until it is just above the heated region, where it is turned and directed radially outward over the bundles. The water, which is directed over the bundles, is colder than the water both above and below so it acts as a cap that inhibits the rise of the hotter water below. Near the back corners, the downward flow through the bundles is sufficiently large to maintain near isothermal conditions in the bundles with the downward flow. This regime is stable and has little effect on the temperature in other regions of the pool. In some instances, farther out from the corner, the cool cap acts in concert with the other forces to produce a small upward or downward flow, as shown in Figures 29 and 31. The effect of a small downward flow rate is most visible in the local inverted temperature distribution where higher temperatures occur at the bottom rather than the top of the bundles. In Figure 29, the temperature inversion is shown to correspond to a bundle grouping that has an upward

velocity. This indicates that the average temperature in these bundles is becoming high enough to change the flow direction and, if the solution were to proceed, the temperature inversion would dissipate in these bundles. This unstable situation prohibits the solution from reaching a true steady state. Even though this flow pattern is unstable and produces temperature oscillations of 8°F, the natural effects of buoyancy keep the temperature from increasing to unacceptable levels.

A large percentage of the available cooling for most of the bundles in the pool comes from the fluid that flows down the rear corner walls and through the high downflow bundles under the inlet. This causes high transverse velocities under the racks in the rear corners. Figures 34 through 43 show the transverse velocity and temperature distribution in the region below the racks and above the pool floor. They show the high (approximately 0.5 ft/s) transverse velocities in the rear corners and also along the side near the cask-handling area. These relatively high velocities produce a slightly lower pressure that tends to increase the relative effect of buoyancy. The velocity and temperature distributions are qualitatively the same for 9 of the 10 runs, but the transverse flow pattern generally terminates at the location of the bundle with the highest local heat generation rate. For the tenth run (Figure 43), the flow in the back right corner is directed around the blocked-off cask-handling area. The higher the local heat generation rate, the greater the effect on the transverse velocities.

A similar transverse velocity pattern exists in the plane just above the bundles, except that the coolant in this case is entrained in the plume rising above the hot bundles. Figures 44 through 53 show these transverse velocity and temperature distributions for the 10 cases run. The temperature distribution along the front side of the pool is fairly homogeneous (less than 4°F temperature difference), with the velocities generally being small (less than 0.1 ft/s) with the direction dependent on the case. In Case 14, where the inlet flow is horizontal, there is a larger region where the flow is downward along the front face (Figure 59). This tends to pull the upper plenum fluid into the region between the wall and the racks. For the case (Figure 57) where the hot bundles are located near the front wall, there is a zone of high upward velocity (\approx 0.6 ft/s) above the fuel bundles.

Three qualitatively similar velocity and flow distributions occur in the bundles above the rack leveling pads. These are shown in Figures 64 through 73. The first type, shown in Figures 64 through 66, has a local power ratio of 1.4 in the bundles above the leveling pads. In the second category, the local power distribution in the bundles is less than 1.0. The typical velocity and temperature distributions for this case are shown in Figures 67 and 70. Figures 68, 69, 71, 72, and 73 show results where the local power ratio is 13.9 in the bundles above the leveling pads. These figures demonstrate that the leveling pads significantly affect the temperature distribution only if the heat generation rate in the bundles above the leveling pads is large. In all of these high local heating ratio cases, the temperature gradients in the high heating bundles are approximately equal. This set of figures also shows

that buoyancy effects tend to equalize temperatures throughout the pool. For example, if the local heating rate increased by a factor of 10 (which is approximately $13.9/1.4$), then the temperature rise through a bundle governed by forced convection would also increase by a factor of approximately 10. However, these results show that, when the local power is increased by a factor of 10, the local temperature rise increases by only 12°F (16° temperature rise of Figures 68, 69, 71, or 72, versus 4°F temperature rise in Figures 64, 65, or 66). This is only a factor of 4. This nonlinear relationship results because buoyancy flows are governed by the Grashoff number (the ratio of buoyancy forces to viscous forces), which is linearly proportional to temperature difference and also approximately proportional to the third power of the local temperature (over the range of 100°F to 200°F). Therefore, the higher the local temperature, the higher will be the buoyancy forces compared to the viscous forces. This is demonstrated by comparing the peak inlet-to-outlet temperature rise in Figures 71 and 72. The only difference between the two cases is the inlet temperature, which is 130°F in Figure 71 and 100°F in Figure 72. The inlet-to-peak temperature rise is only 56°F for the 130°F inlet case, while it is 60°F for the colder 100°F inlet.

In the pool above the fuel bundles, the coolant tends to roll with a large scale on the order of one-fourth of the linear dimensions of the open pool region. This large rolling maintains the upper pool approximately isothermal except for a slight high temperature cone or plume that forms above the heated regions. There are also small regions of high temperature gradients near the inlets.

These results combine to demonstrate that the good mixing in the upper plenum, the relatively open flow area below the fuel, and the 2-in. gaps around the periphery of the racks all combine to provide adequate cooling, regardless of the inlet flow orientation or the location and magnitude of "loading patterns" of the hot bundles within the pool. The major factor controlling pool performance is the total pool heating rate to total pool recirculation flow rate. The maximum temperature rise of 56°F calculated for the 13.9 local power ratio is 15° less than that calculated by the utility.

By assuming an axial power factor of 1.2 and using a coolant to clad heat transfer coefficients of $50 \text{ Btu/h-ft}^2 \text{ }^{\circ}\text{F}$, the clad temperature rise above that of the coolant was determined to be 15°F for the assemblies with a heating ratio of 13.9. The fuel temperature rise is highly dependent on the fuel clad heat transfer coefficient about which there is little reliable information at these low temperatures. However, it is believed that its value lies between 200 and $1000 \text{ Btu/h-ft}^2 \text{ }^{\circ}\text{F}$. The maximum fuel-to-clad temperature rise was calculated to be less than 6°F using the conservatively low heat transfer coefficient of $200 \text{ Btu/h-ft}^2 \text{ }^{\circ}\text{F}$ and values of 1.2 and 13.9 for the axial and assembly heat rate peaking factors, respectively. These temperature rises are negligible when compared to the pool coolant temperature rise.

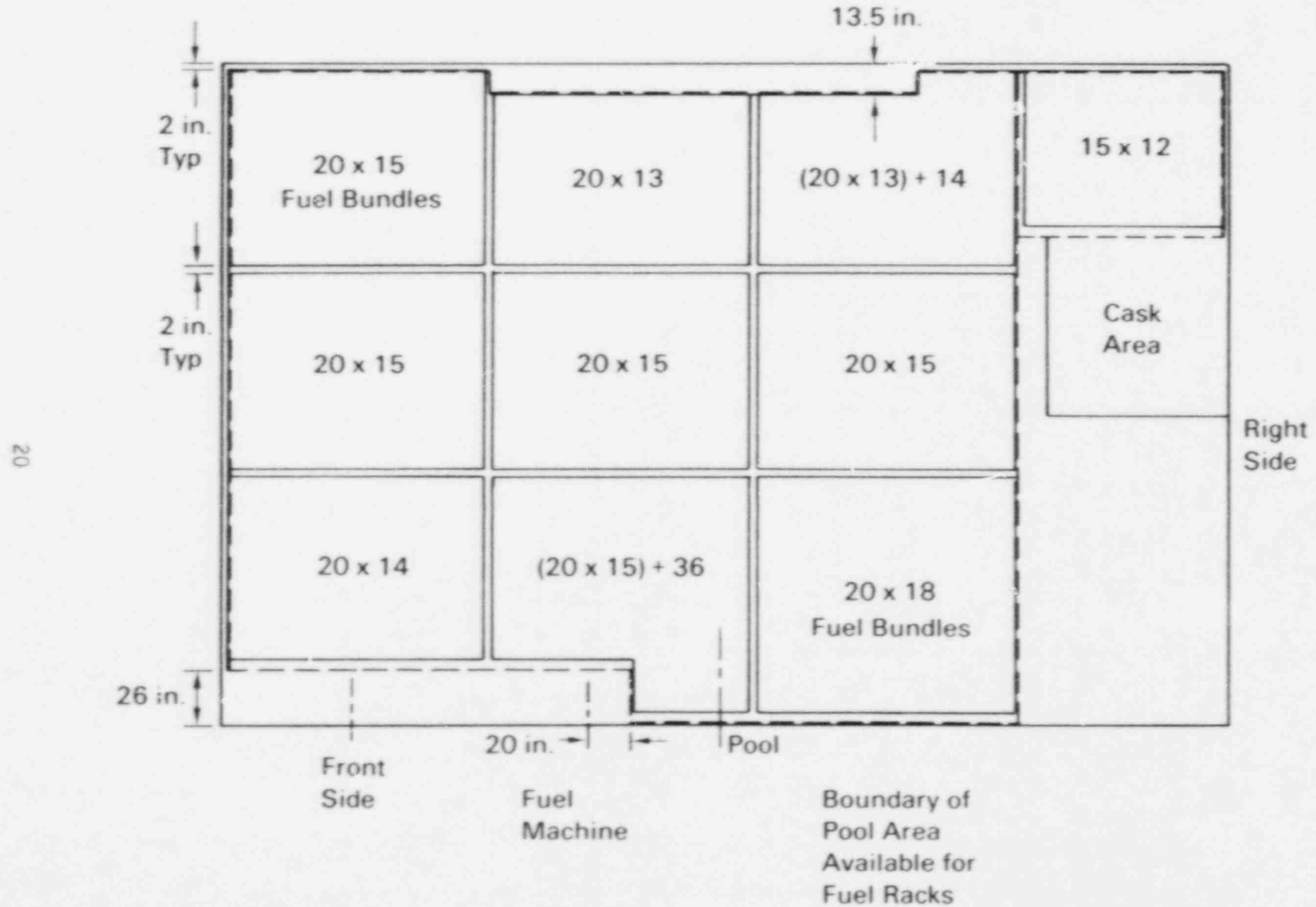


FIGURE 1. Cross Section of Vermont Yankee Spent-Fuel Pool Showing Proposed Storage Rack Layout

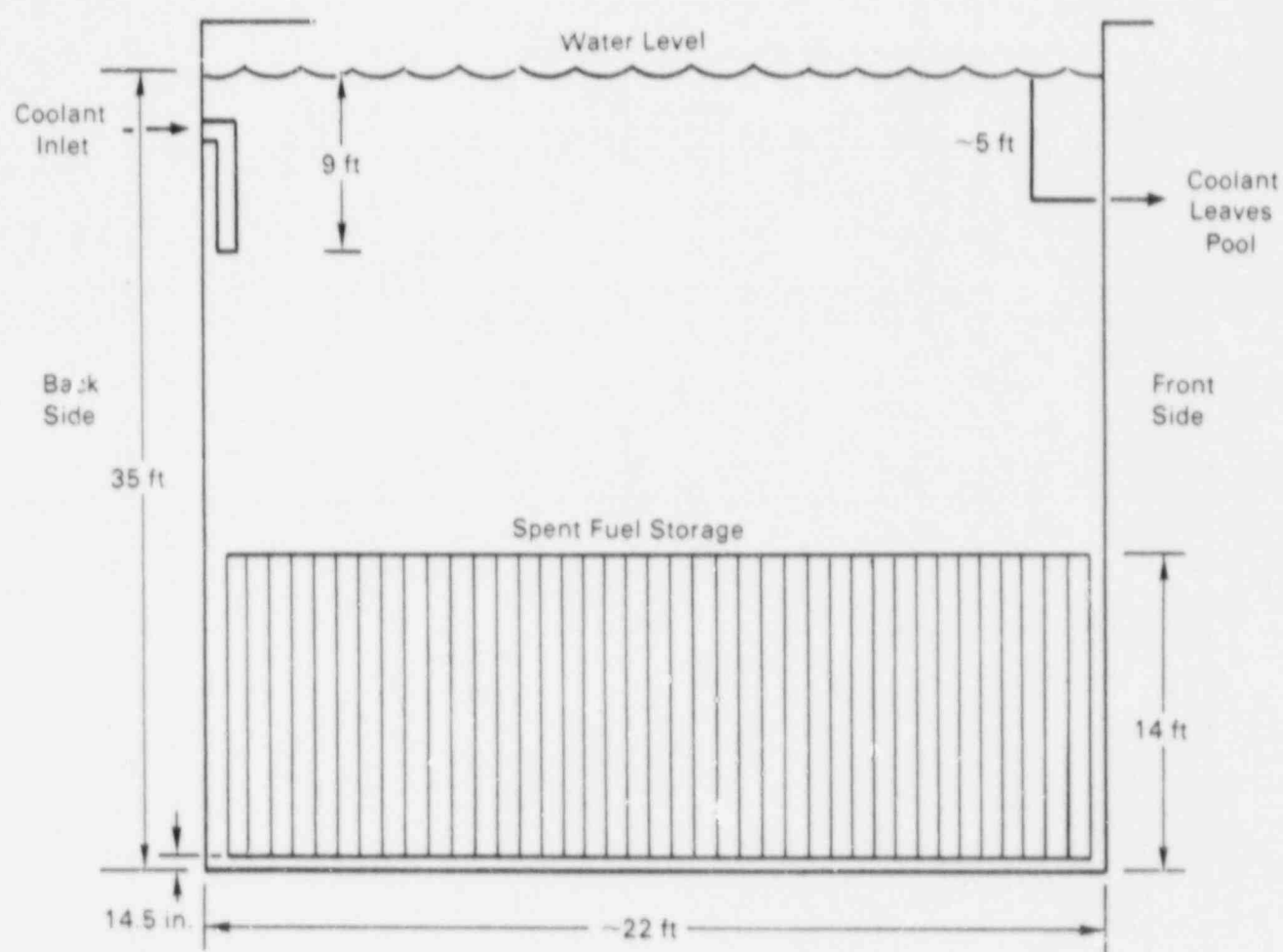


FIGURE 2. Vertical Cross Section of Vermont Yankee Spent-Fuel Pool

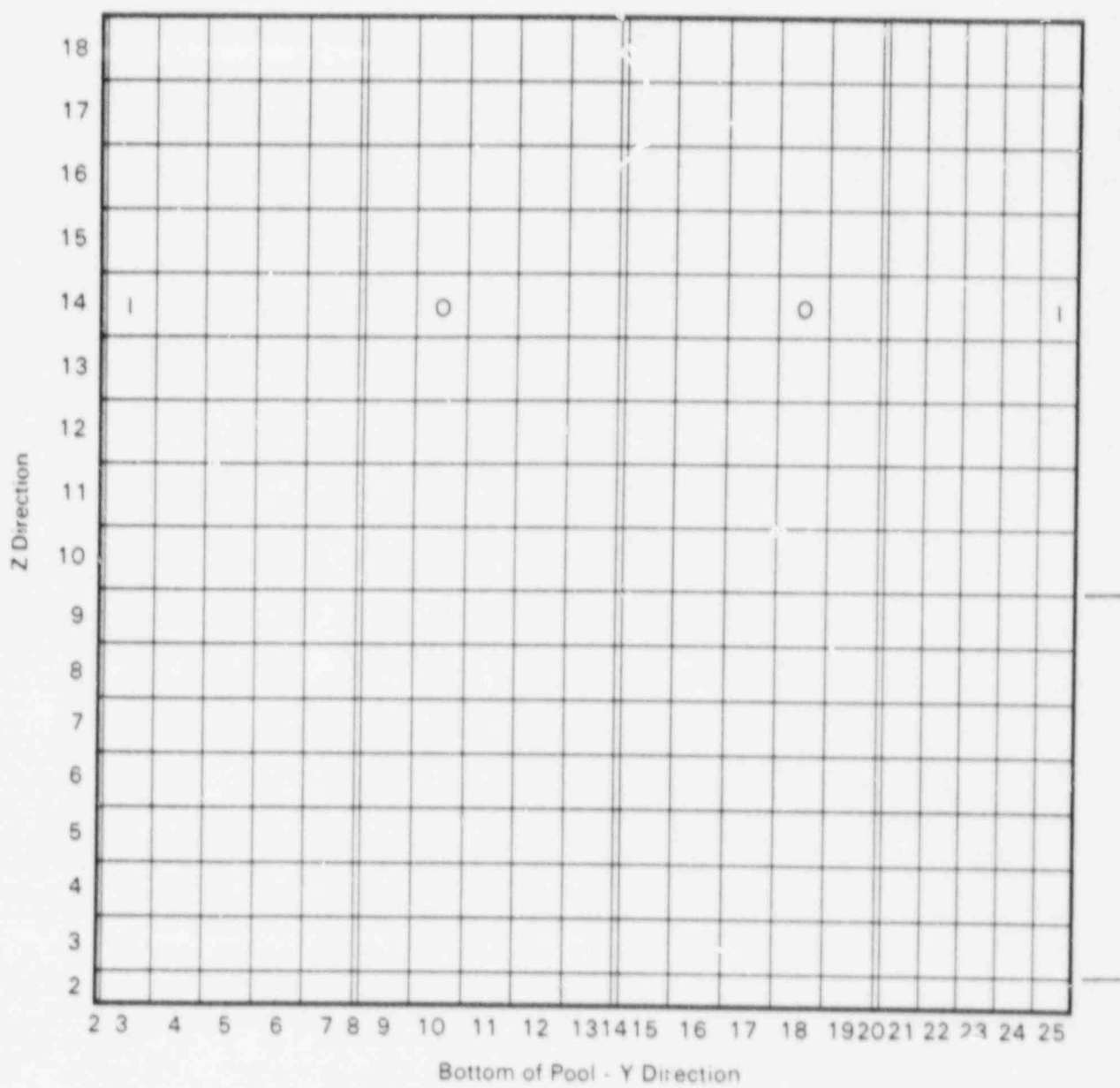
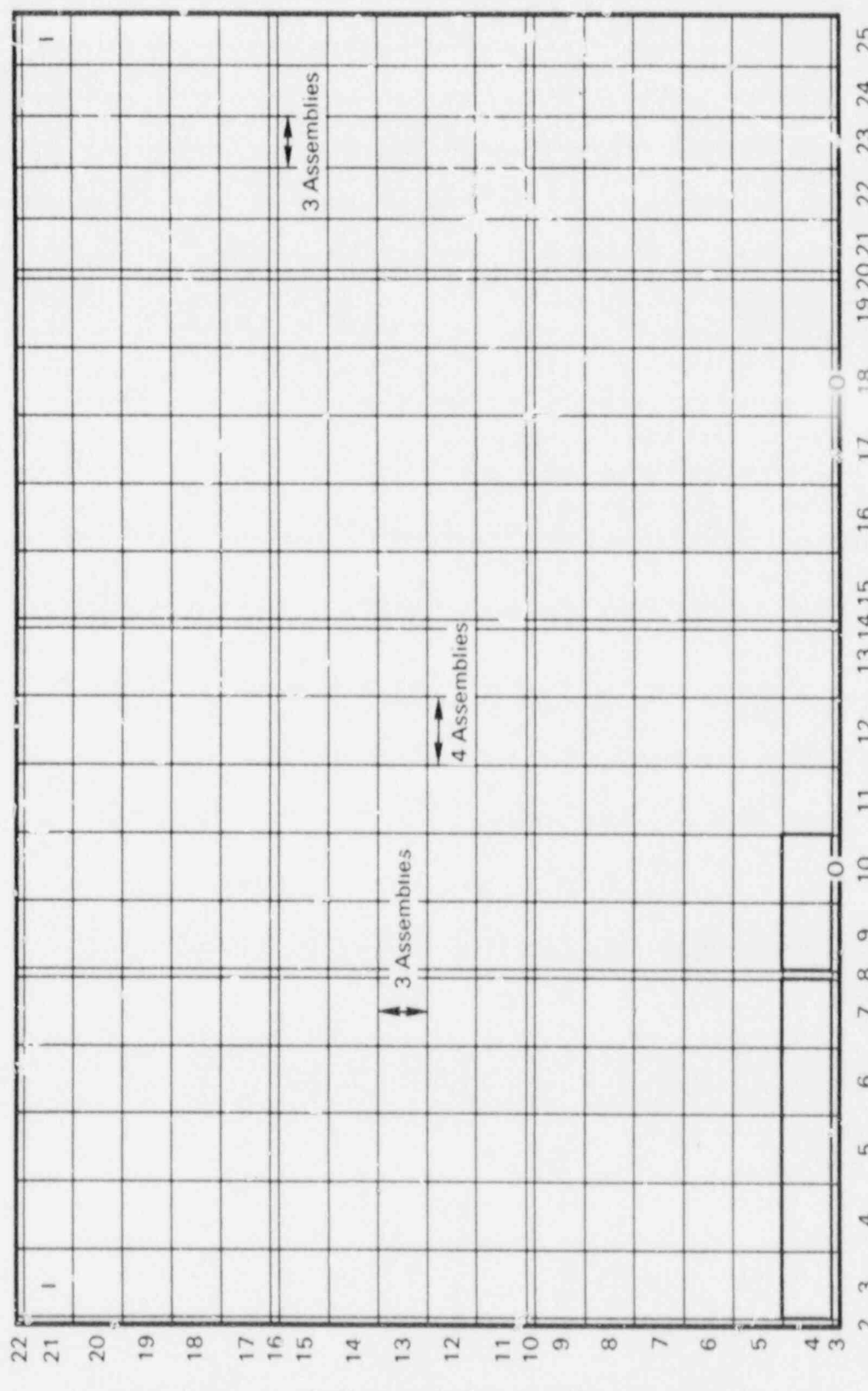


FIGURE 3. TEMPEST Noding Model in X-Y Plane

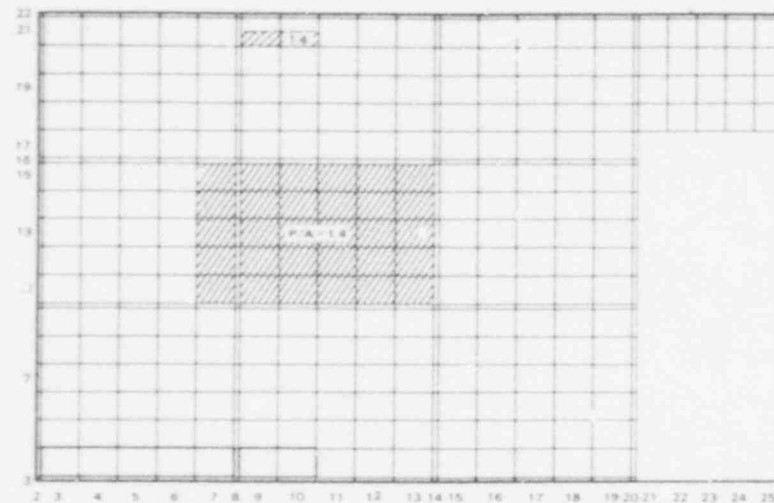
| = Inlet
O = Outlet



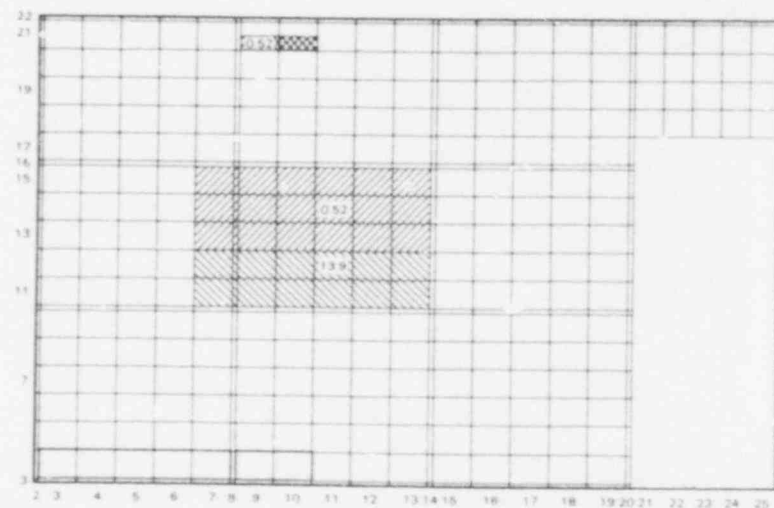
Left-Hand Side - X Direction

Front Side (Outlet Side of Pool) - Y Direction

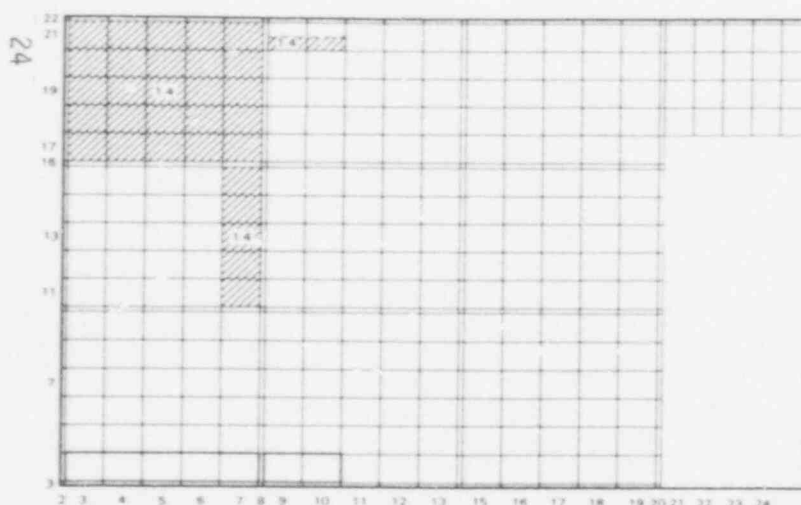
FIGURE 4. TEMPEST Nodding Model in X-Y Plane



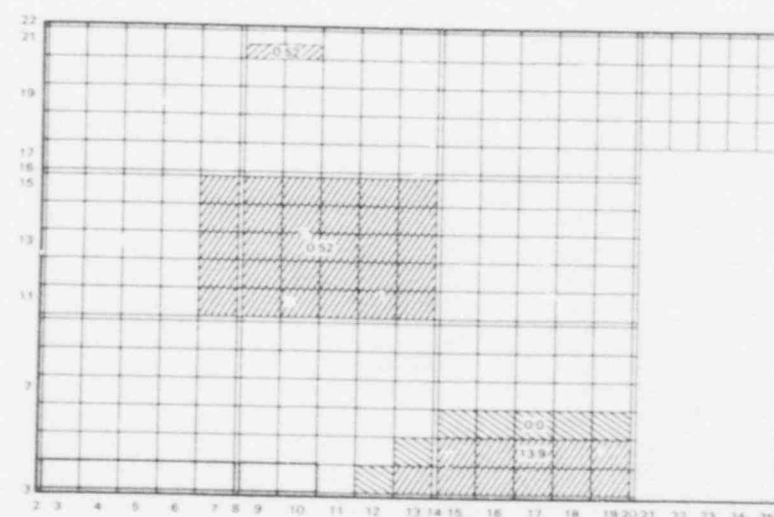
a. Configuration 1



b. Configuration 2



c. Configuration 3



d. Configuration 4

FIGURE 5. Normalized Local Heat Generation Rate Distributions

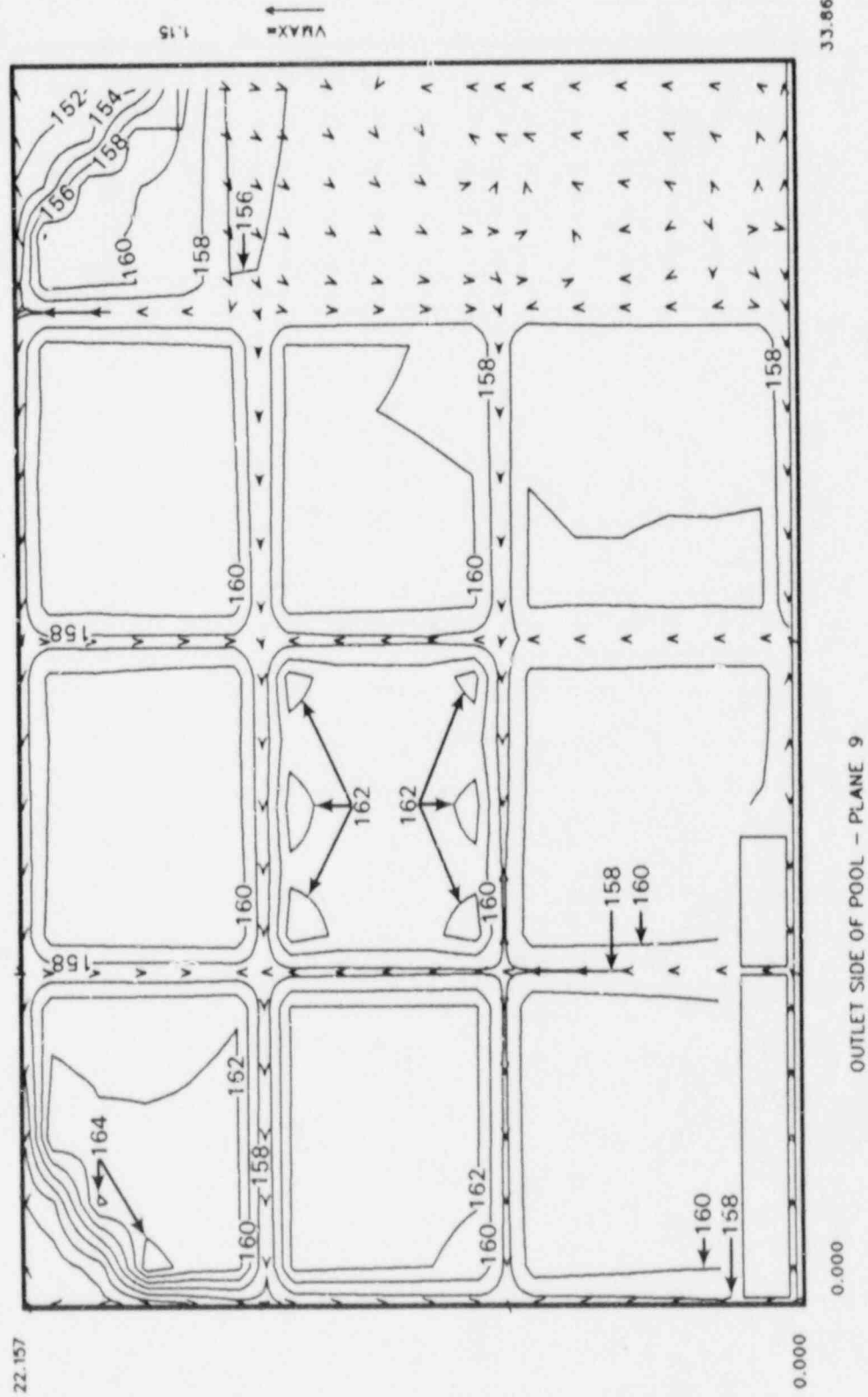


FIGURE 6. Temperature Distribution at the Top of the Fuel Bundles for Case Number 5. ($Q = 4187 \text{ GPM}$, $T_{INLET} = 150^\circ\text{F}$, $P_L/\rho = 1.4$, inlet flow down, peak heat generation near center of pool)

22.157

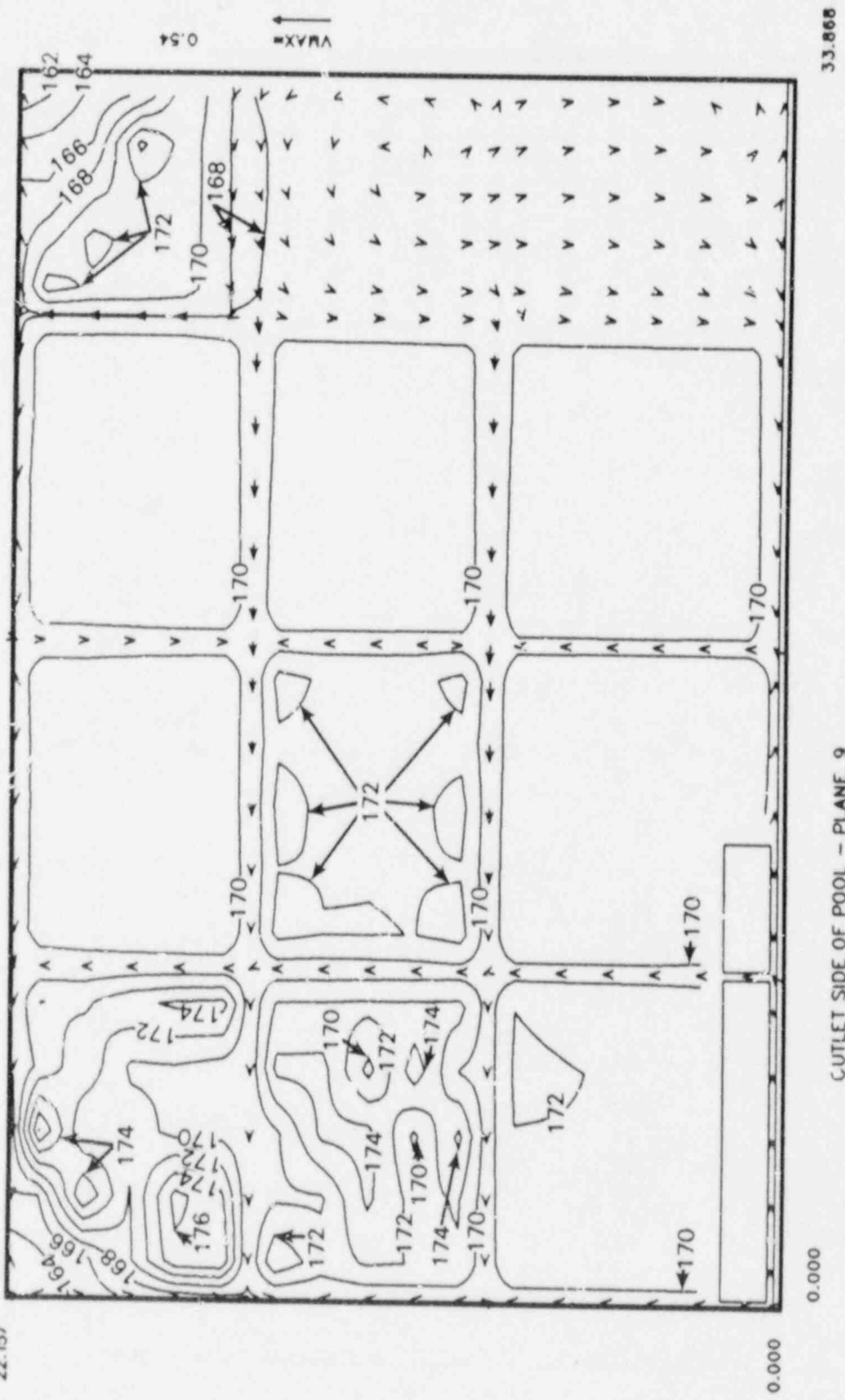


FIGURE 7. Temperature Distribution at the Top of the Fuel Bundles for Case Number 9. ($Q = 1048 \text{ GPM}$, $T_{INLET} = 150^\circ\text{F}$, $P_L/P = 1.4$, inlet flow down, peak heat generation near center of pool)

33.868

27

22.157

0.000

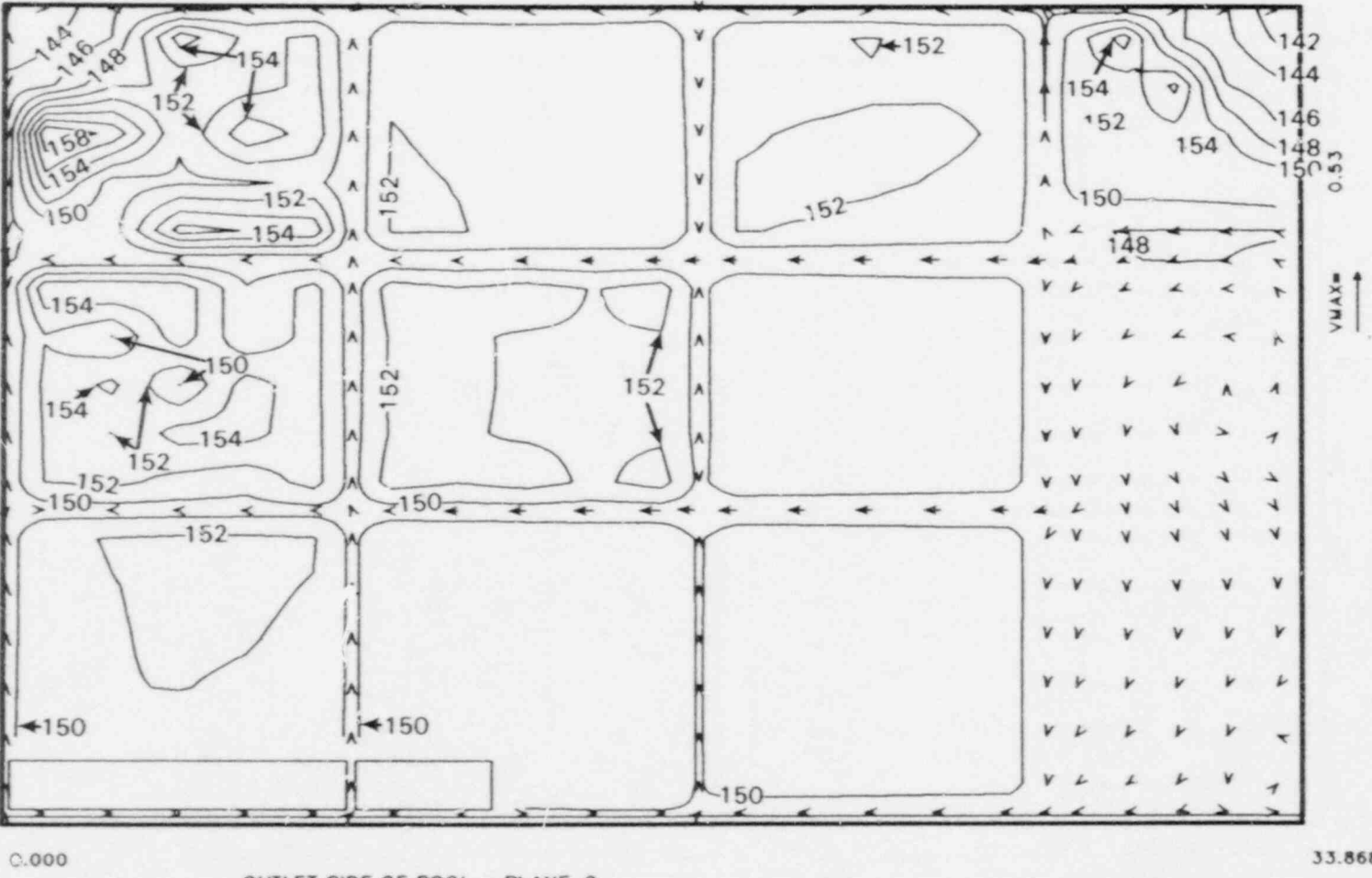


FIGURE 8. Temperature Distribution at the Top of the Fuel Bundles for Case Number 10. ($Q = 1048 \text{ GPM}$, $T_{INLET} = 130^\circ\text{F}$, $P_L/P = 1.4$, inlet flow down, peak heat generation near center of pool)

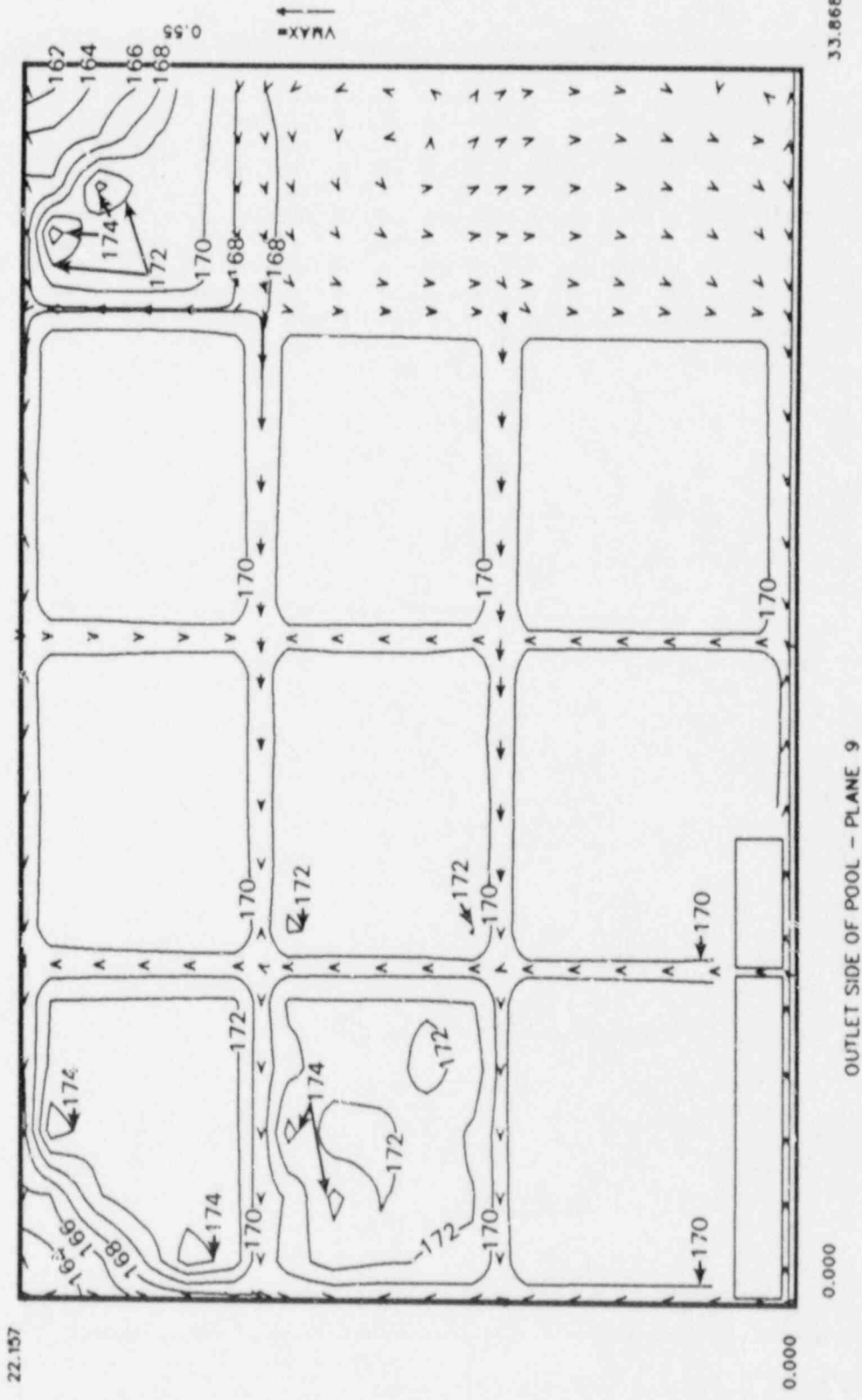


FIGURE 9. Temperature distribution at the top of the fuel bunules for GPM, TINLET = 150°F, $P_L/P = 1.4$, inlet flow down, peak heat generation under inlet)

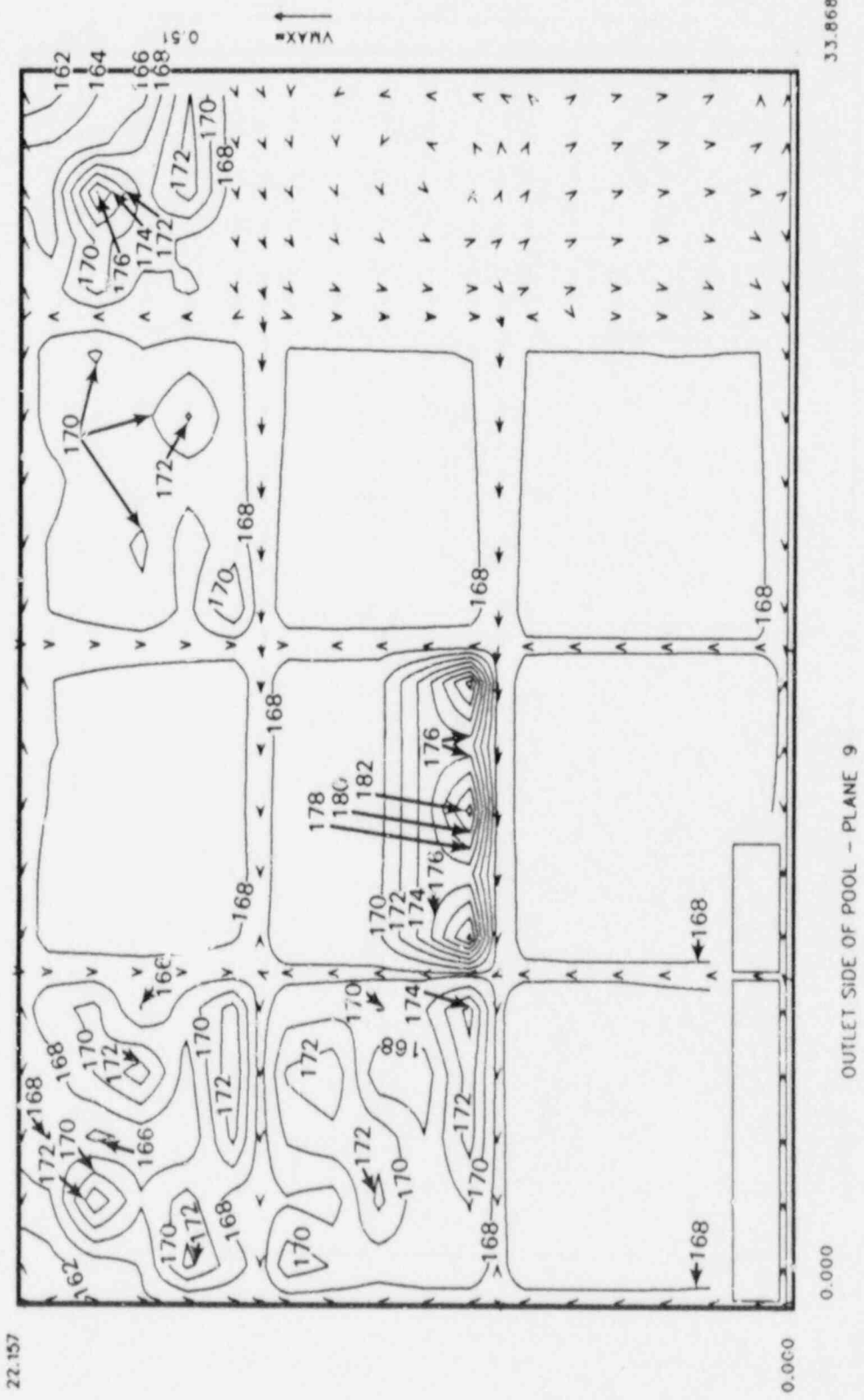


FIGURE 10. Temperature Distribution at the Top of the Fuel Bundles for GPM, TINLET = 150°F, inlet flow down, peak heat generation near center of pool

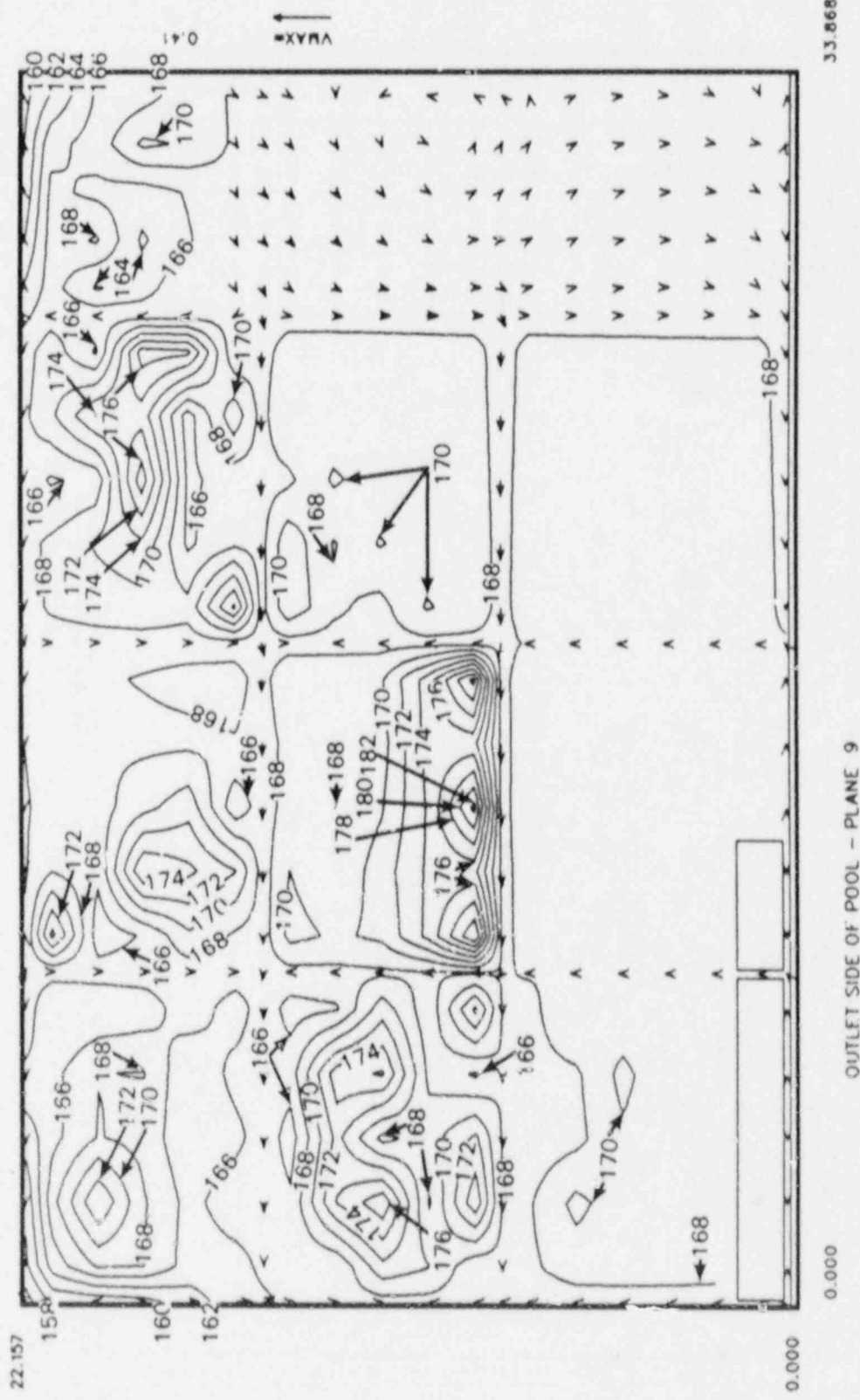


FIGURE 11. Temperature Distribution at the Top of the Fuel Bundles for Case Number 14. ($Q = 1048 \text{ GPM}$, $T_{INLET} = 150^\circ\text{F}$, $P_L/P = 13.9$, inlet flow horizontal, peak heat generation near center of pool)

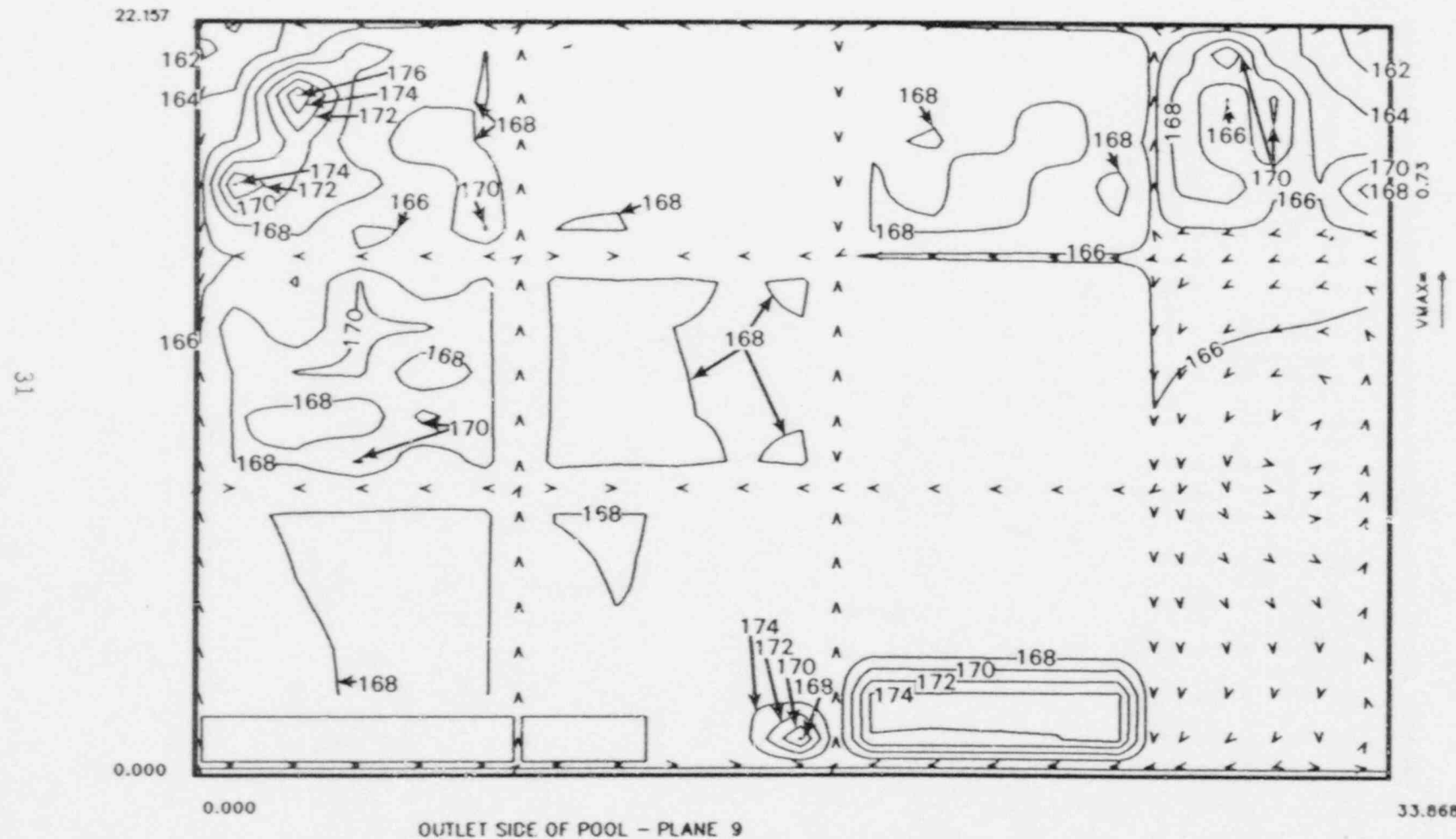


FIGURE 12. Temperature Distribution at the Top of the Fuel Bundles for Case Number 16. ($Q = 1048 \text{ GPM}$, $T_{INLET} = 150^\circ\text{F}$, $P_L/P = 13.9$, inlet flow down, peak heat generation near edge of pool)

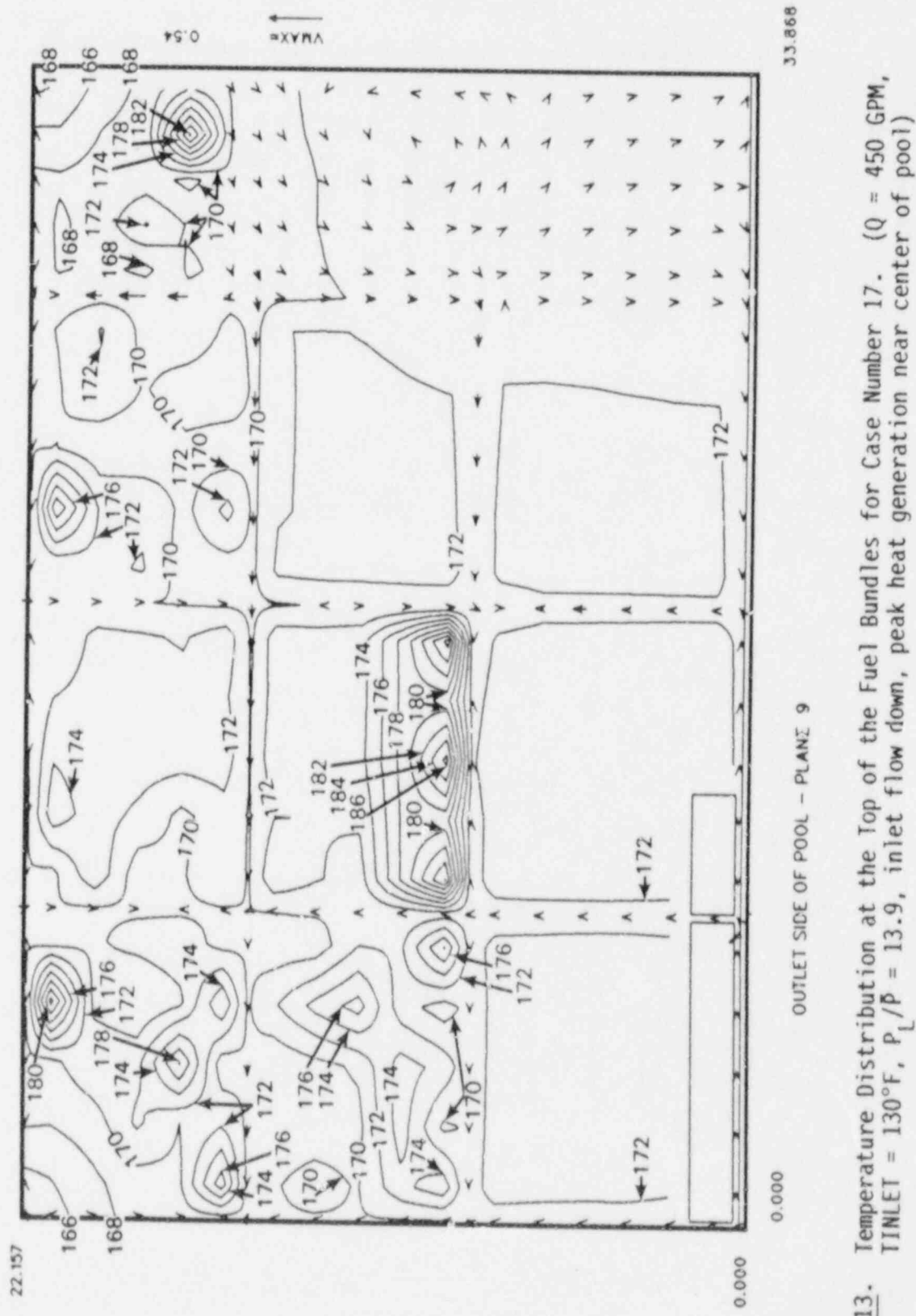


FIGURE 13. Temperature Distribution at the Top of the Fuel Bundles for Case Number 17. ($Q = 450 \text{ GPM}$, TINLET = 130°F , $P_L/P = 13.9$, inlet flow down, peak heat generation near center of pool)

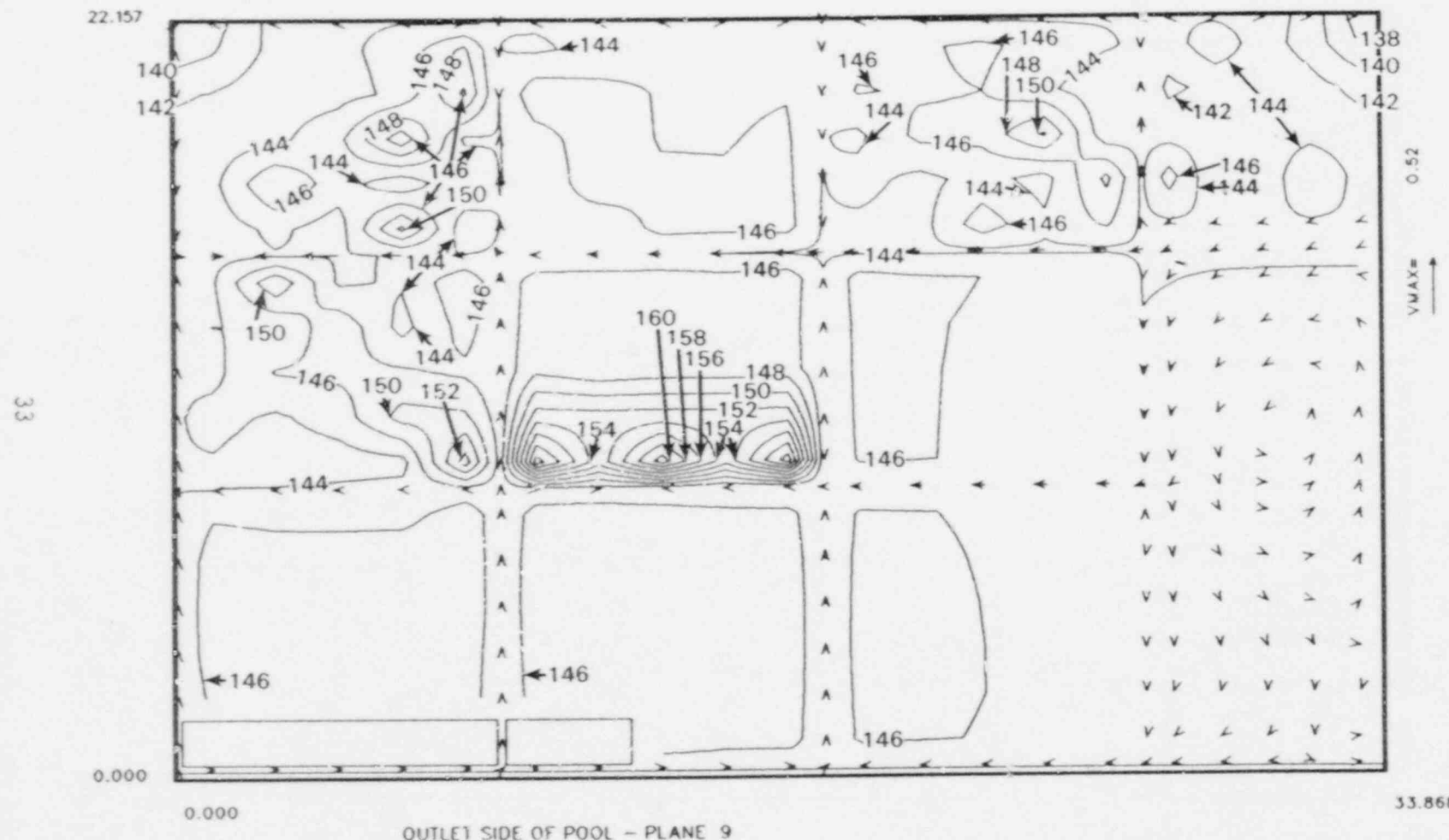


FIGURE 14. Temperature Distribution at the Top of the Fuel Bundles for Case Number 18. ($Q = 450$ GPM, TINLET = 100°F , $P_1/\bar{P} = 13.9$, inlet flow down, peak heat generation near center of pool)

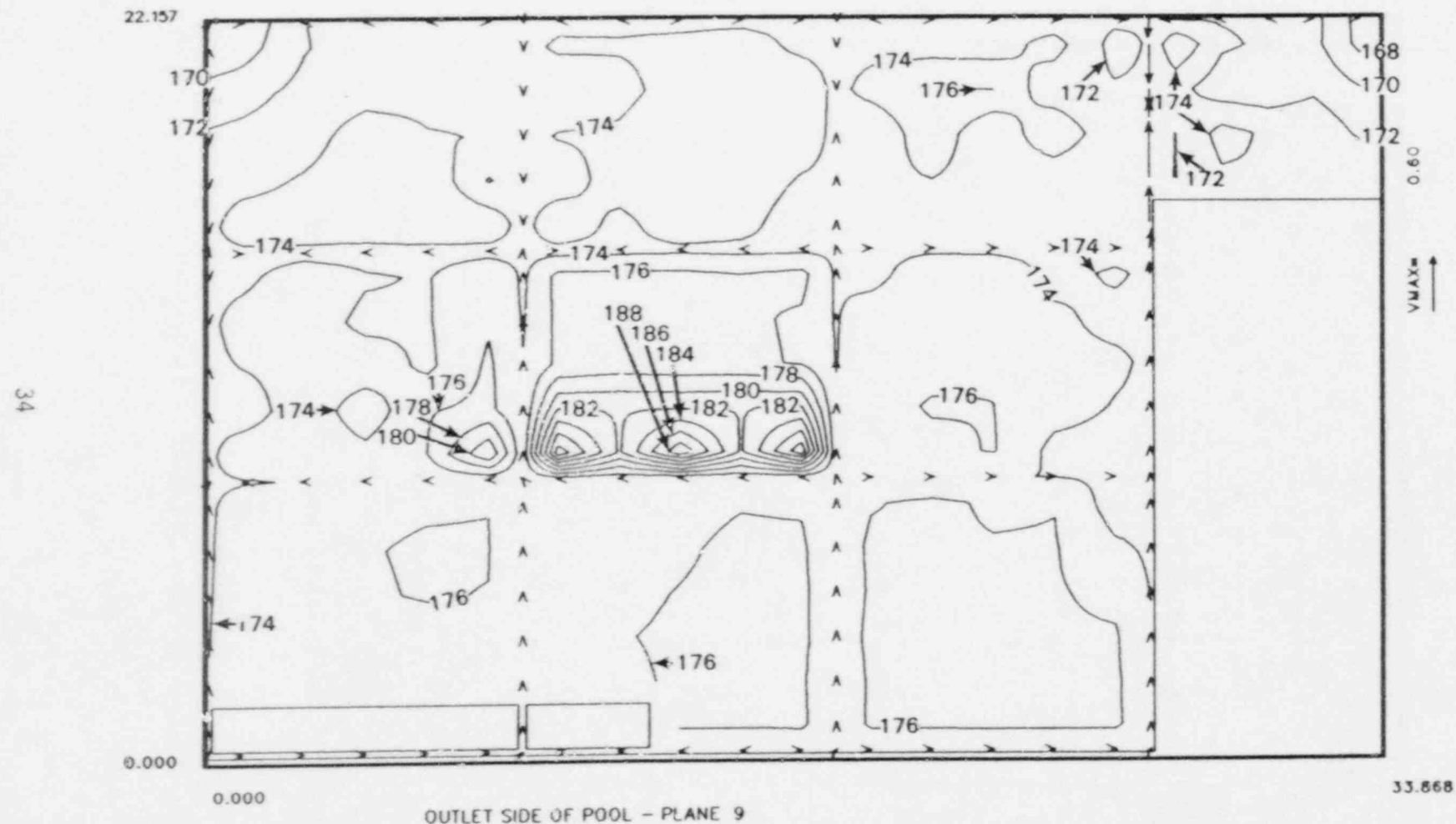


FIGURE 15. Temperature Distribution at the Top of the Fuel Bundles for Case Number 19. ($Q = 450 \text{ GPM}$, TINLET = 130°F , $P_e/P_0 = 13.9$, inlet flow down, peak heat generation near center of pool, large open flow region of cask area removed from model)

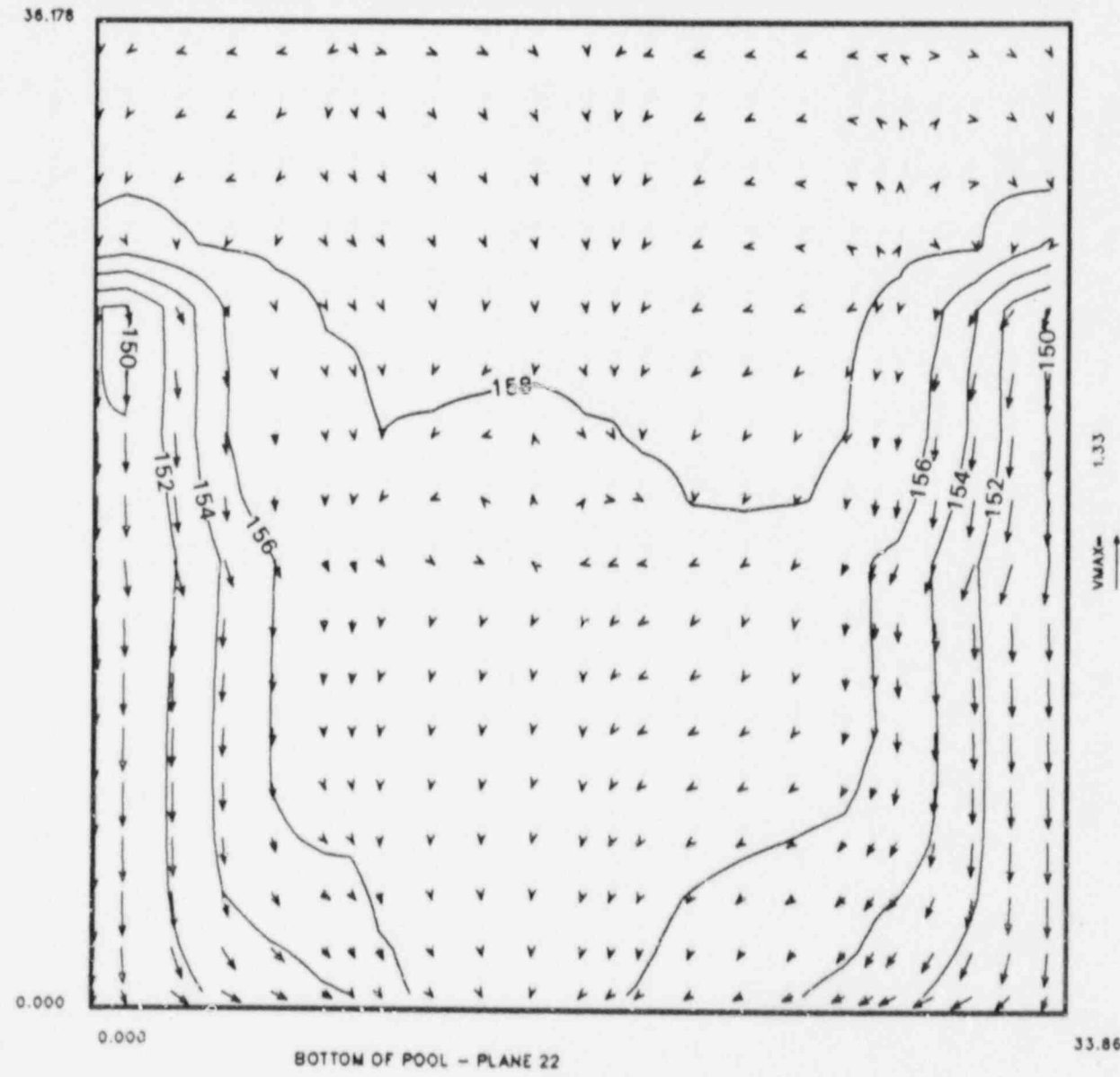


FIGURE 16. Temperature and Flow Distribution along the Back Wall of the Pool for Case Number 5. ($Q = 4187 \text{ GPM}$, $T_{INLET} = 150^\circ\text{F}$, $P_L/P = 1.4$, inlet flow down, peak heat generation near center of pool)

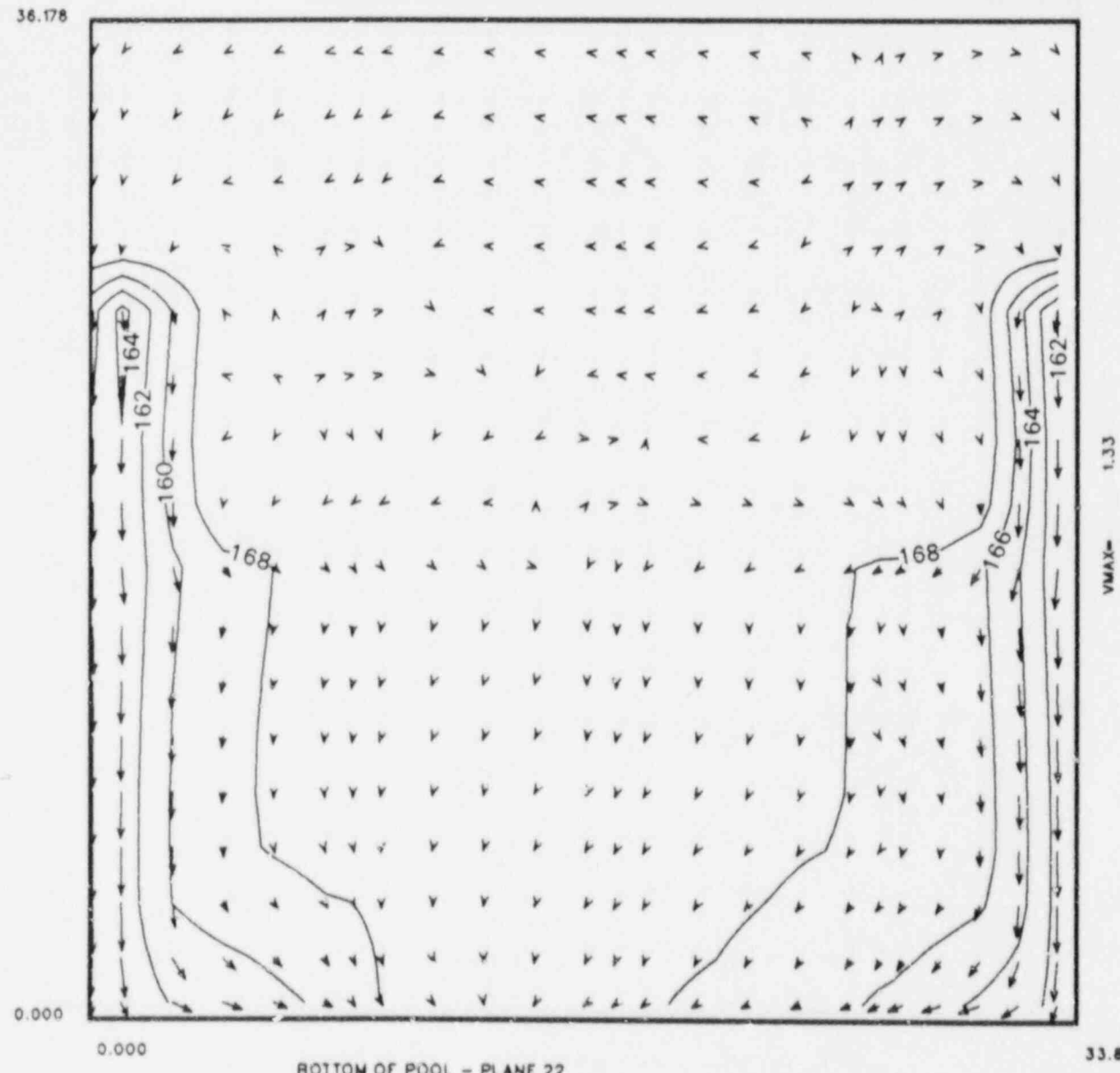


FIGURE 17. Temperature and Flow Distribution along the Back Wall of the Pool for Case Number 9. ($Q = 1048 \text{ GPM}$, $T_{INLET} = 150^\circ\text{F}$, $P_L/P = 1.4$, inlet flow down, peak heat generation near center of pool)

38.178

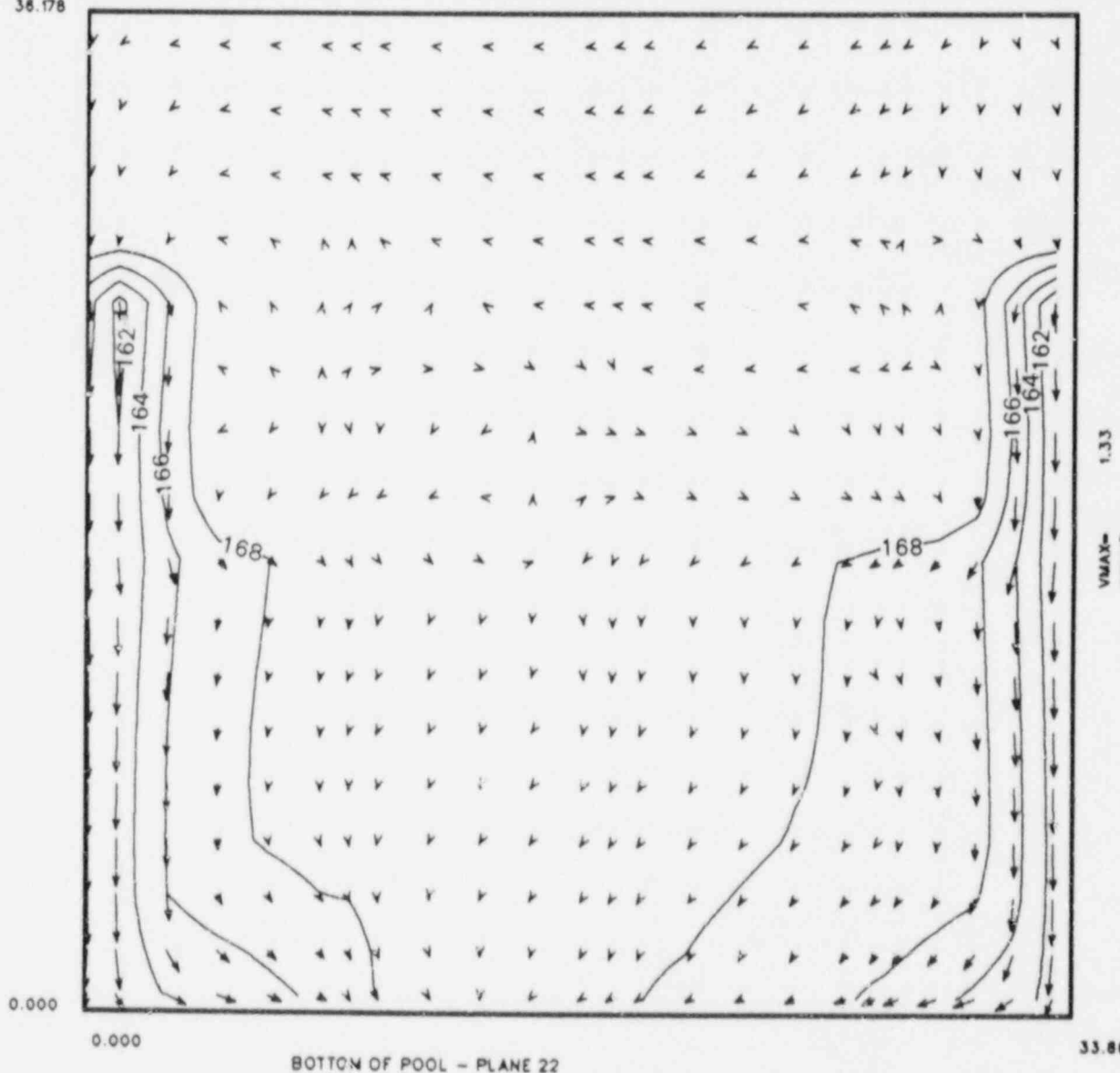


FIGURE 18. Temperature and Flow Distribution along the Back Wall of the Pool for Case Number 11. ($Q = 1048 \text{ GPM}$, $T_{INLET} = 150^\circ\text{F}$, $P_L/P = 1.4$, inlet flow down, peak heat generation under inlet)

36.178

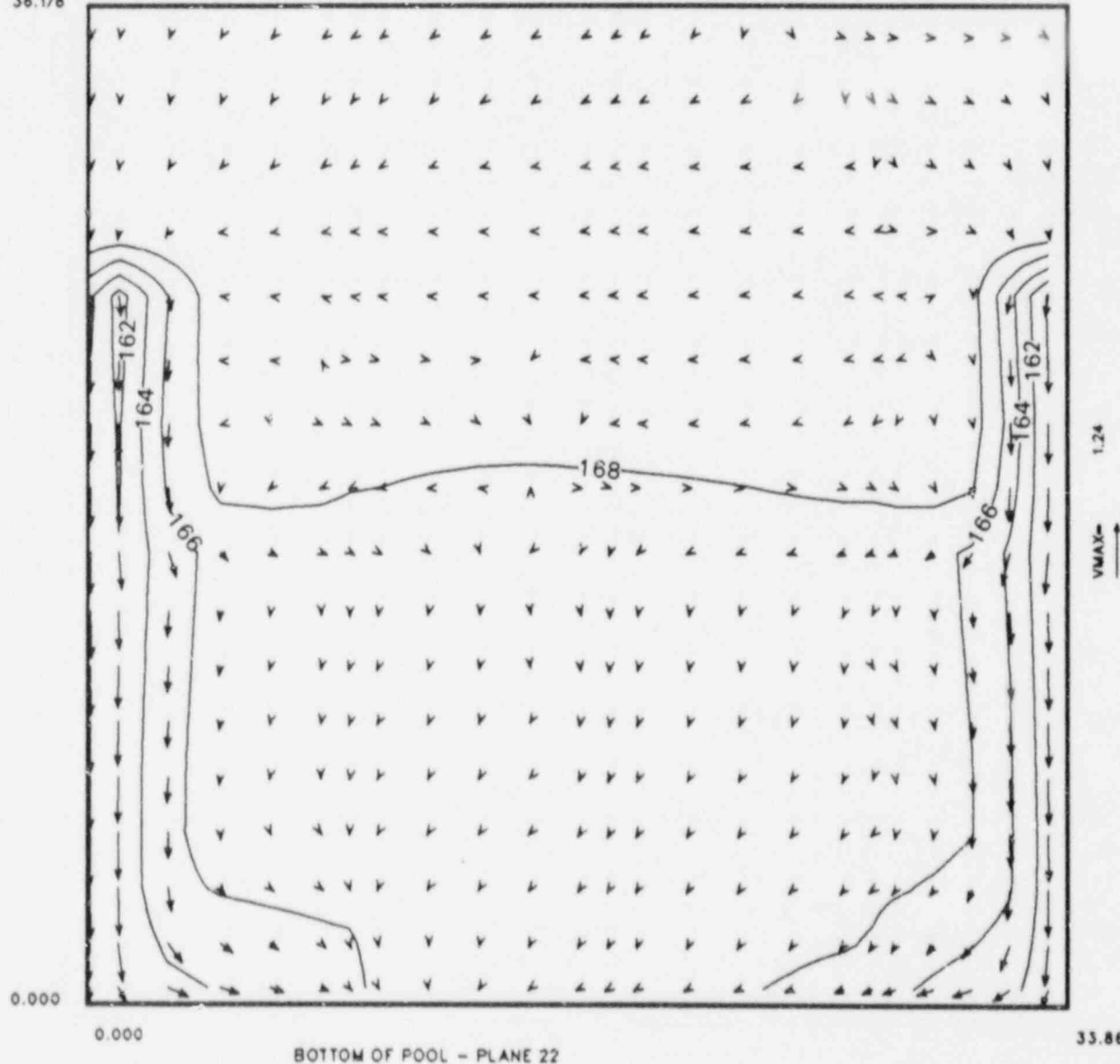


FIGURE 19. Temperature and Flow Distribution along the Back Wall of the Pool for Case Number 12. ($Q = 1048 \text{ GPM}$, $T_{INLET} = 150^\circ\text{F}$, $P_e/P_0 = 13.9$, inlet flow down, peak heat generation near center of pool)

36.178

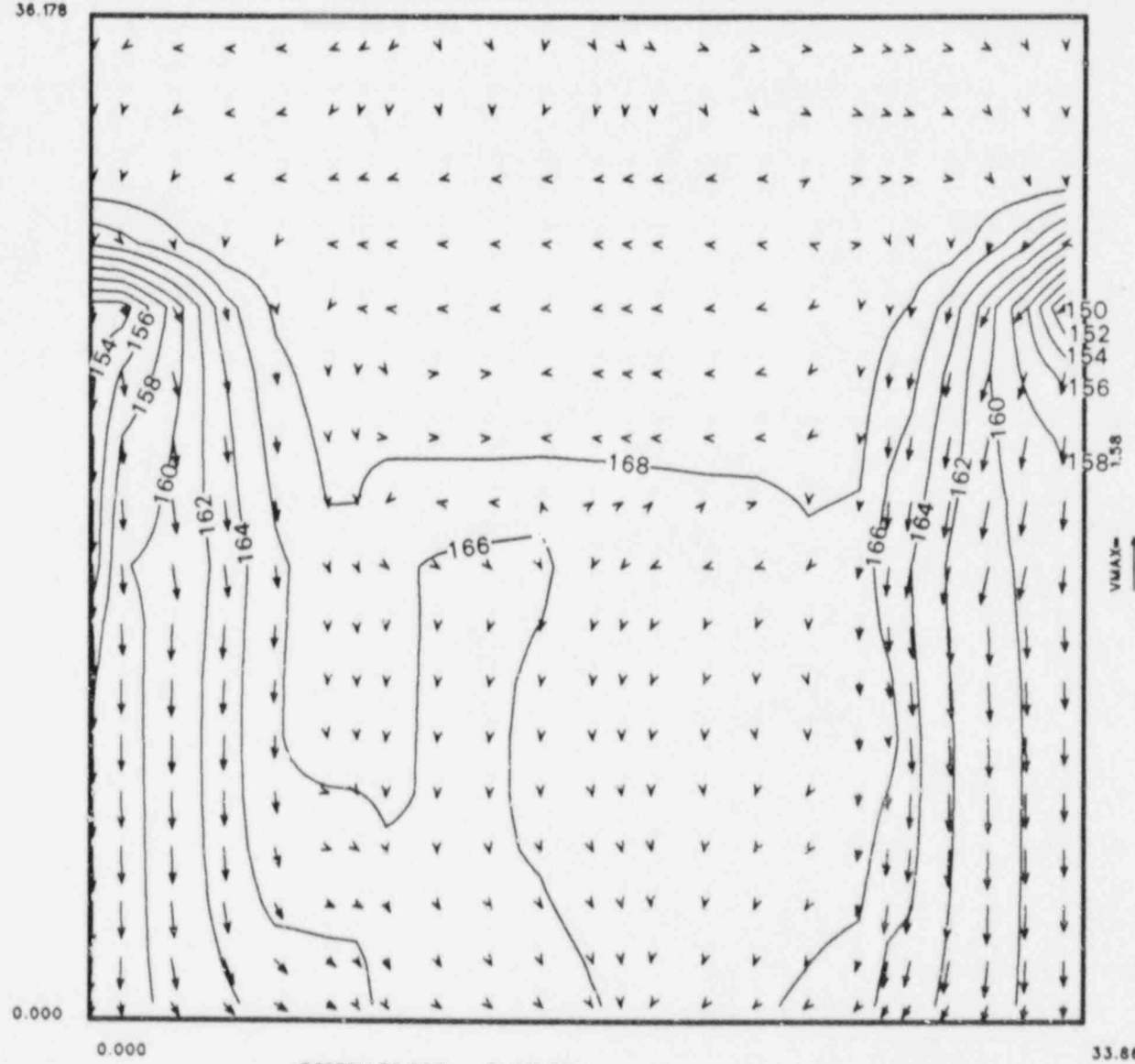


FIGURE 20. Temperature and Flow Distribution along the Back Wall of the Pool for Case Number 14. ($Q = 1048 \text{ GPM}$, $T_{INLET} = 150^\circ\text{F}$, $P_L/P = 13.9$, inlet flow horizontal, peak heat generation near center of pool)

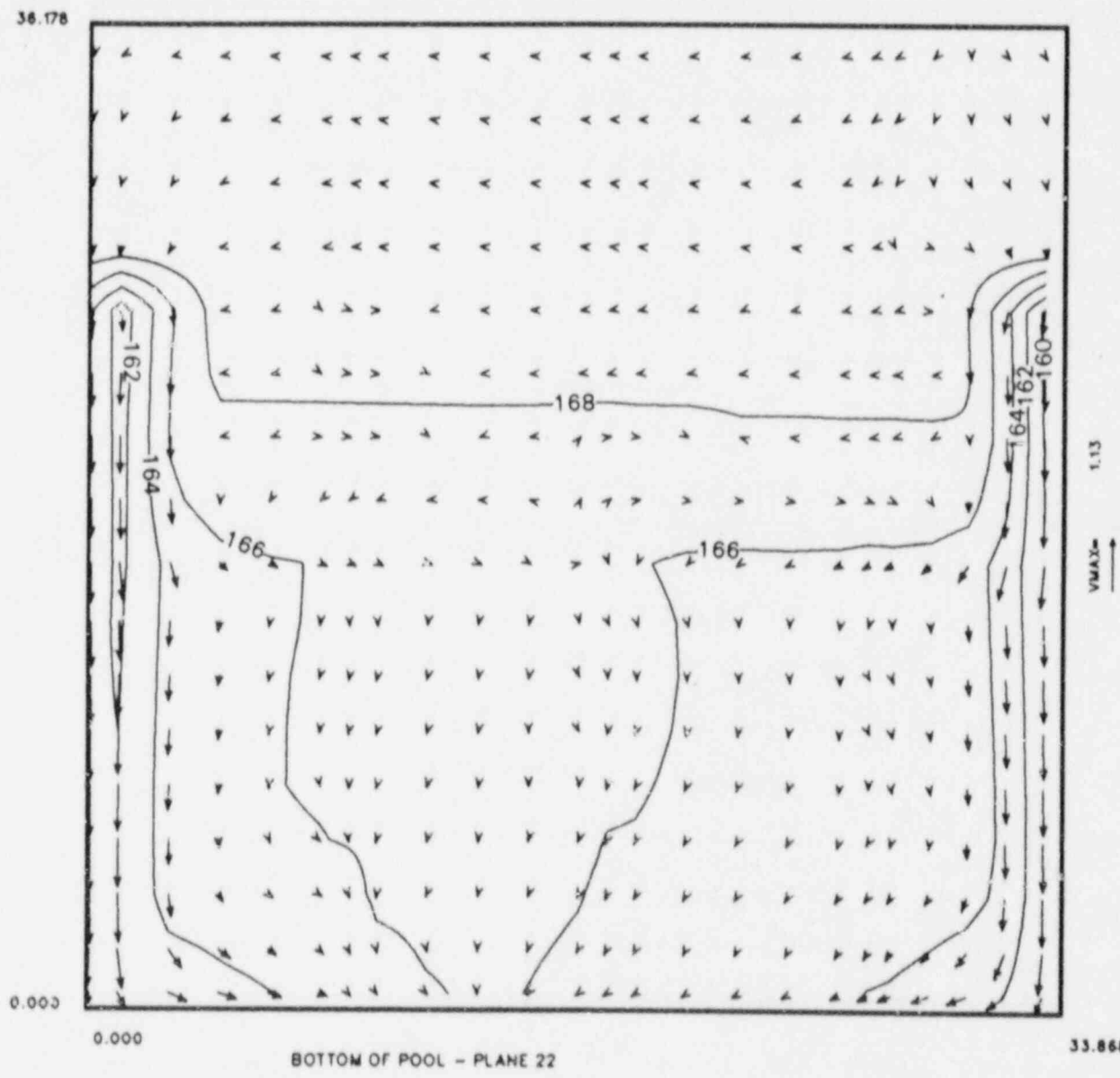


FIGURE 21. Temperature and Flow Distribution along the Back Wall of the Pool for Case Number 16. ($Q = 1048 \text{ GPM}$, $T_{INLET} = 150^\circ\text{F}$, $P_e/P_0 = 13.9$, inlet flow down, peak heat generation near edge of pool)

36.178

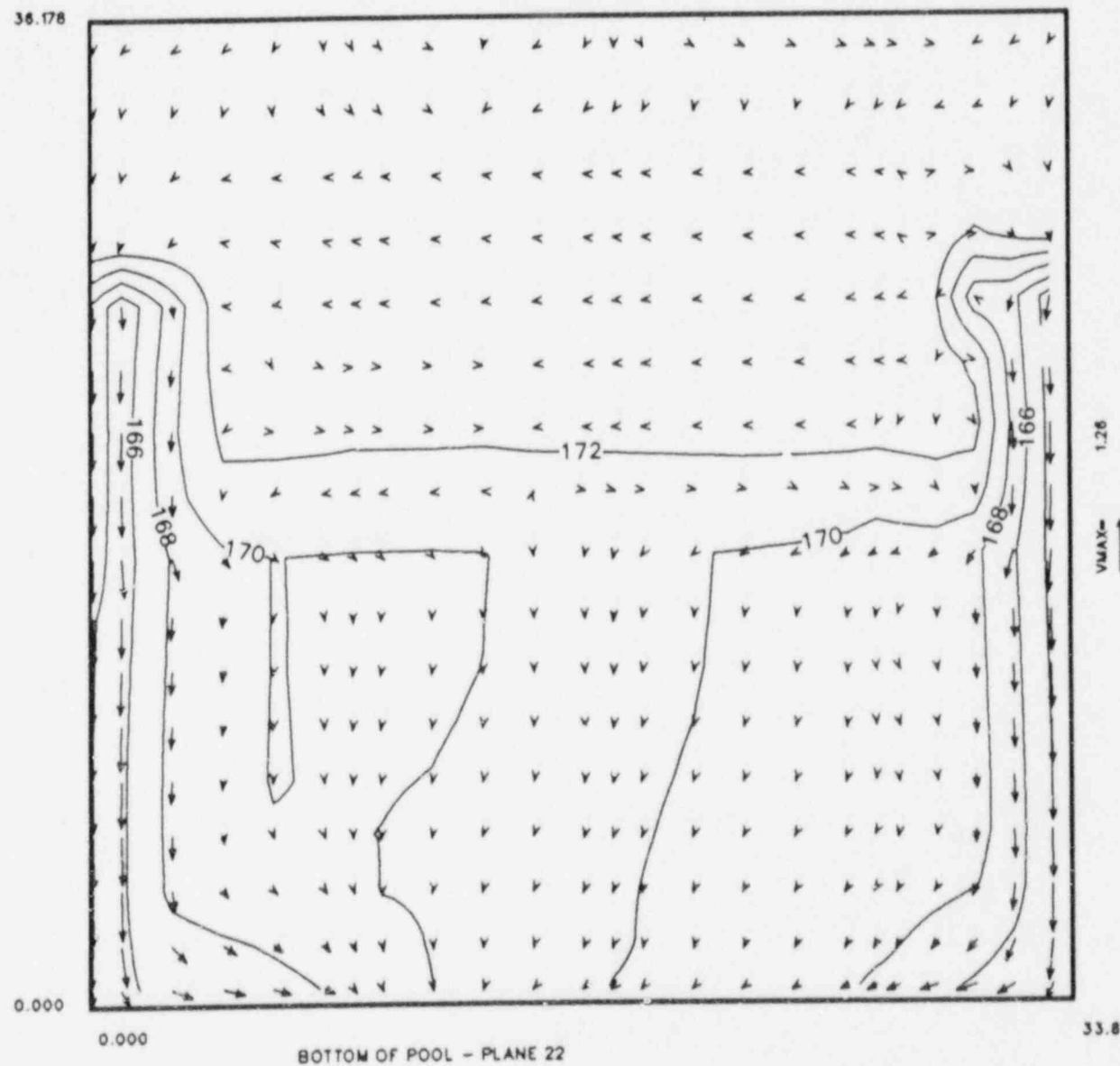


FIGURE 22. Temperature and Flow Distribution along the Back Wall of the Pool for Case Number 17. ($Q = 450 \text{ GPM}$, $T_{INLET} = 130^\circ\text{F}$, $P_L/P = 13.9$, inlet flow down, peak heat generation near center of pool)

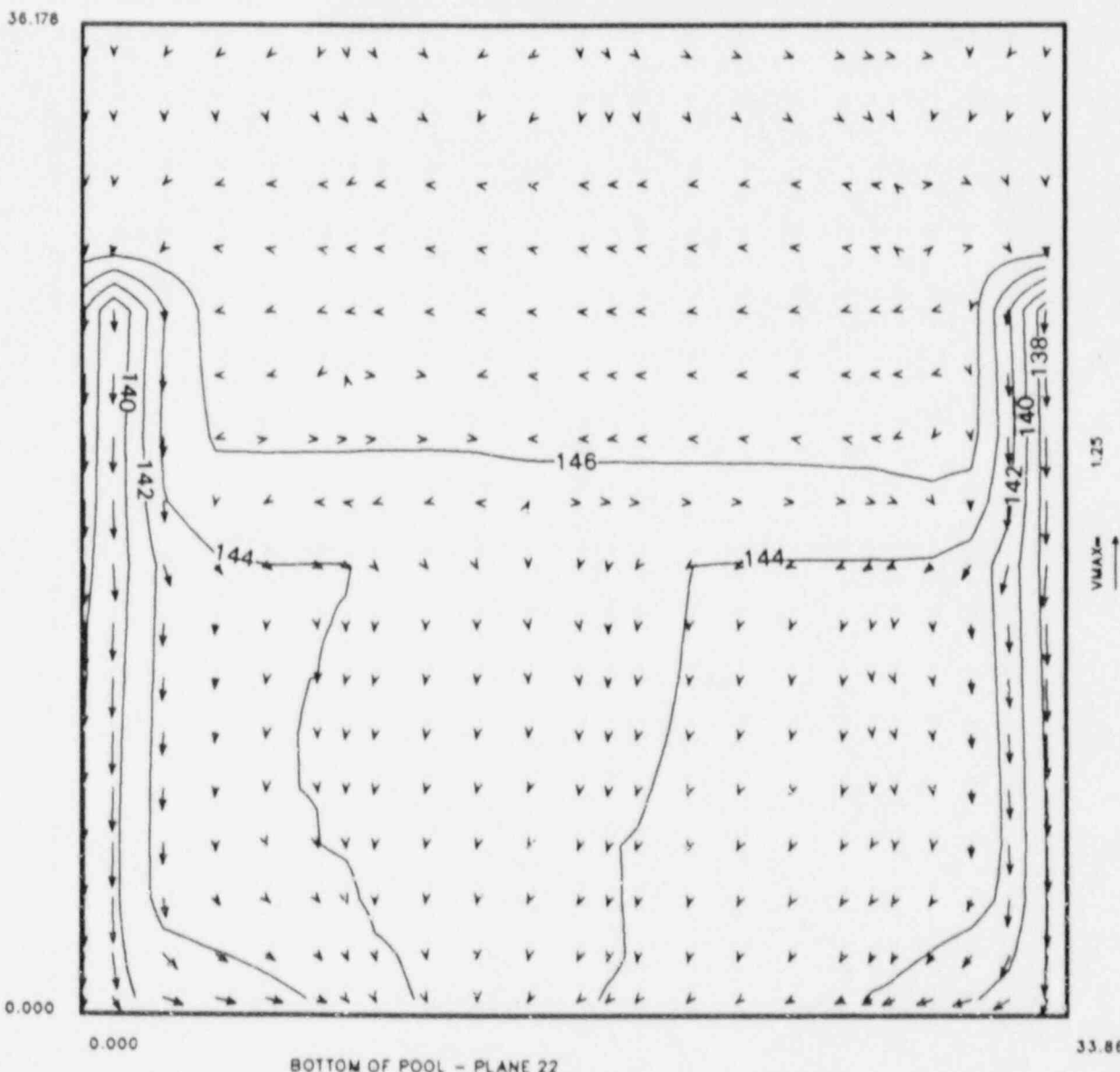


FIGURE 23. Temperature and Flow Distribution along the Back Wall of the Pool for Case Number 18. ($Q = 450 \text{ GPM}$, $T_{INLET} = 100^\circ\text{F}$, $P_L/P = 13.9$, inlet flow down, peak heat generation near center of pool)

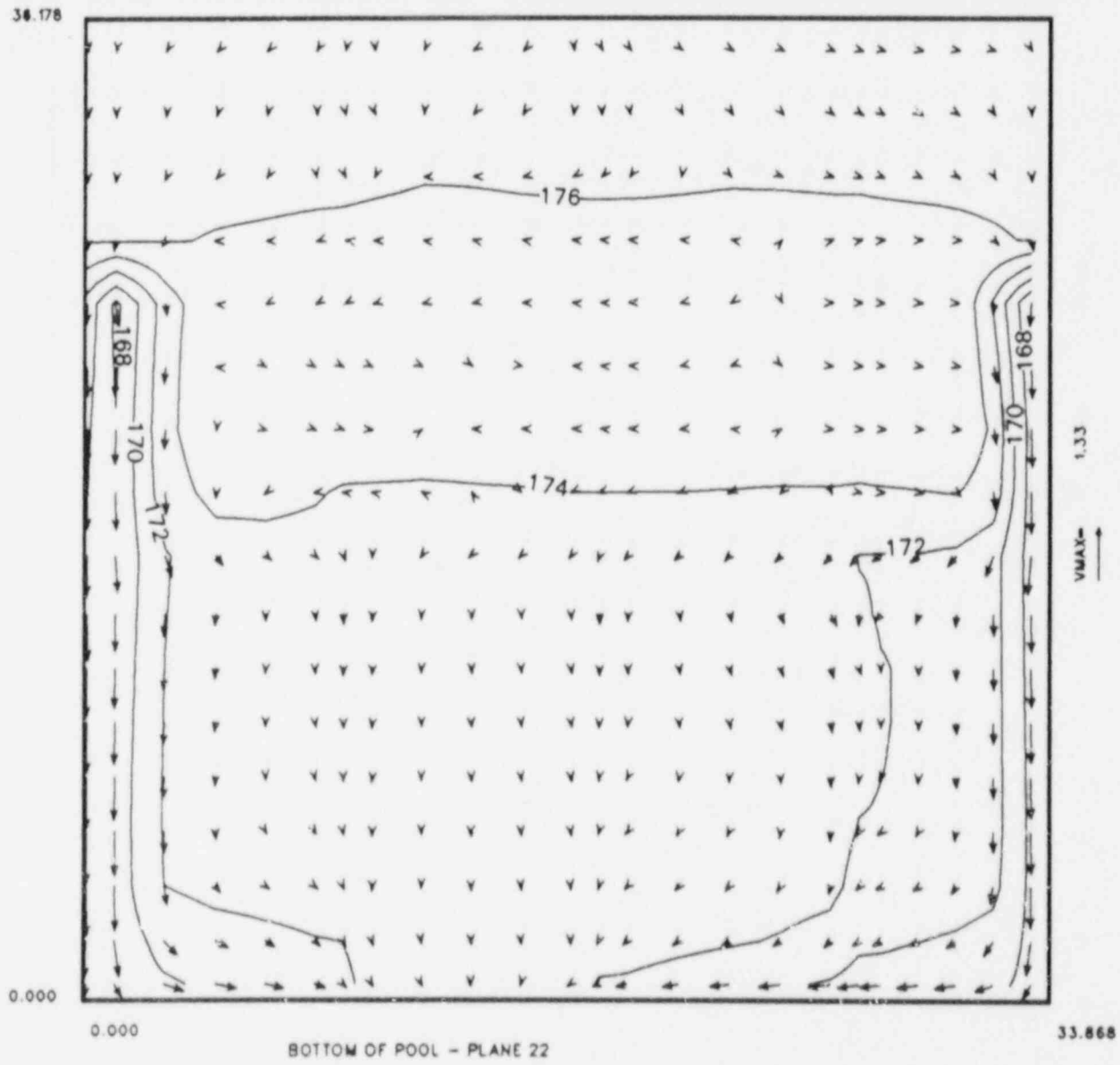


FIGURE 24. Temperature and Flow Distribution along the Back Wall of the Pool for Case Number 19. ($Q = 450 \text{ GPM}$, $\text{TINLET} = 130^\circ\text{F}$, $P_L/P = 13.9$, inlet flow down, peak heat generation near center of pool, large open flow region of cask area removed from model)

36.178

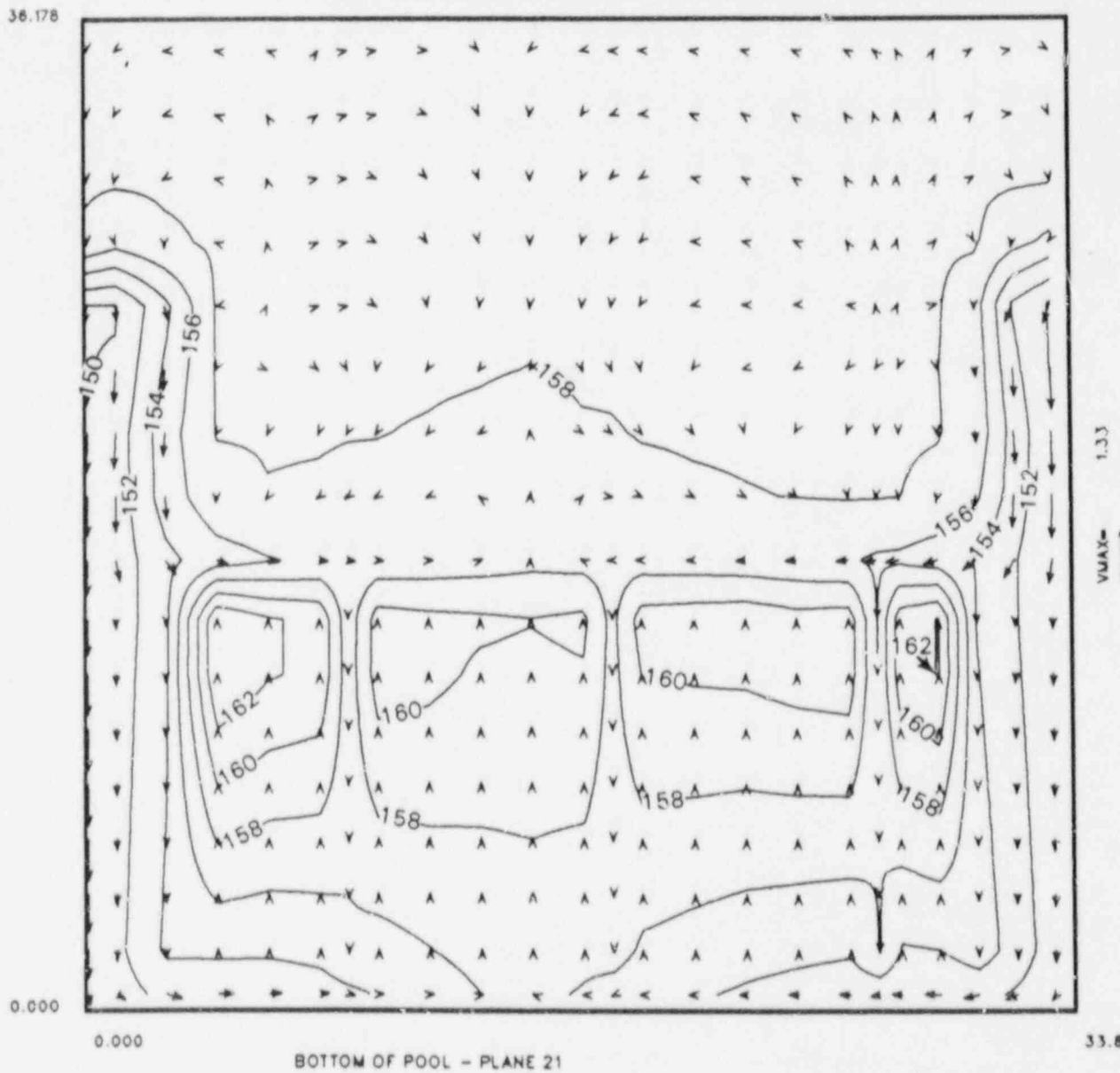


FIGURE 25. Temperature and Flow Distribution in Bundles next to the Back Wall of the Pool for Case Number 5. ($Q = 4187 \text{ GPM}$, TINLET = 150°F , $P_t/\bar{P} = 1.4$, inlet flow down, peak heat generation near center of pool)

36.178

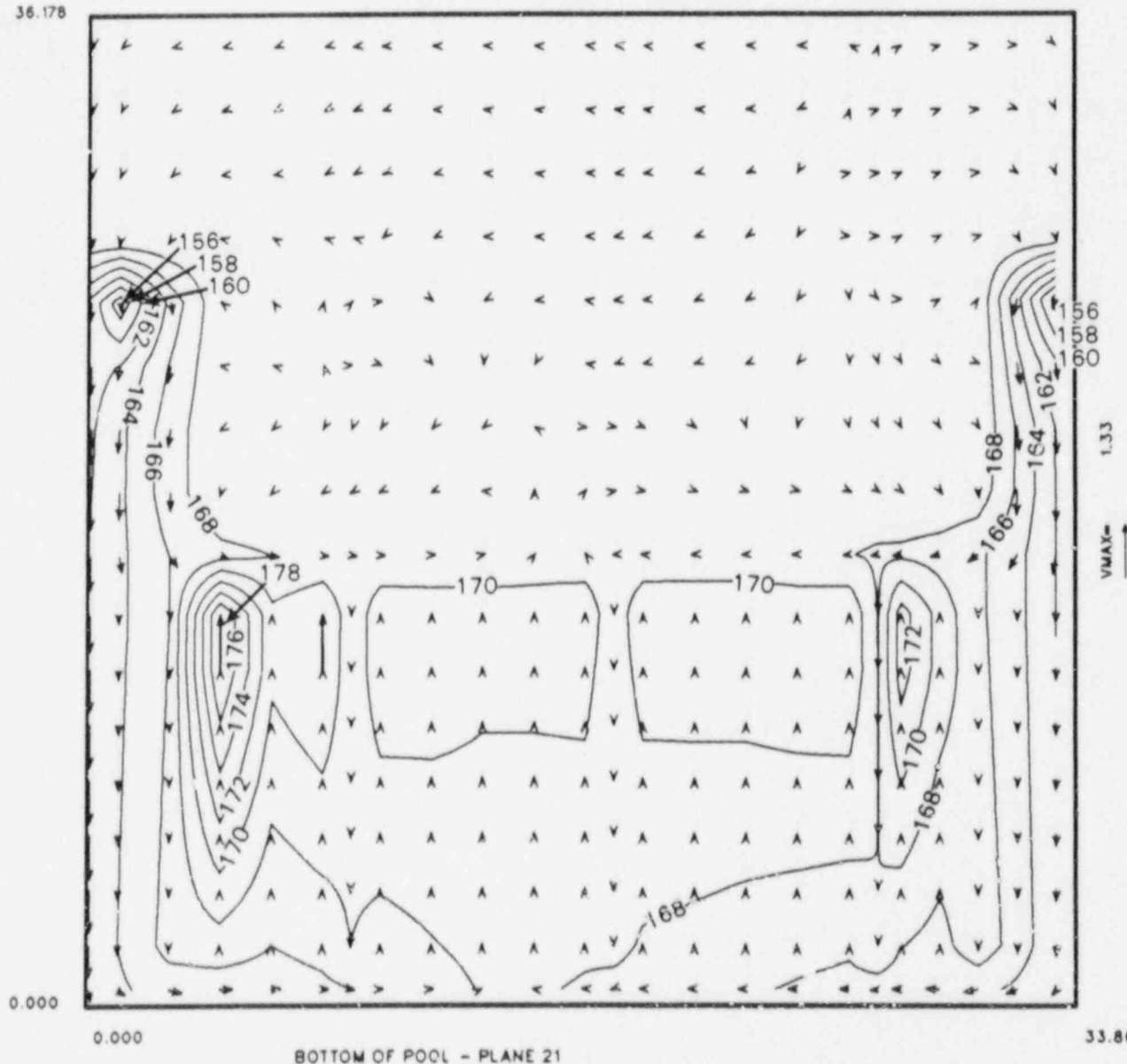


FIGURE 26. Temperature and Flow Distribution in Bundles next to the Back Wall of the Pool for Case Number 9. ($Q = 1048$ GPM, TINLET = 150°F , $P_t/P = 1.4$, inlet flow down, peak heat generation near center of pool)

36.178

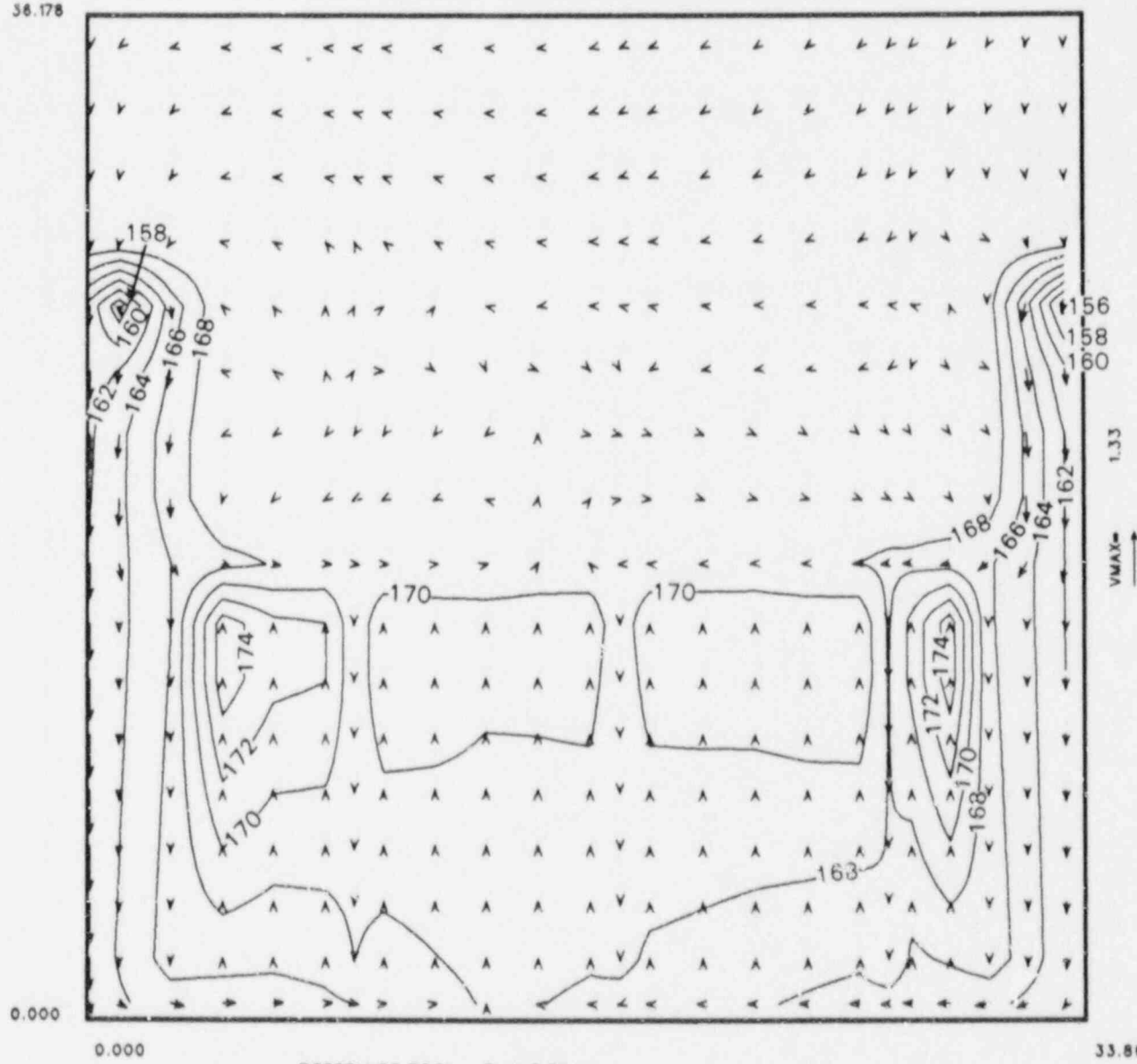


FIGURE 27. Temperature and Flow Distribution in Bundles next to the Back Wall of the Pool for Case Number 11. ($Q = 1048 \text{ GPM}$, $T_{INLET} = 150^\circ\text{F}$, $P_L/P = 1.4$, inlet flow down, peak heat generation under inlet)

36.178

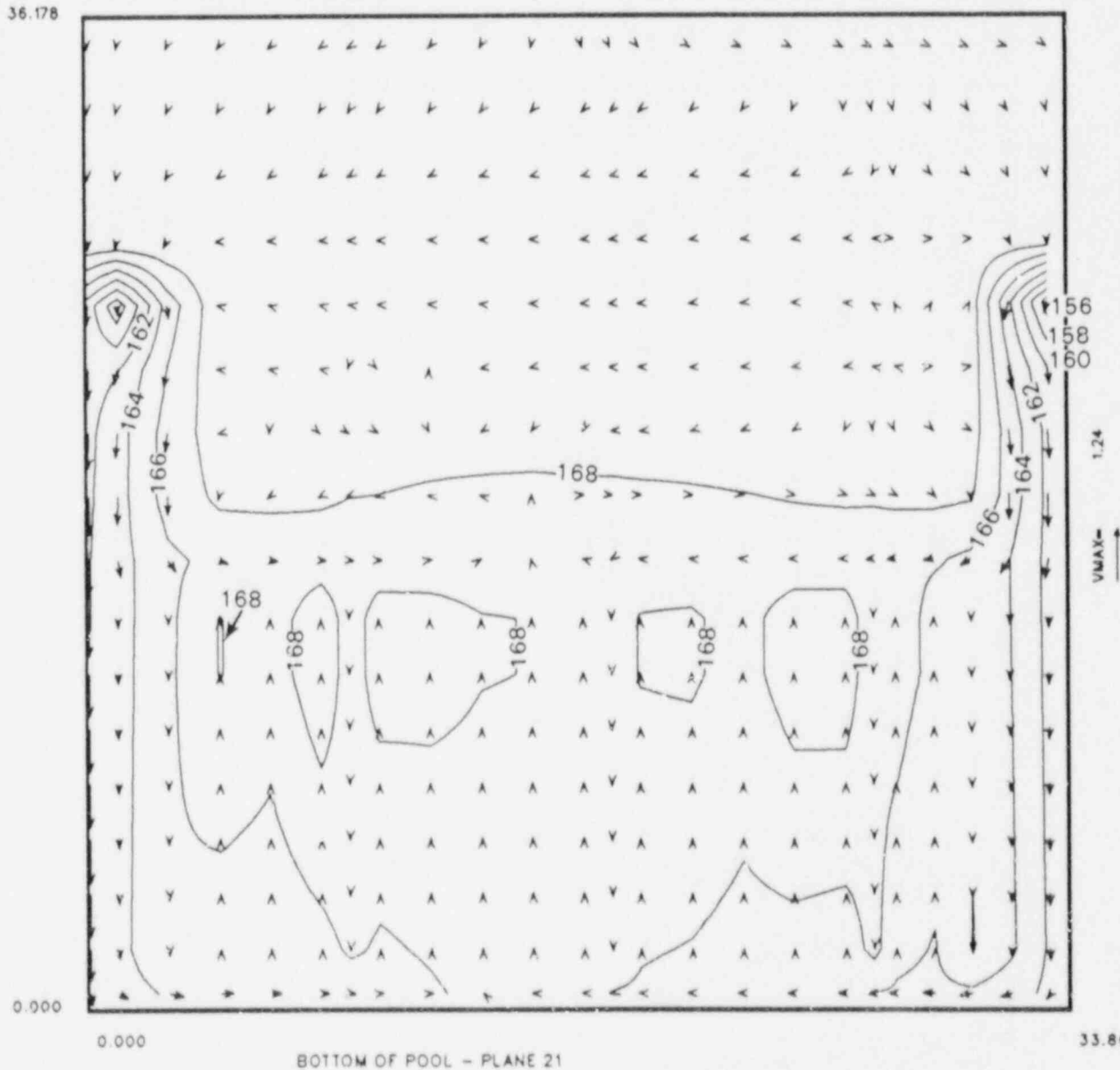


FIGURE 28. Temperature and Flow Distribution in Bundles next to the Back Wall of the Pool for Case Number 12. ($Q = 1048 \text{ GPM}$, $T_{INLET} = 150^\circ\text{F}$, $P_i/P = 13.9$, inlet flow down, peak heat generation near center of pool)

36.178

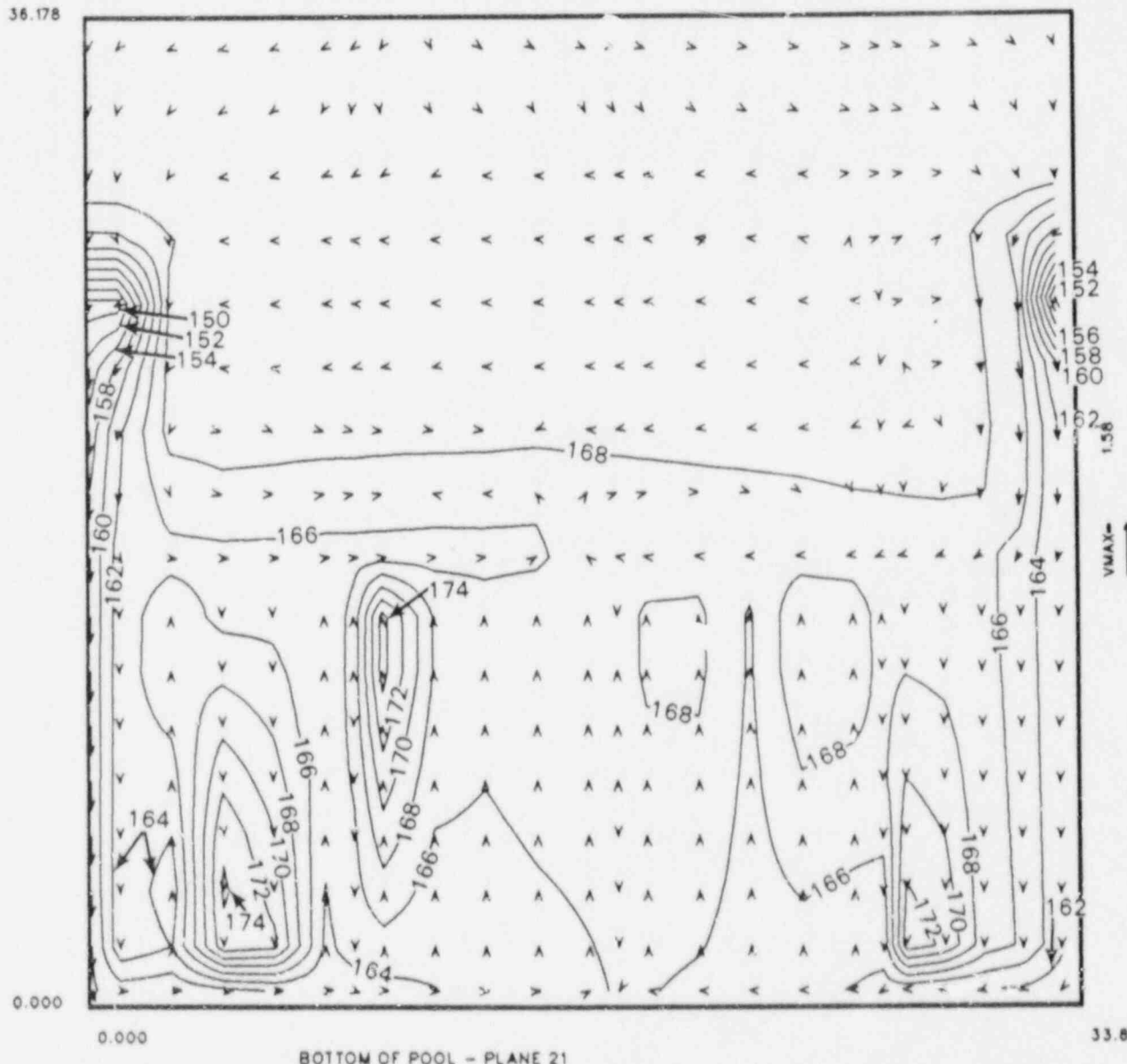


FIGURE 29. Temperature and Flow Distribution in Bundles next to the Back Wall of the Pool for Case Number 14. ($Q = 1048 \text{ GPM}$, $T_{INLET} = 150^\circ\text{F}$, $P_i/P = 13.9$, inlet flow horizontal, peak heat generation near center of pool)

36.178

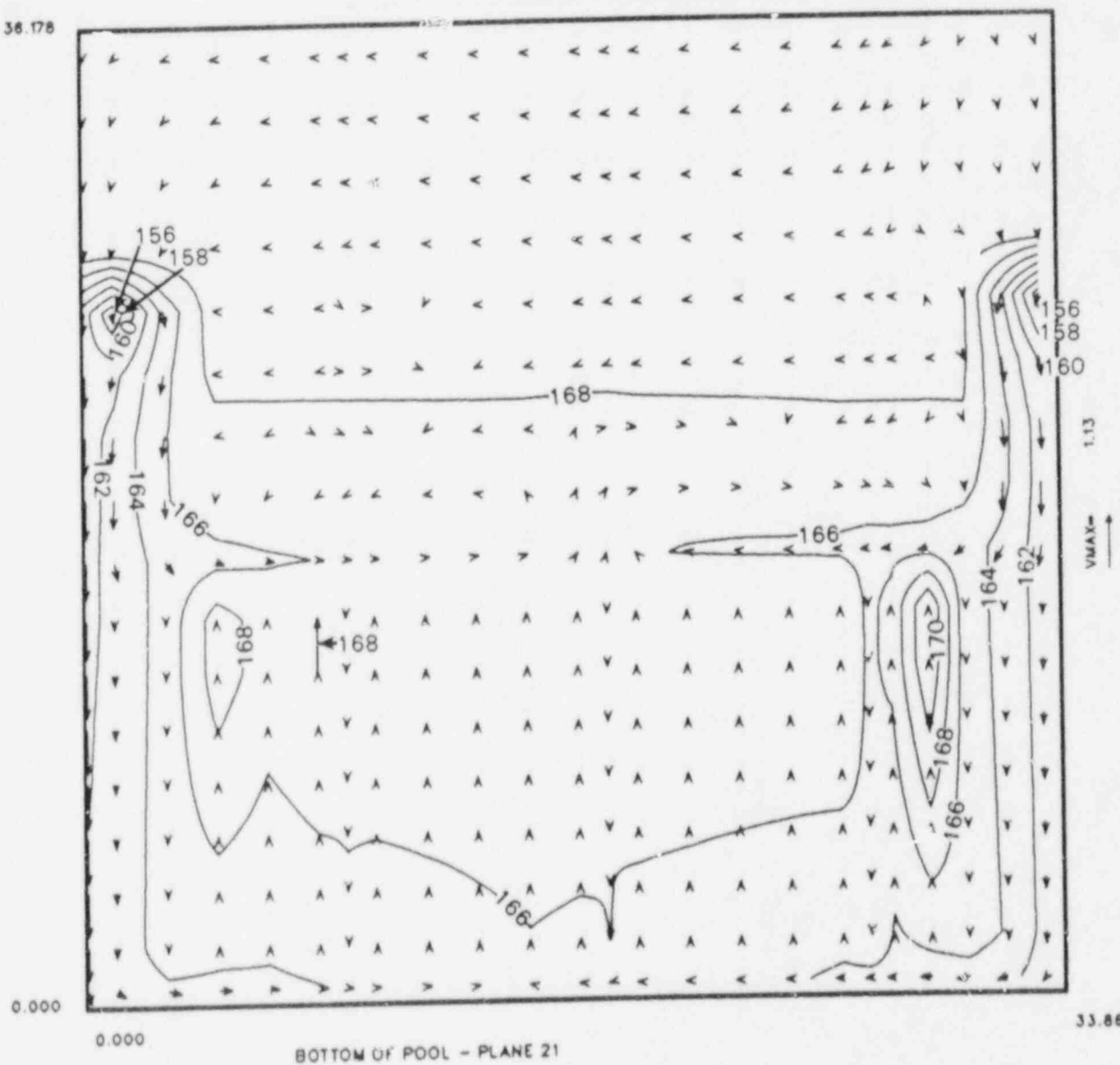


FIGURE 30. Temperature and Flow Distribution in Bundles next to the Back Wall of the Pool for Case Number 16. ($Q = 1048 \text{ GPM}$, $T_{INLET} = 150^\circ\text{F}$, $P/\bar{P} = 13.9$, inlet flow down, peak heat generation near edge of pool)

36.178

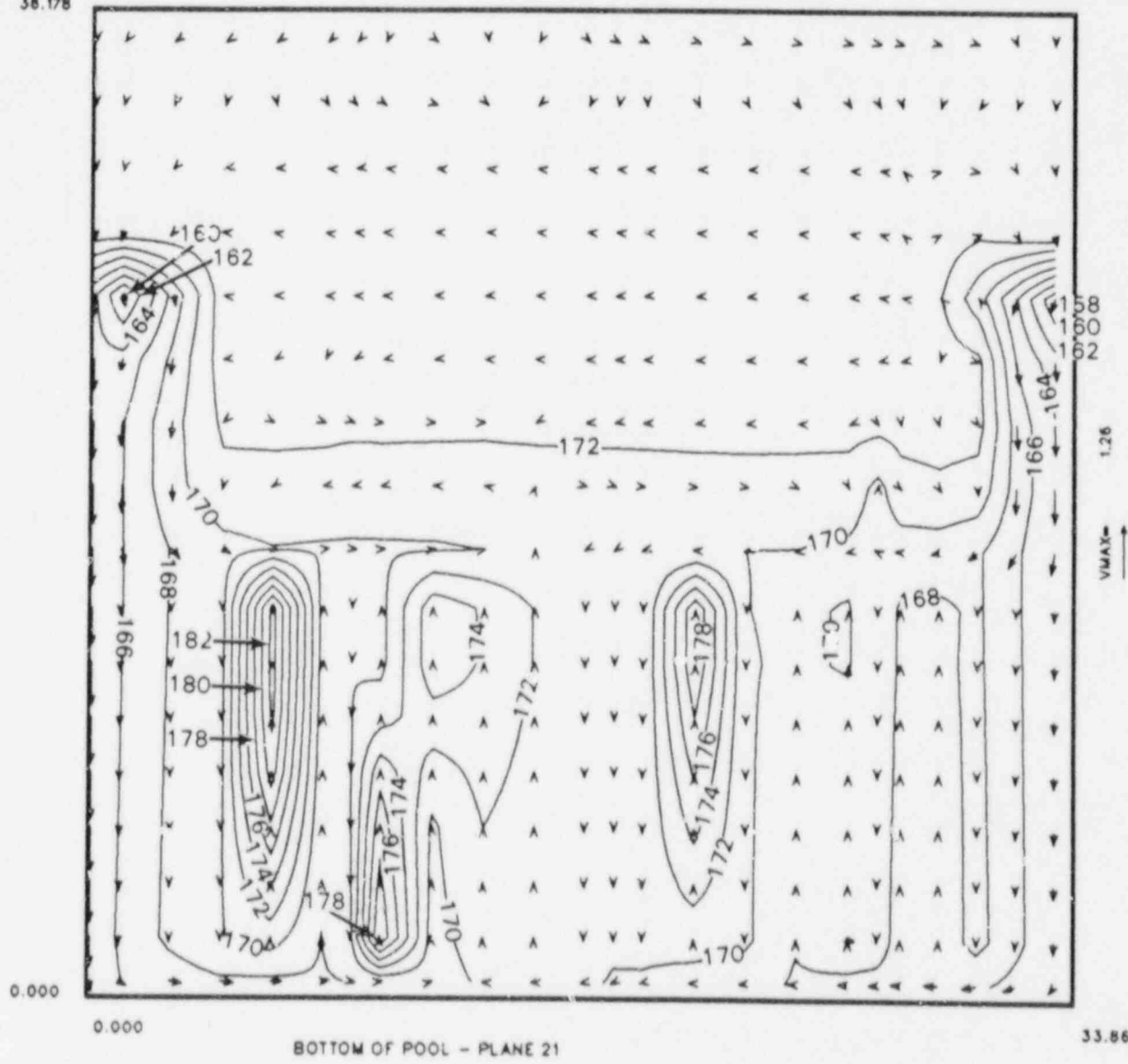


FIGURE 31. Temperature and Flow Distribution in Bundles next to the Back Wall of the Pool for Case Number 17. ($Q = 450 \text{ GPM}$, TINLET = 130°F , $P_t/P = 13.9$, inlet flow down, peak heat generation near center of pool)

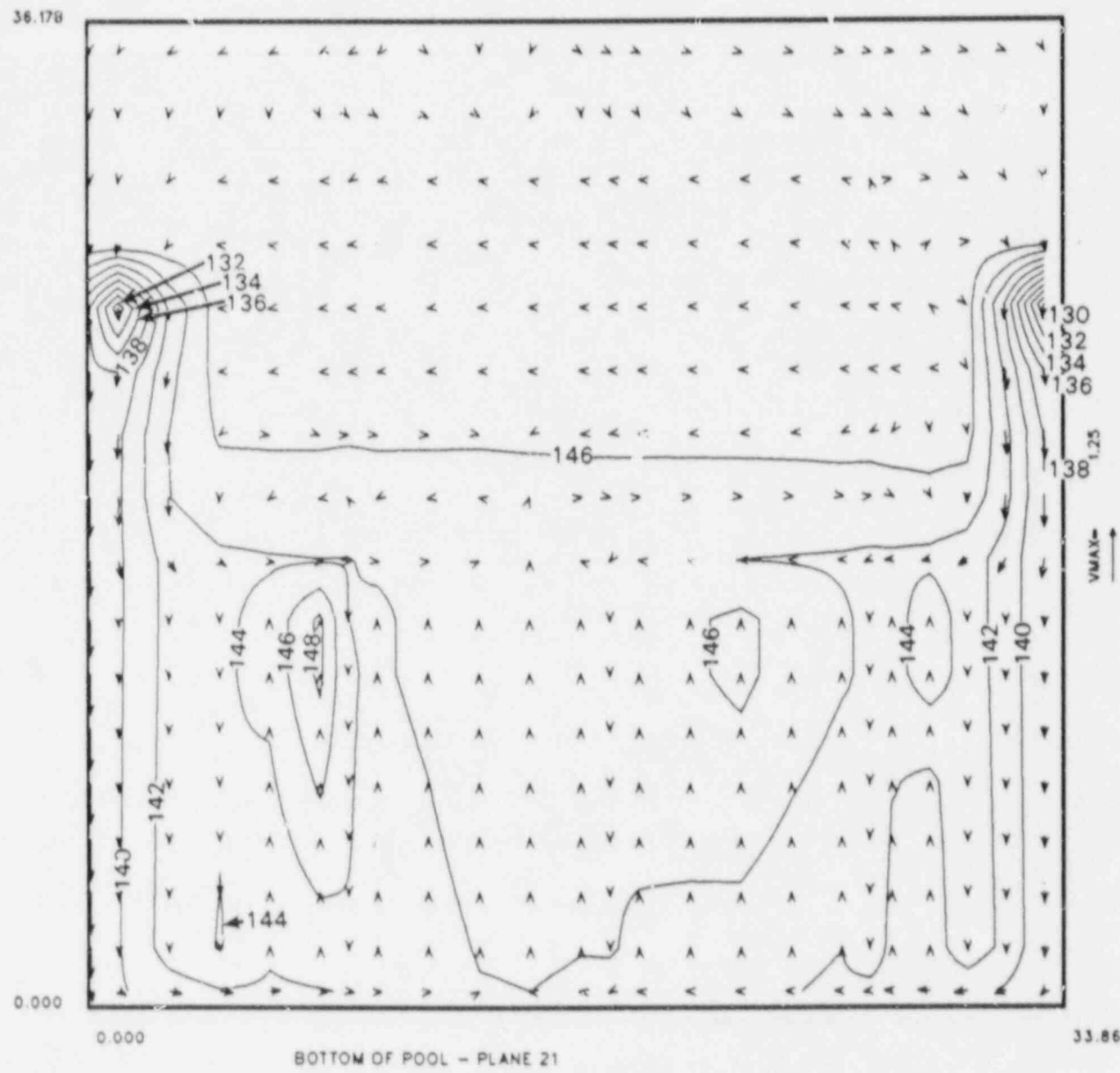


FIGURE 32. Temperature and Flow Distribution in Bundles next to the Back Wall of the Pool for Case Number 18. ($Q = 450 \text{ GPM}$, TINLET = 100°F , $P_t/P = 13.9$, inlet flow down, peak heat generation near center of pool)

36.178

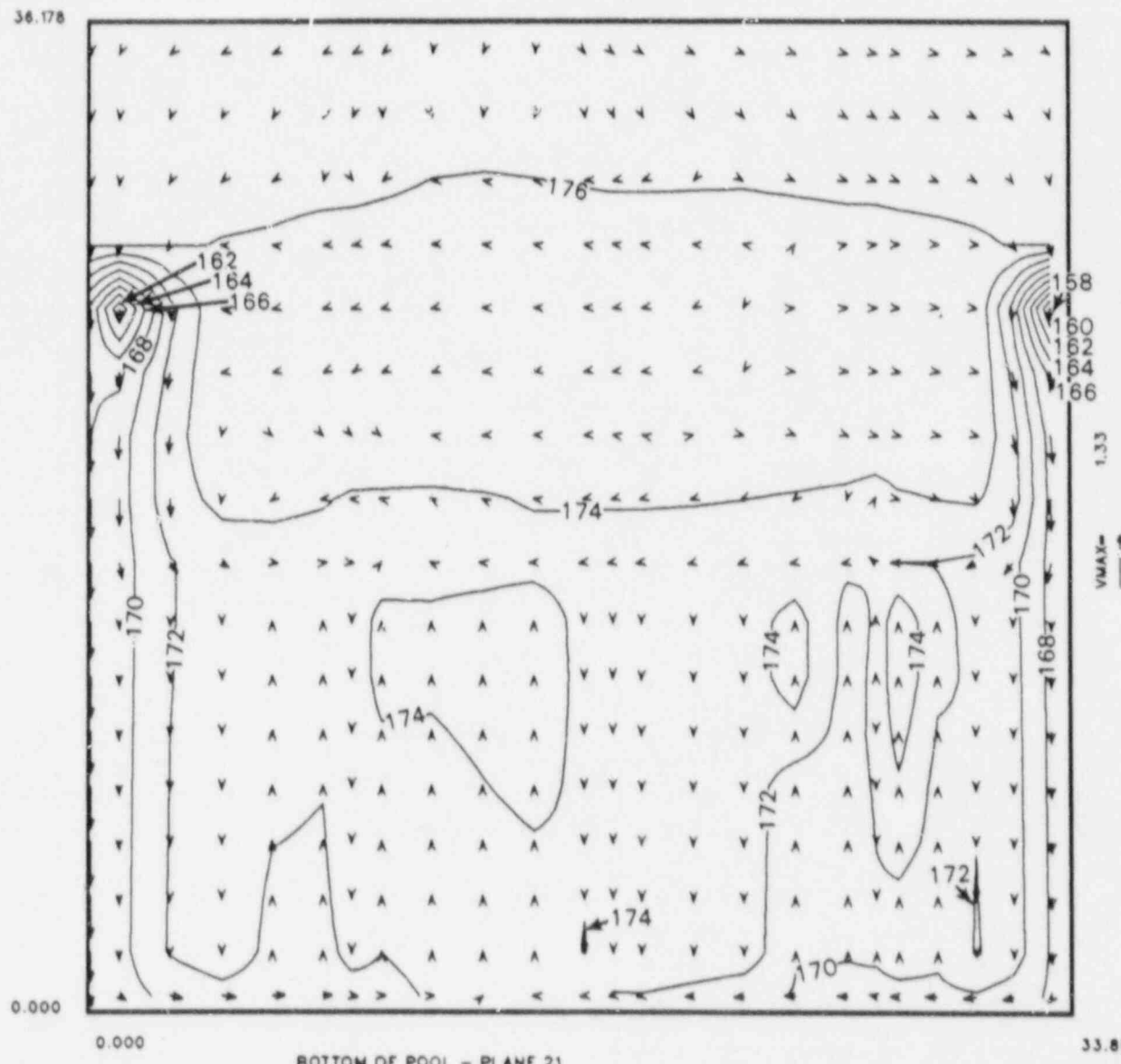


FIGURE 33. Temperature and Flow Distribution in Bundles next to the Back Wall of the Pool for Case Number 19. ($Q = 450 \text{ GPM}$, $T_{INLET} = 130^\circ\text{F}$, $P_t/P = 13.9$, inlet flow down, peak heat generation near center of pool, large open flow region of cask area removed from model)

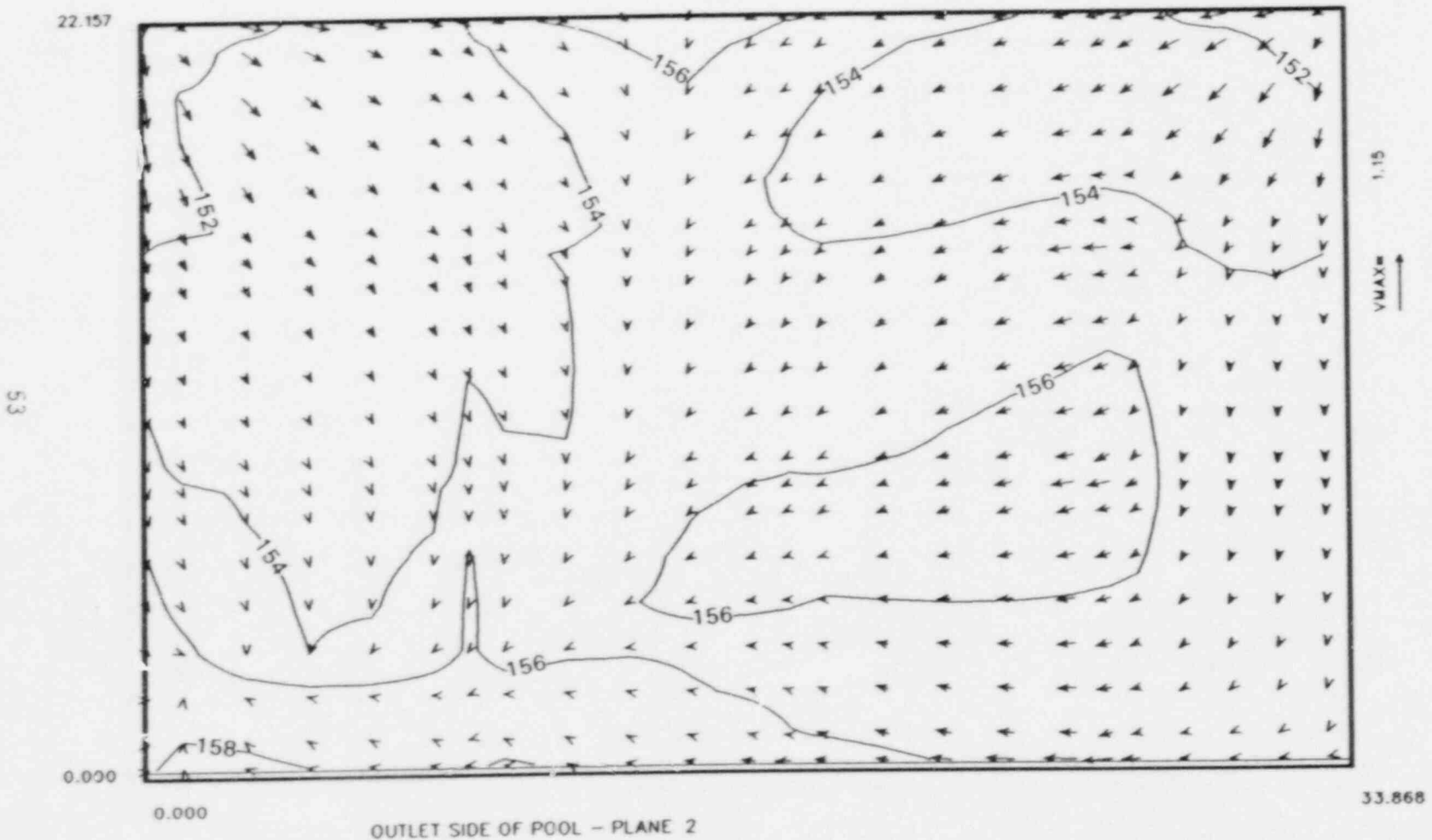


FIGURE 34. Temperature and Flow Distribution below the Fuel Bundles for Case Number 5. ($Q = 4187 \text{ GPM}$,
 $T_{INLET} = 150^\circ\text{F}$, $P_L/\bar{P} = 1.4$, inlet flow down, peak heat generation near center of pool)

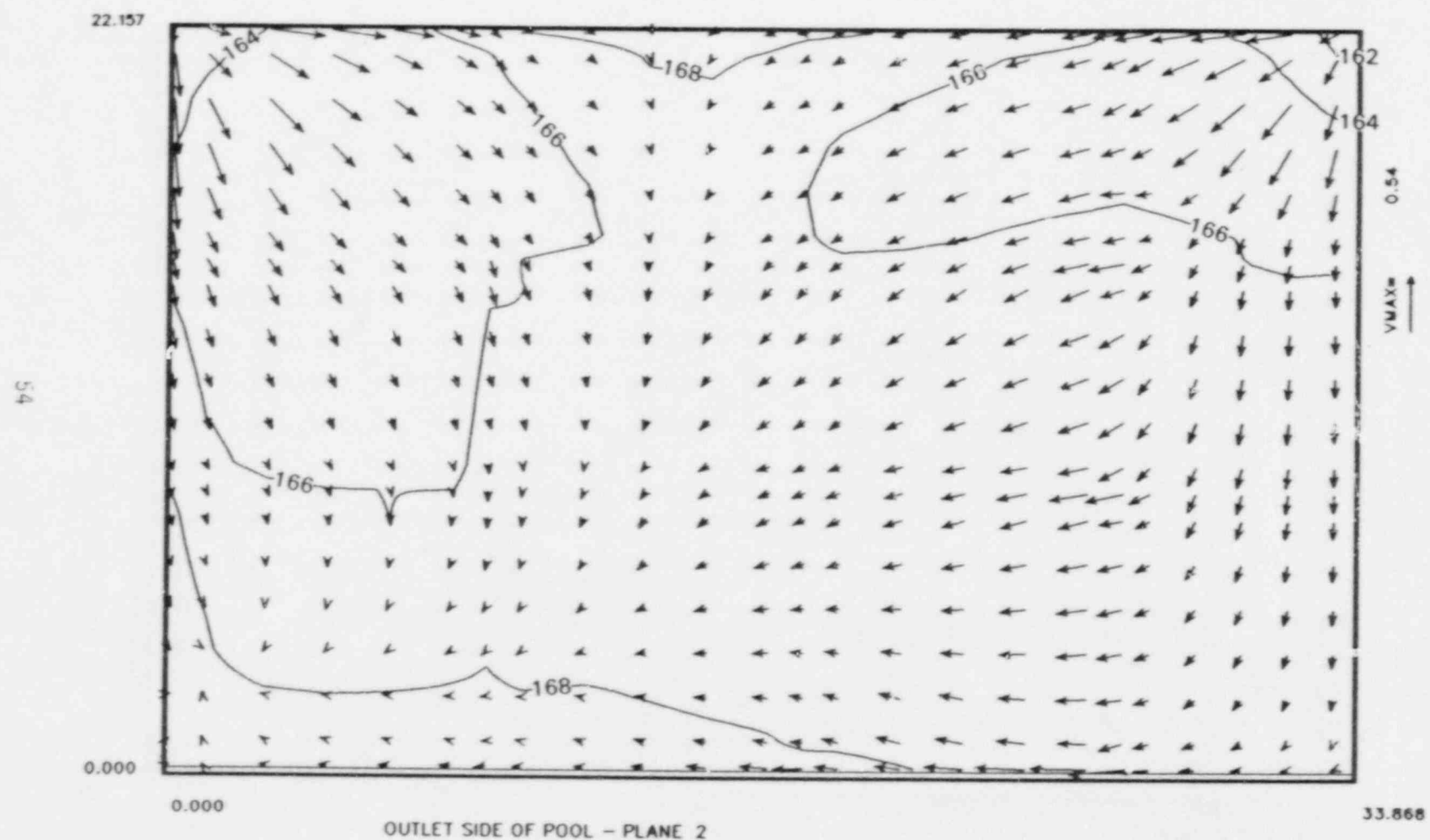


FIGURE 35. Temperature and Flow Distribution below the Fuel Bundles for Case Number 9. ($Q = 1048 \text{ GPM}$, $T_{INLET} = 150^\circ\text{F}$, $P_L/P = 1.4$, inlet flow down, peak heat generation near center of pool)

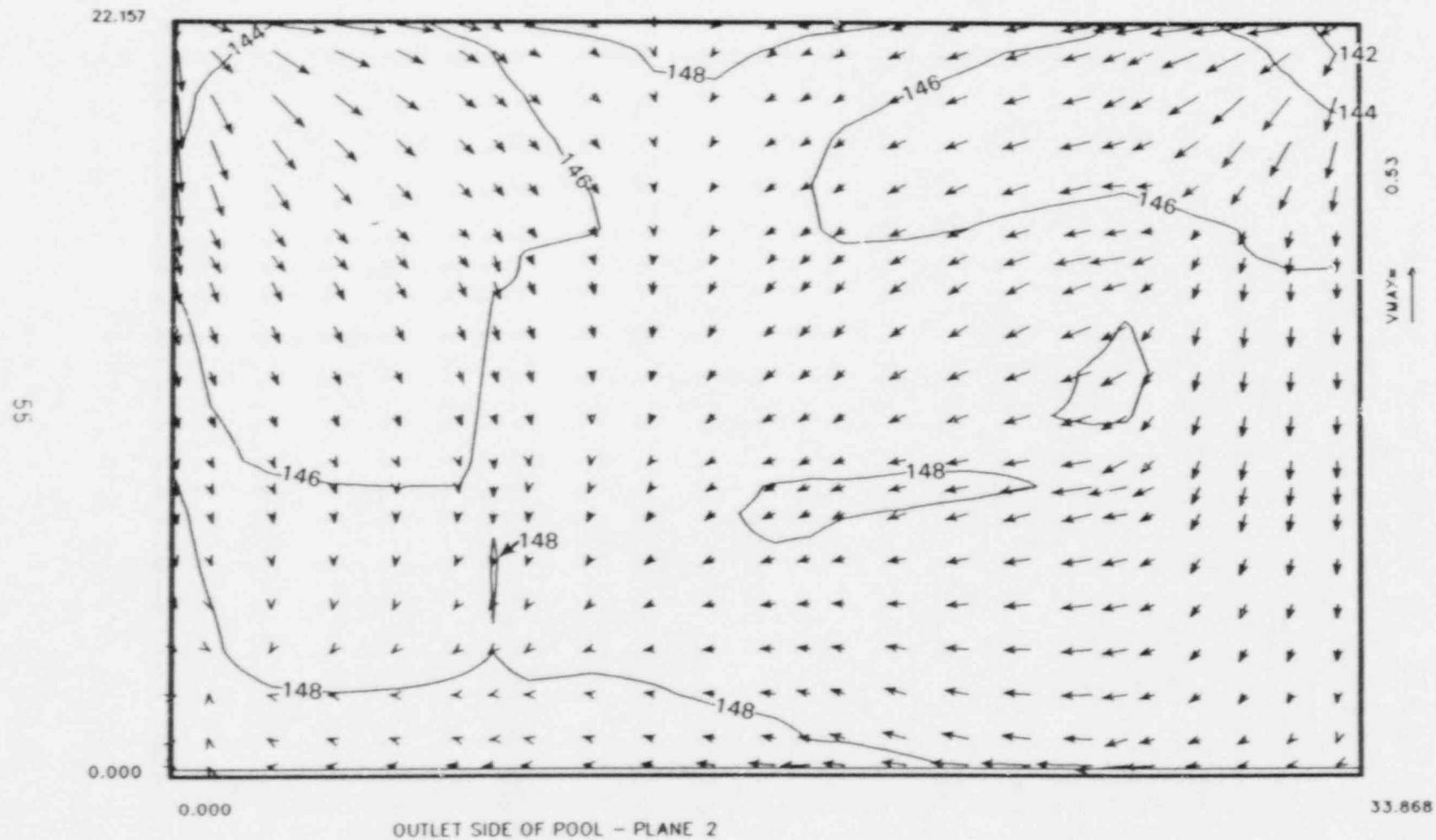


FIGURE 36. Temperature and Flow Distribution below the Fuel Bundles for Case Number 10. ($Q = 1048 \text{ GPM}$, $T_{INLET} = 130^\circ\text{F}$, $P_L/P = 1.4$, inlet flow down, peak heat generation near center of pool)

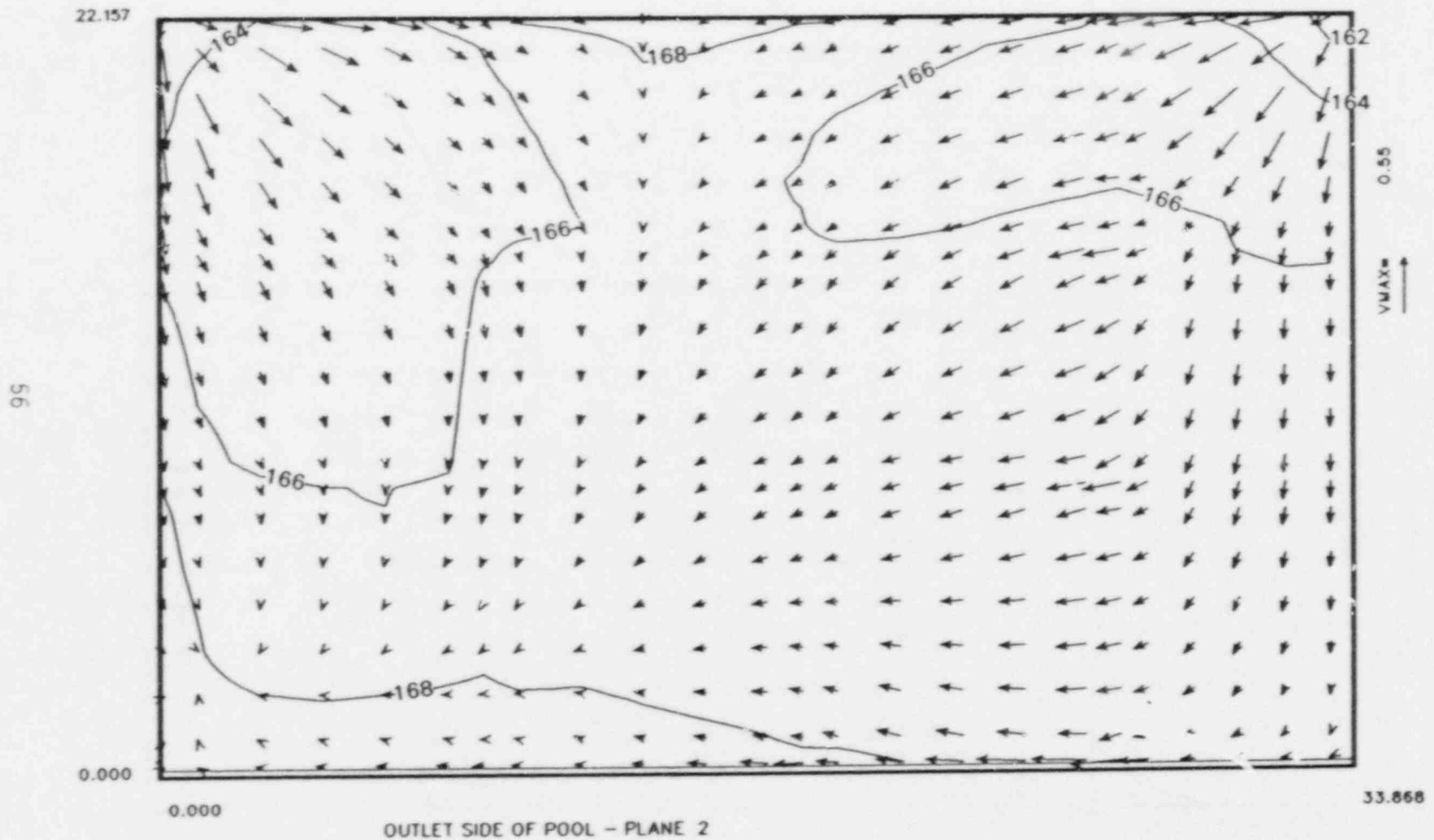


FIGURE 37. Temperature and Flow Distribution below the Fuel Bundles for Case Number 11. ($Q = 1048 \text{ GPM}$, $T_{INLET} = 150^\circ\text{F}$, $P_L/P = 1.4$, inlet flow down, peak heat generation under inlet)

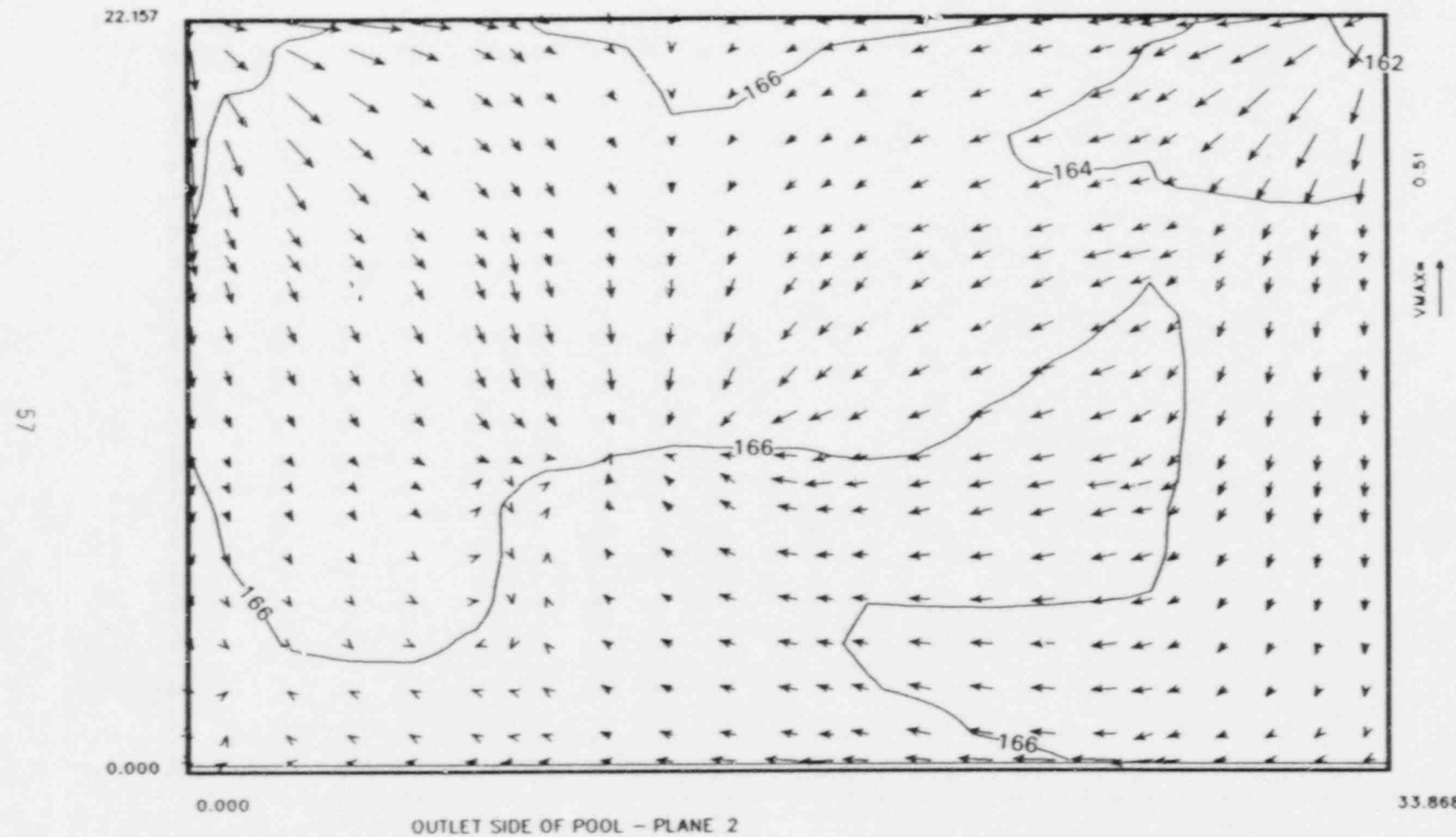


FIGURE 38. Temperature and Flow Distribution below the Fuel Bundles for Case Number 12. ($Q = 1048 \text{ GPM}$, $T_{INLET} = 150^\circ\text{F}$, $P_L/P = 13.9$, inlet flow down, peak heat generation near center of pool)

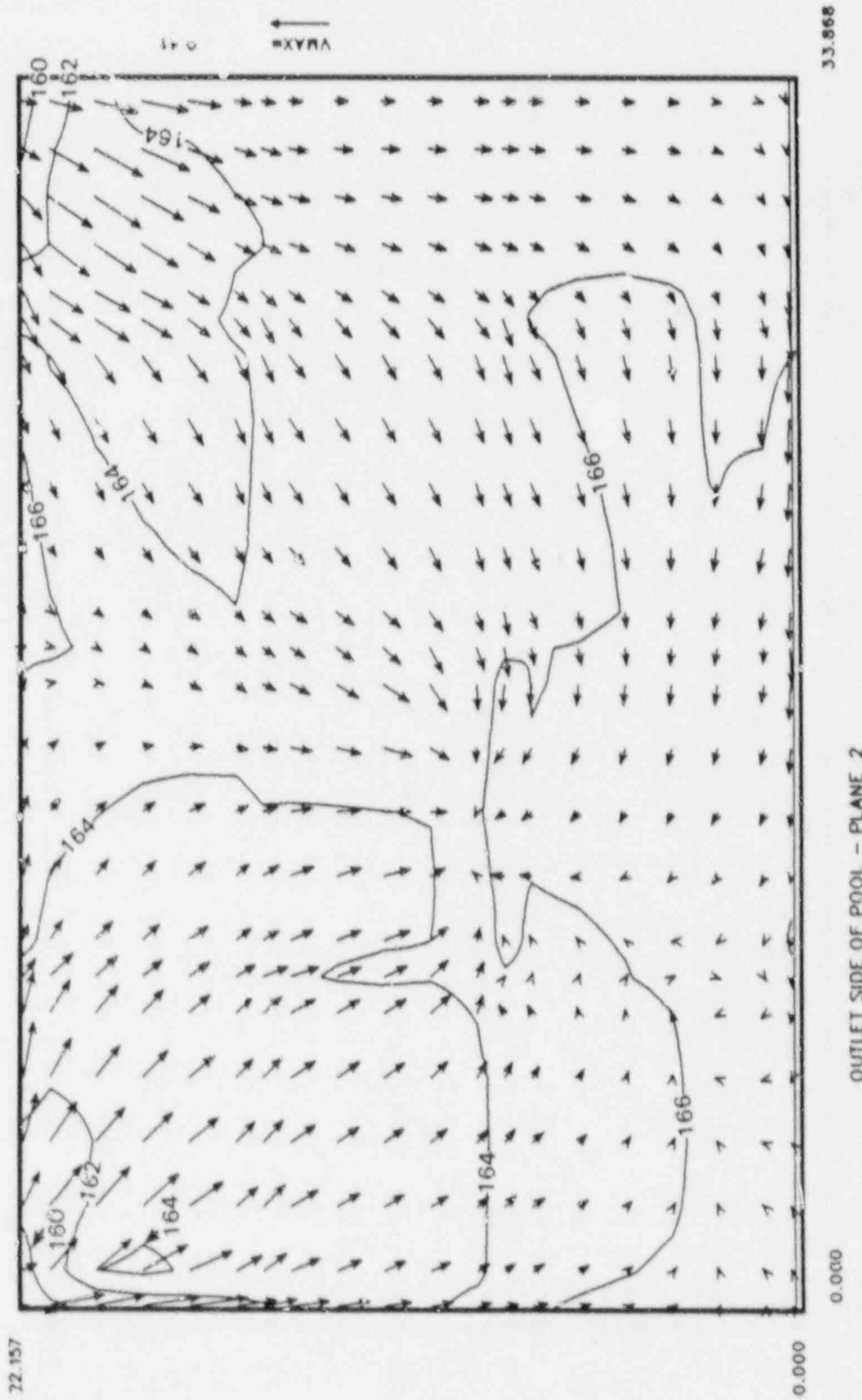


FIGURE 39. Temperature and Flow Distribution below the Fuel Bundles for Case Number 14. ($Q = 1048 \text{ GPM}$, $T_{INLET} = 150^\circ\text{F}$, $P_L/P = 13.9$, inlet flow horizontal, peak heat generation near center of pool)

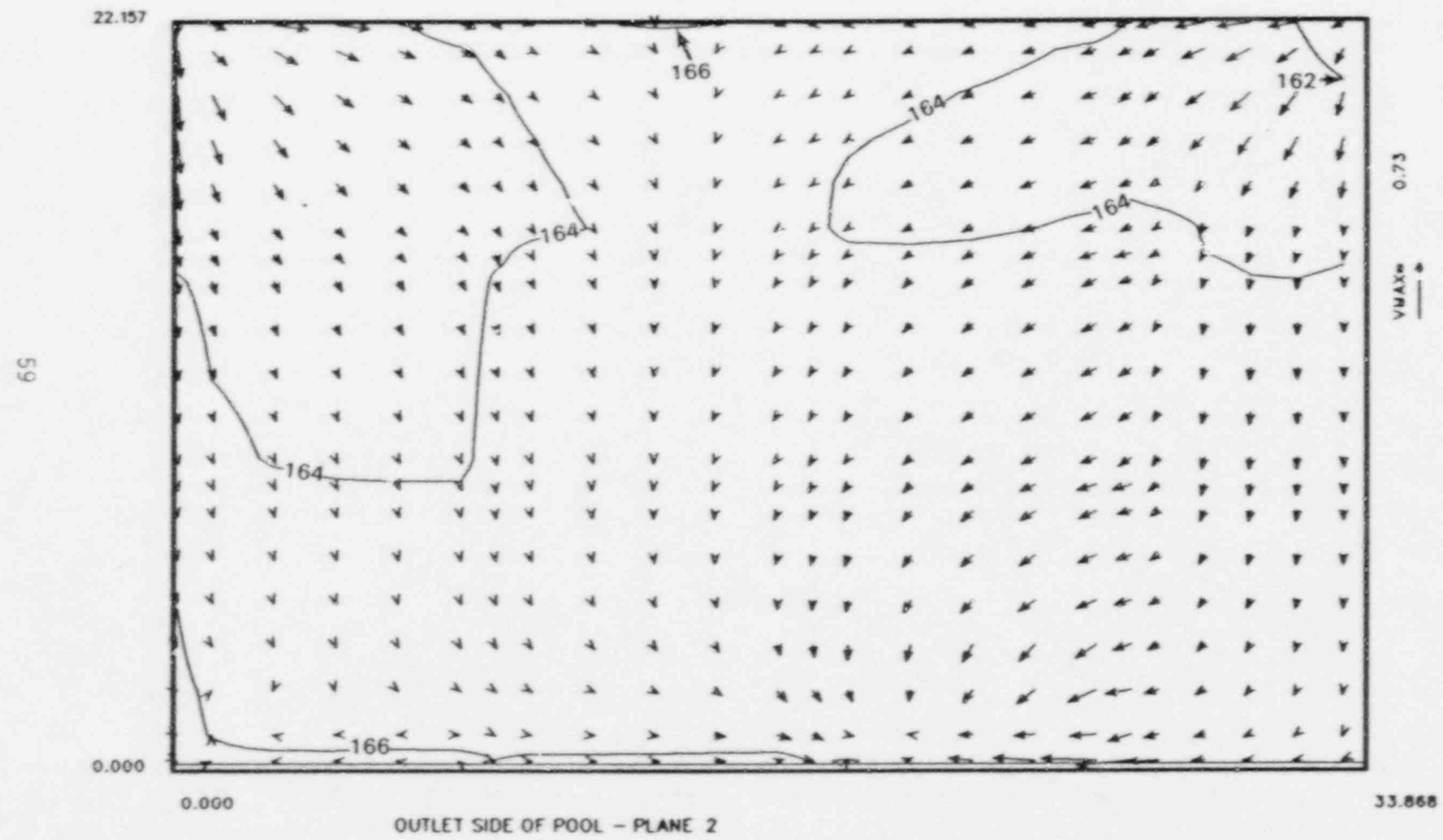


FIGURE 40. Temperature and Flow Distribution below the Fuel Bundles for Case Number 16. ($Q = 1048 \text{ GPM}$, $T_{INLET} = 150^\circ\text{F}$, $P_L/P = 13.9$, inlet flow down, peak heat generation near edge of pool)

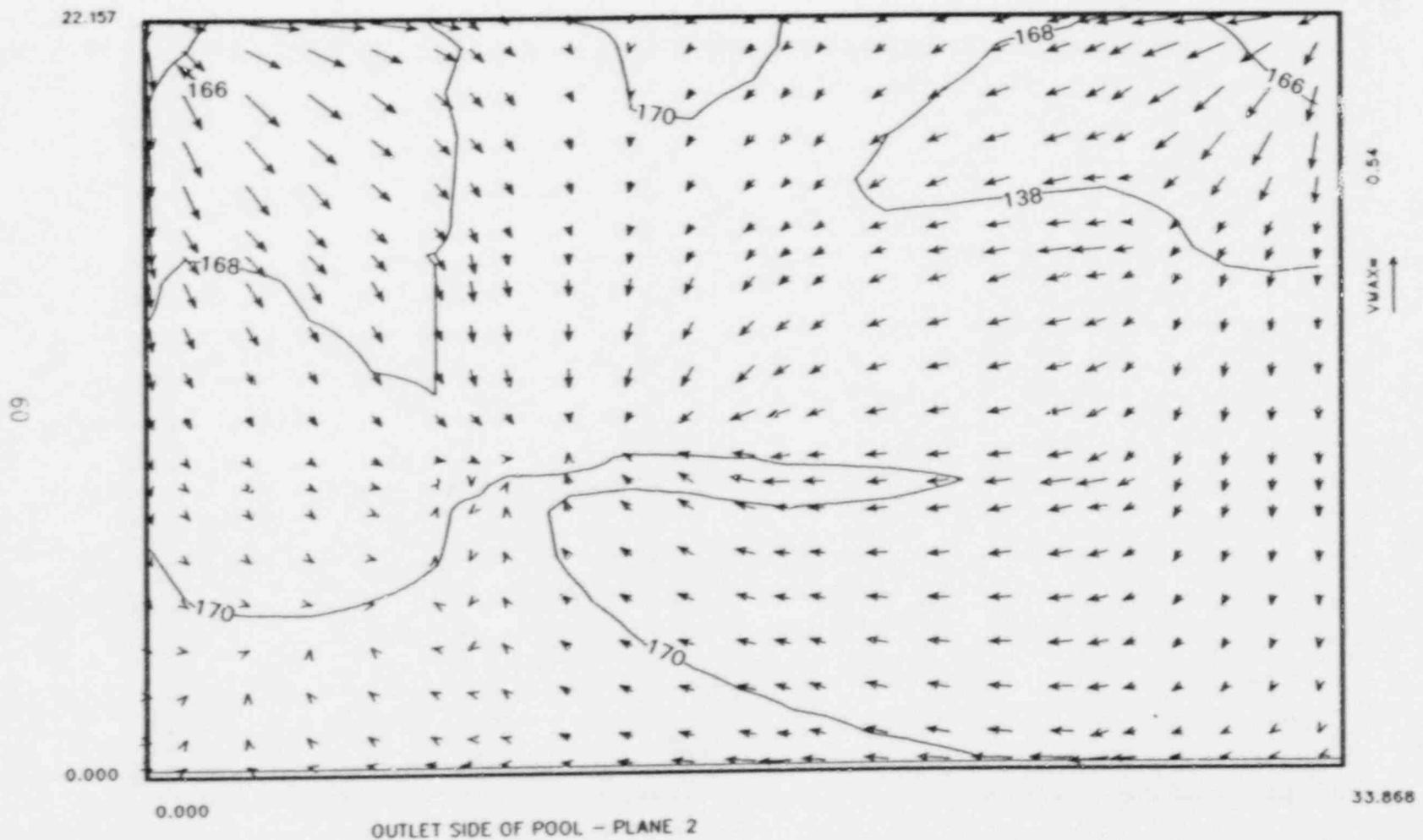


FIGURE 41. Temperature and Flow Distribution below the Fuel Bundles for Case Number 17. ($Q = 450 \text{ GPM}$, TINLET = 130°F , $P_L/P = 13.9$, inlet flow down, peak heat generation near center of pool)

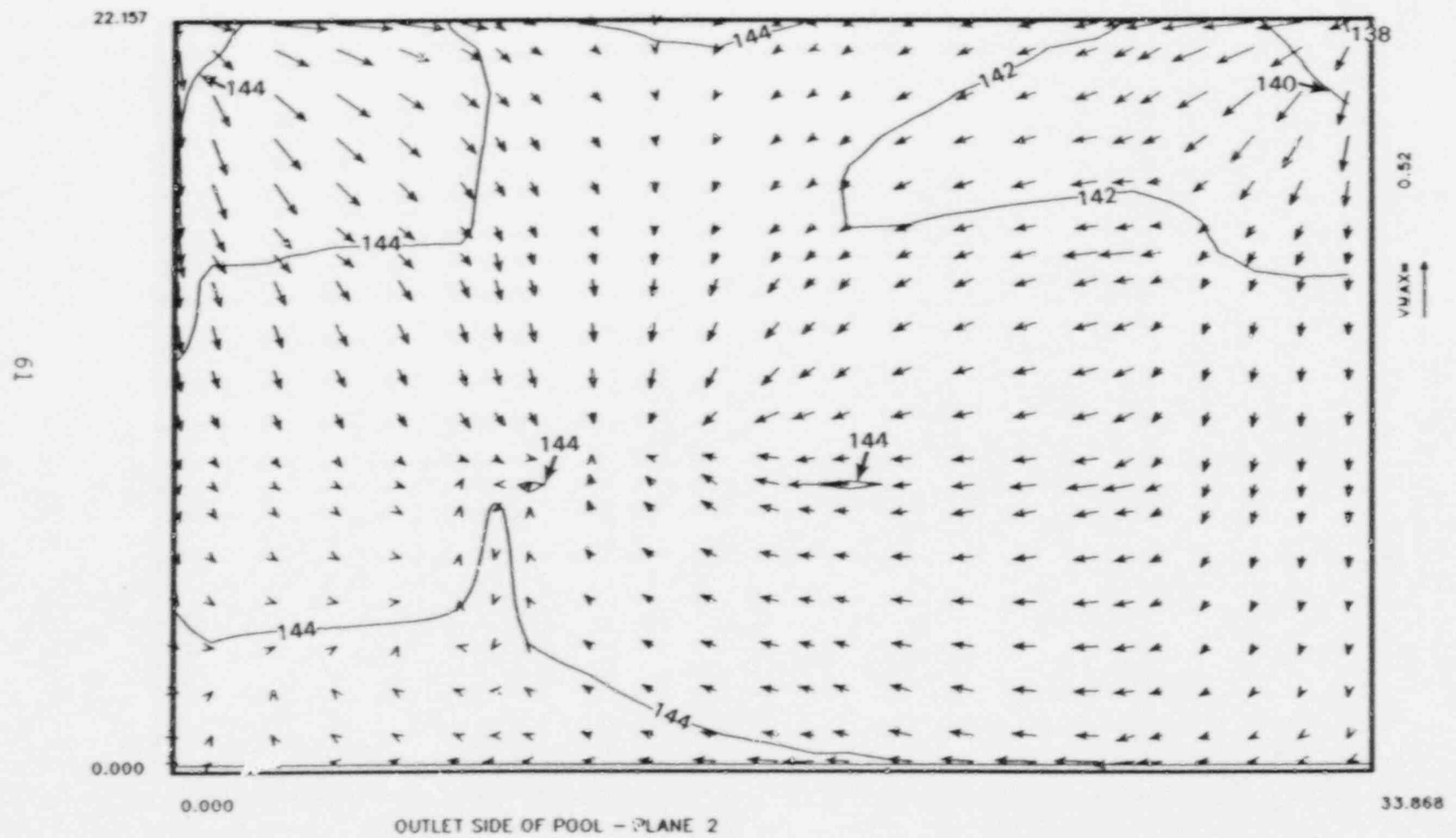


FIGURE 42. Temperature and Flow Distribution below the Fuel Bundles for Case Number 18. ($Q = 450 \text{ GPM}$, $T_{INLET} = 100^\circ\text{F}$, $P_L/P = 13.9$, inlet flow down, peak heat generation near center of pool)

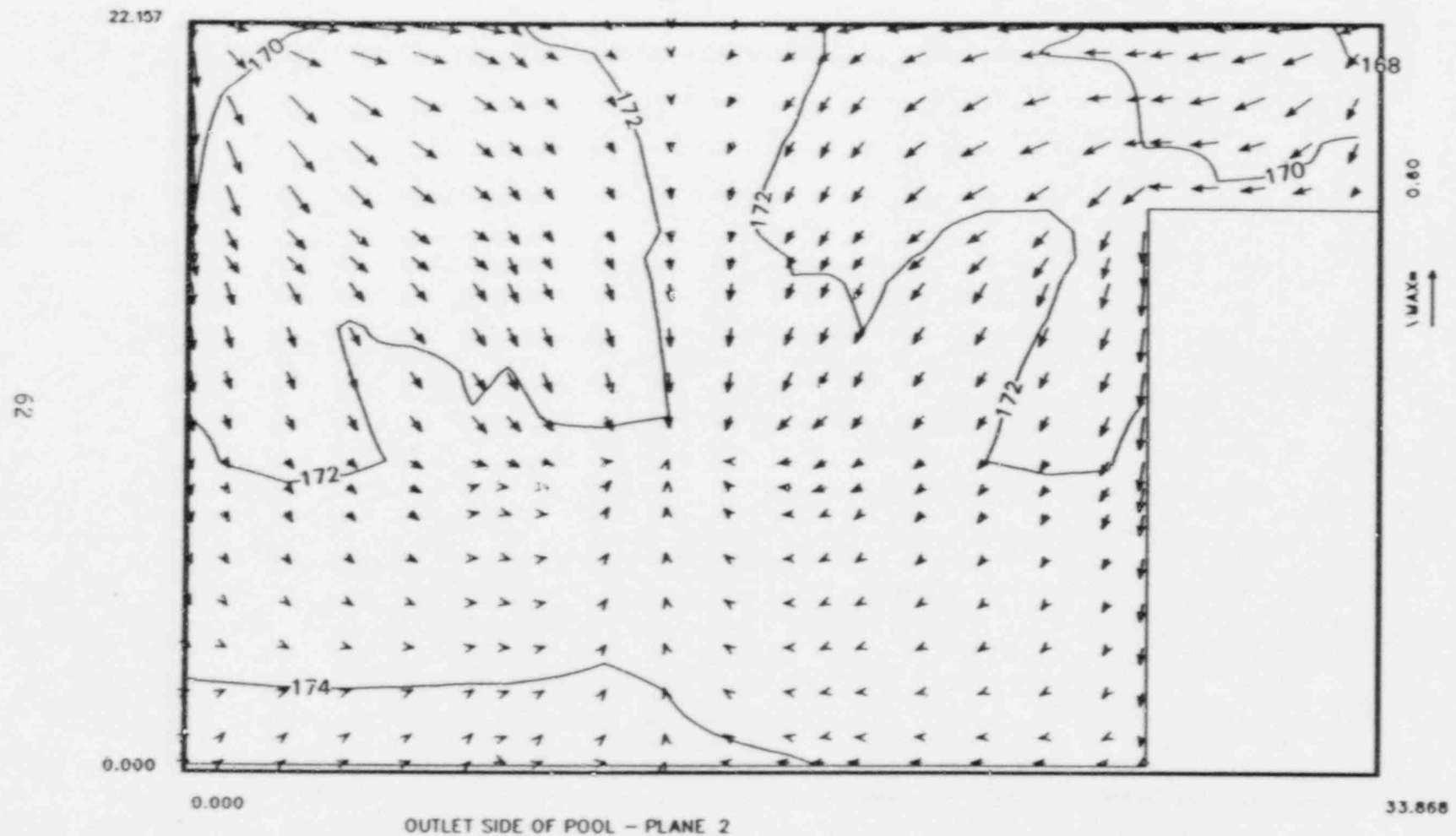


FIGURE 43. Temperature and Flow Distribution below the Fuel Bundles for Case Number 19. ($Q = 450 \text{ GPM}$, $T_{INLET} = 130^\circ\text{F}$, $P_i/P_o = 13.9$, inlet flow down, peak heat generation near center of pool, large open flow region of cask area removed from model)

FIGURE 44. Temperature and Flow Distribution above the Fuel Bundles for Case Number 5. ($Q = 4187 \text{ GPM}$, $T_{INLET} = 150^\circ\text{F}$, $P_e/P = 1.4$, inlet flow down, peak heat generation near center of pool)

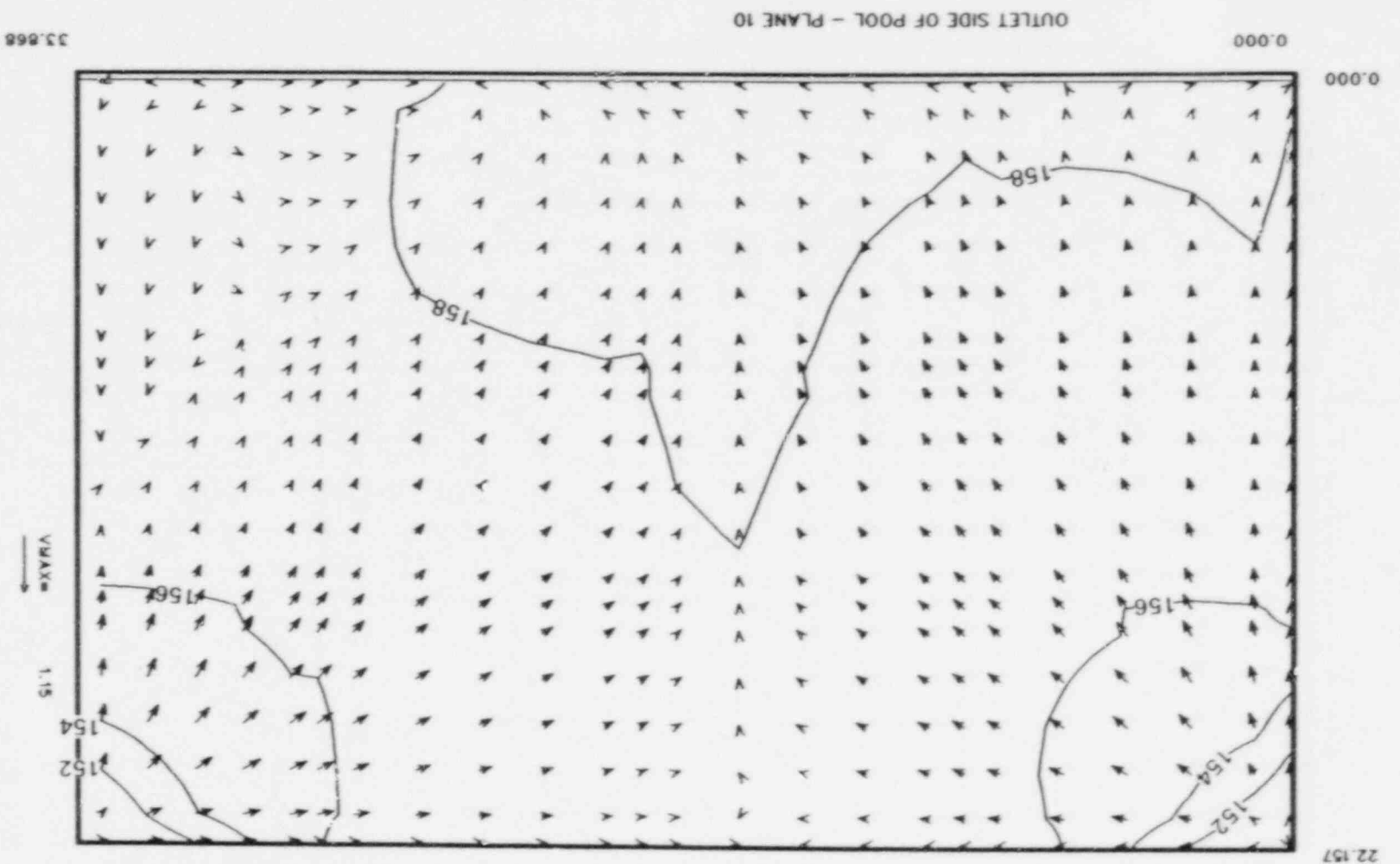


FIGURE 45. Temperature and Flow distribution above the Fuel Bundles for Case Number 9. ($Q = 1048 \text{ GPM}$, TINLET = 150°F , $P_e/P = 1.4$, inlet flow down, peak heat generation near center of pool)

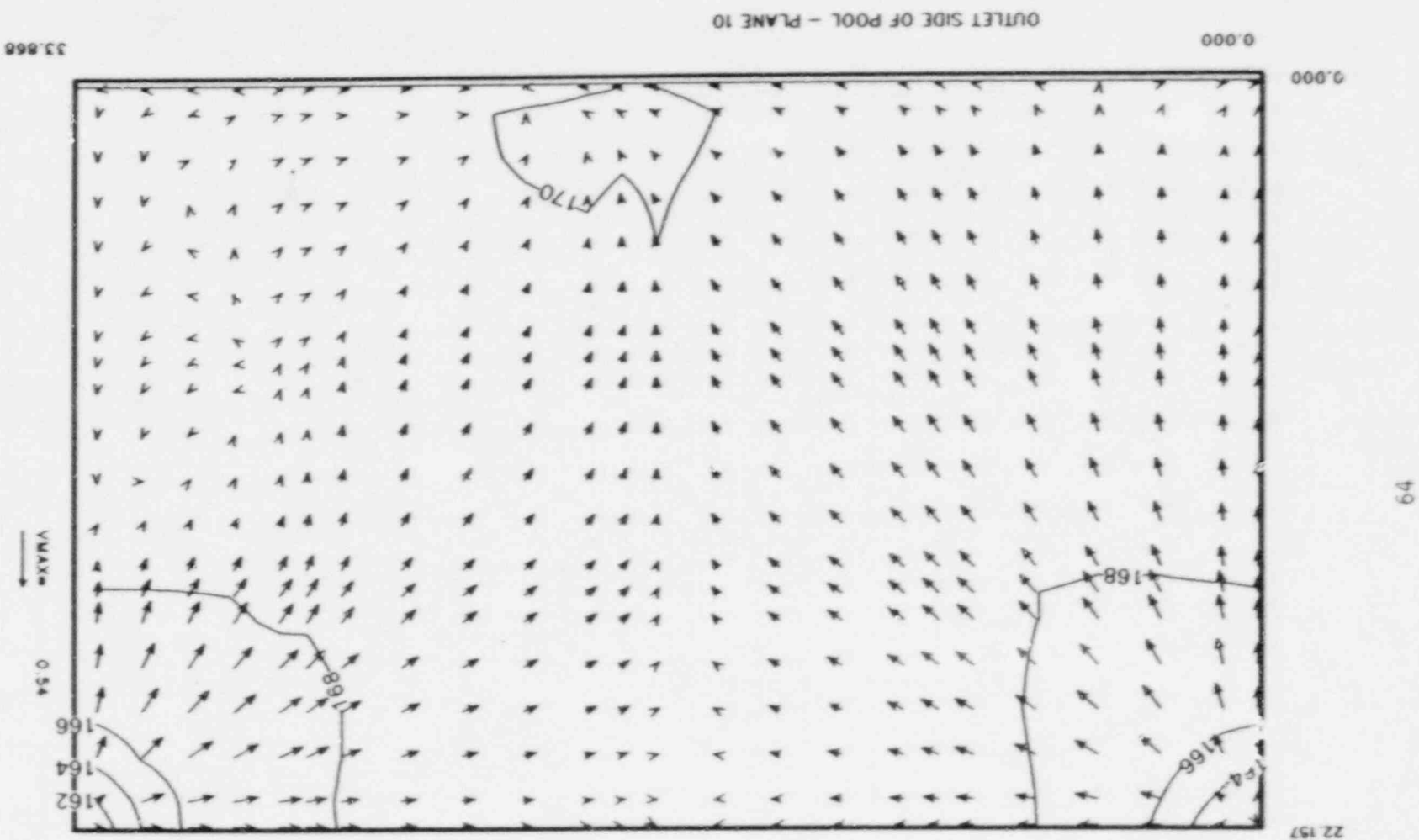


FIGURE 46. Temperature and Flow Distribution above the Fuel Bundles for Case Number 10. ($Q = 1048 \text{ GPM}$, $T_{INLET} = 130^\circ\text{F}$, $P_L/P = 1.4$, inlet flow down, peak heat generation near center of pool)

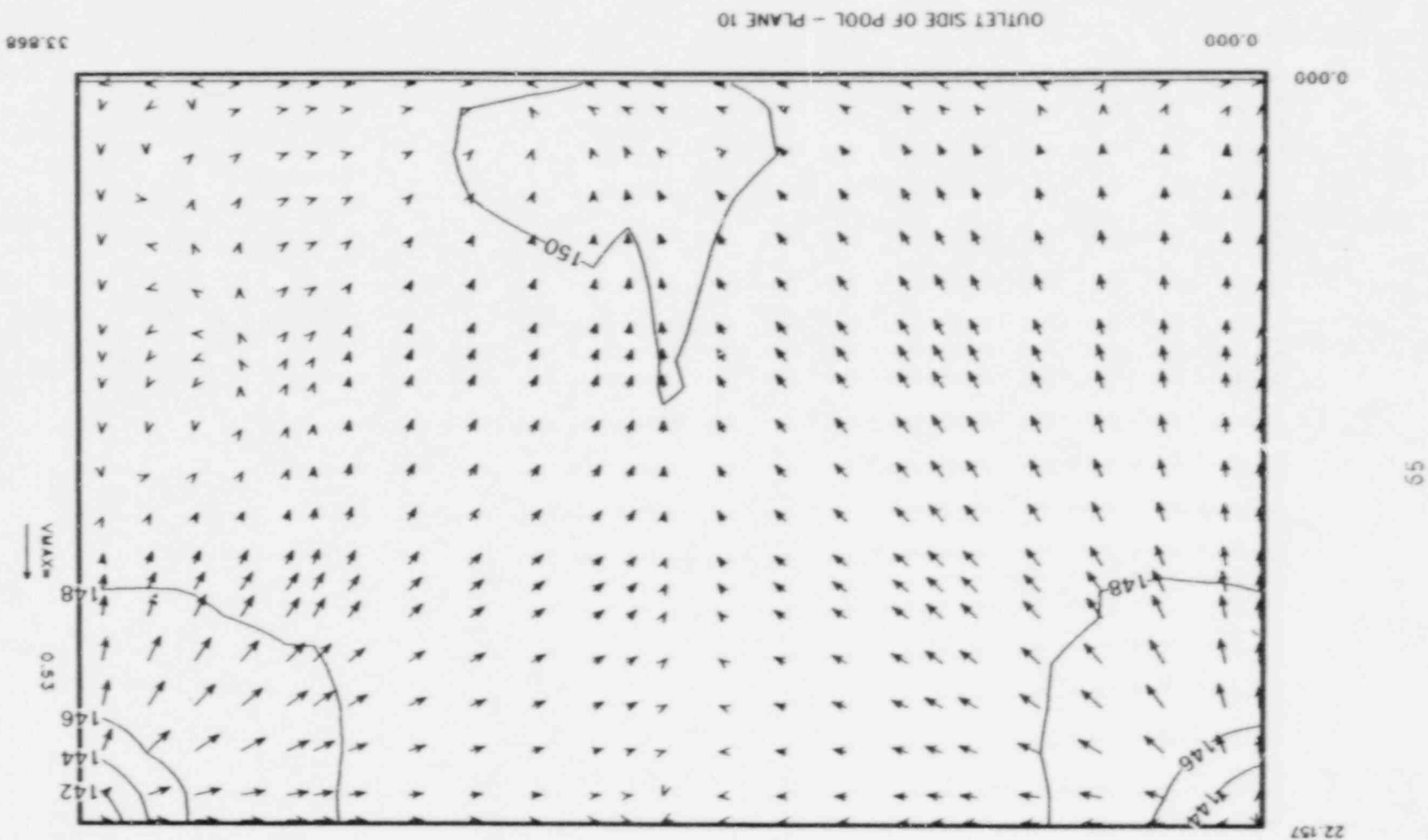
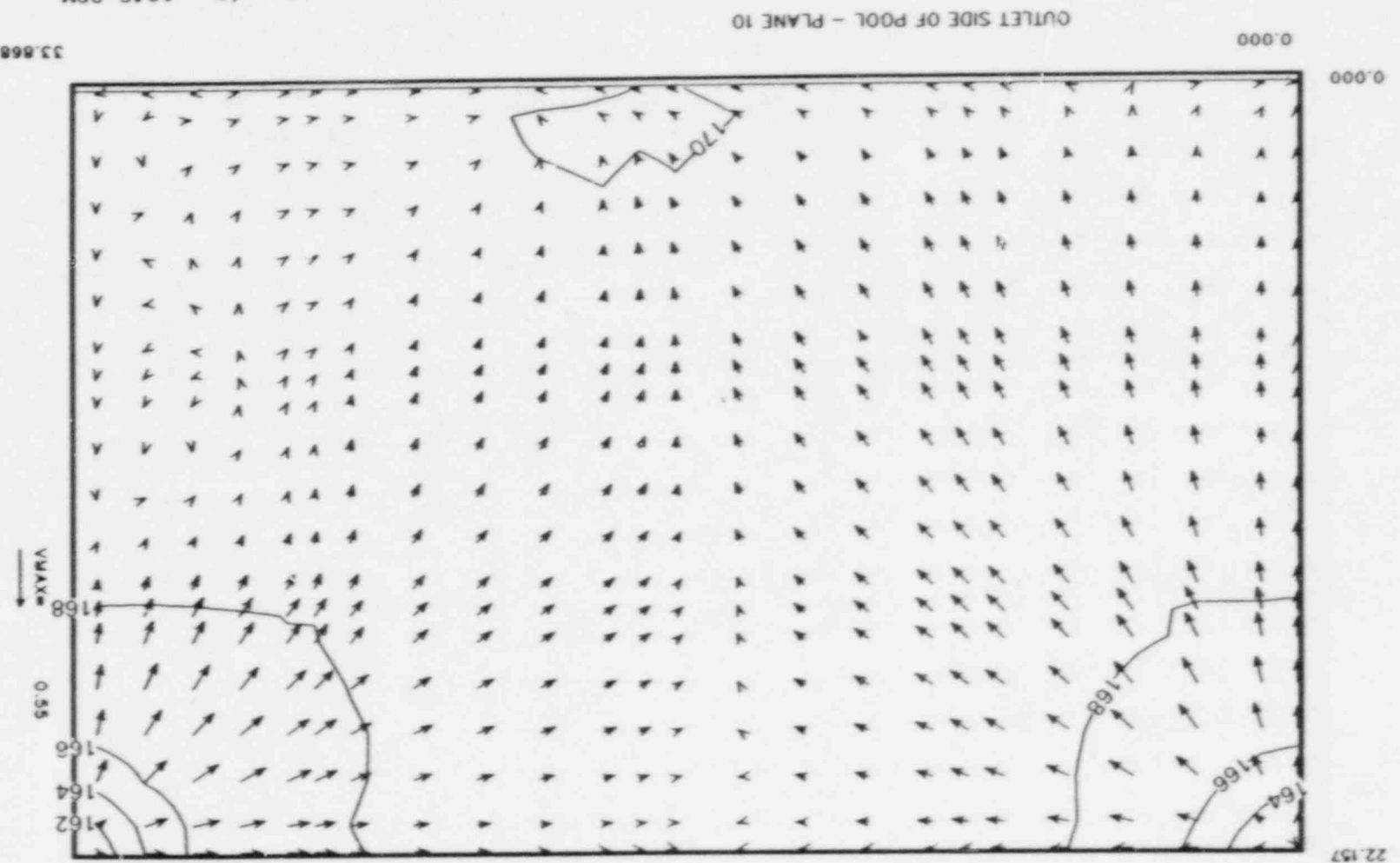


FIGURE 47. Temperature and Flow Distribution above the Fuel Bundles for Case Number 11. ($Q = 1048 \text{ GPM}$,
 TINLET = 150°F , $P_e/P_i = 1.4$, inlet flow down, peak heat generation under inlet)



22.157

L7

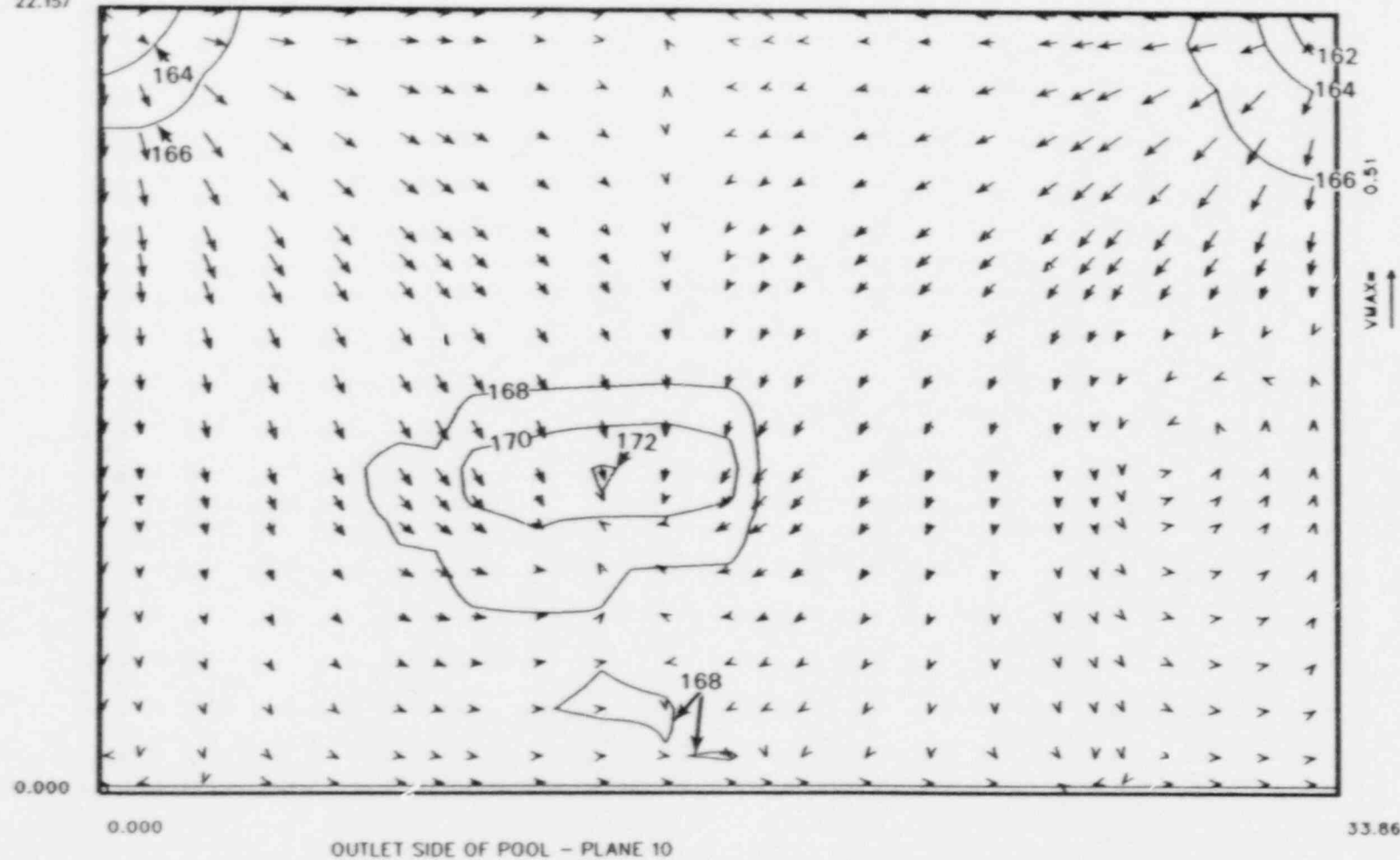


FIGURE 48. Temperature and Flow Distribution above the Fuel Bundles for Case Number 12. ($Q = 1048 \text{ GPM}$, $T_{INLET} = 150^\circ\text{F}$, $P_L/P = 13.9$, inlet flow down, peak heat generation near center of pool)

FIGURE 49. Temperature and Flow Distribution above the Fuel Bundles for Case Number 14. ($Q = 1048 \text{ GPM}$, $T_{INLET} = 150^\circ\text{F}$, $P_e/P = 13.9$, inlet flow horizontal, peak heat generation near center of pool)

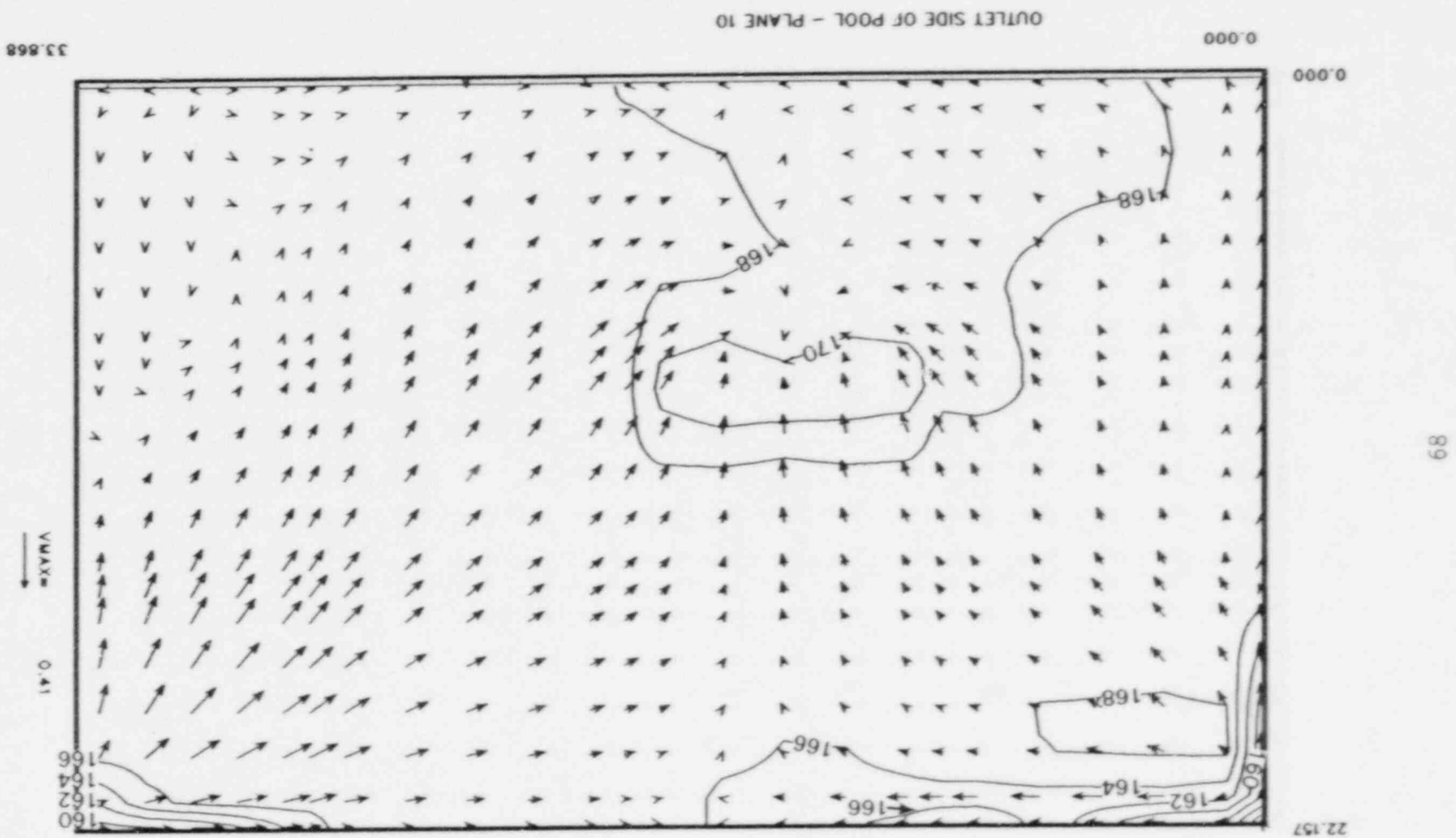
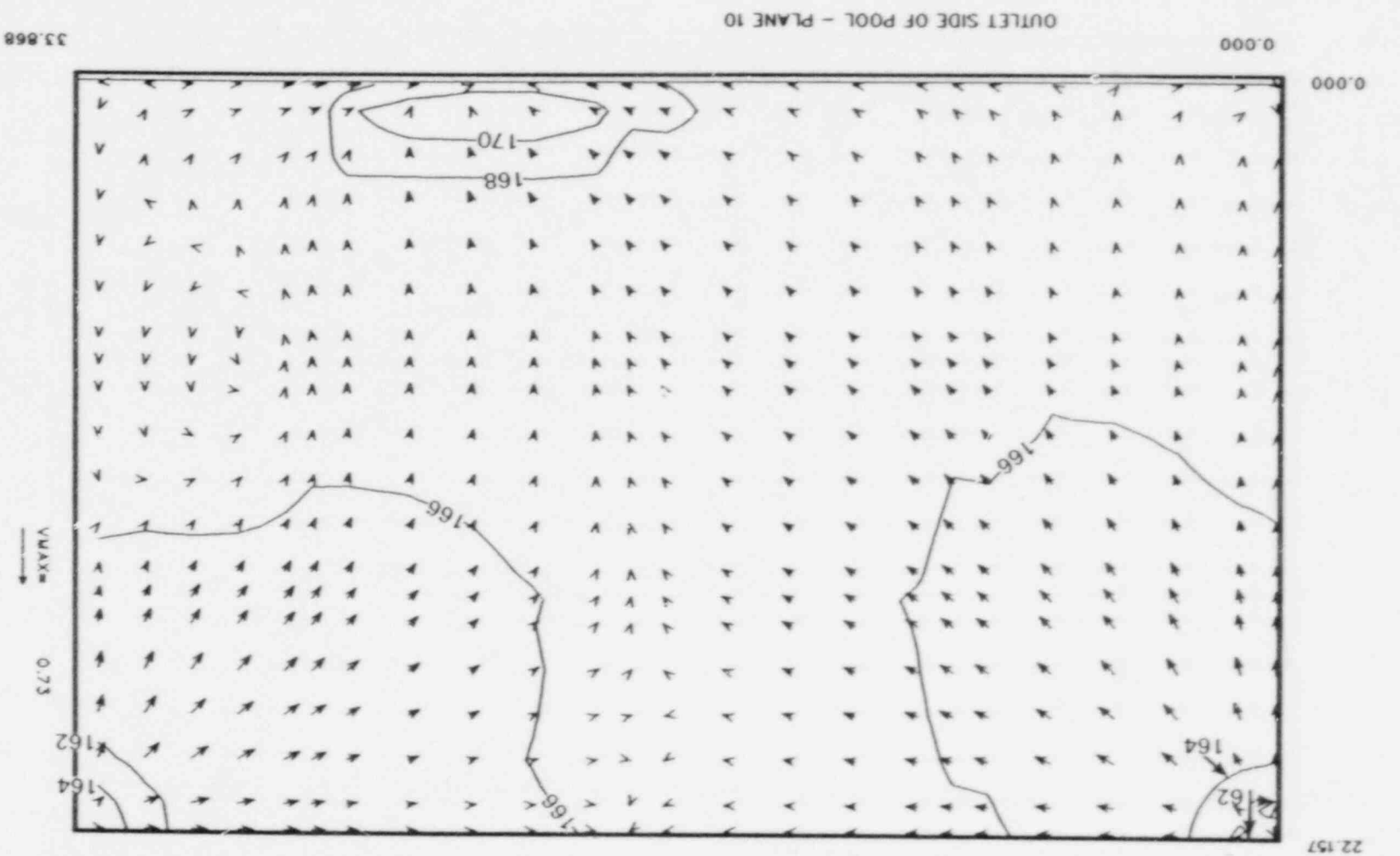


FIGURE 50. Temperature and Flow Distribution above the Fuel Bundles for Case Number 16. ($Q = 1048 \text{ GPM}$,
 TINLET = 150°F , $P_e/P = 13.9$, inlet flow down, peak heat generation near edge of pool)



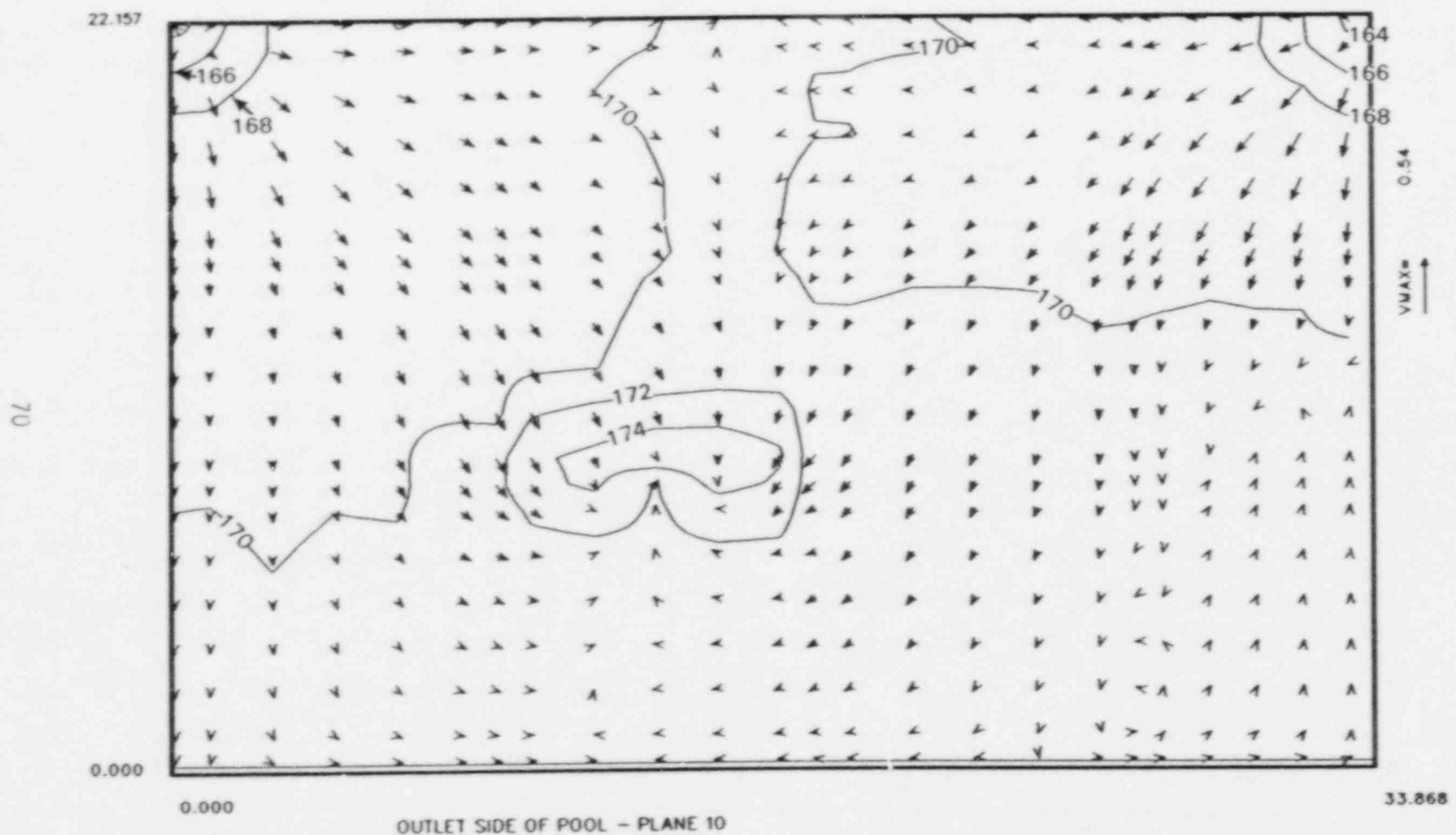


FIGURE 51. Temperature and Flow Distribution above the Fuel Bundles for Case Number 17. ($Q = 450$ GPM, TINLET = 130°F , $P_L/P = 13.9$, inlet flow down, peak heat generation near center of pool)

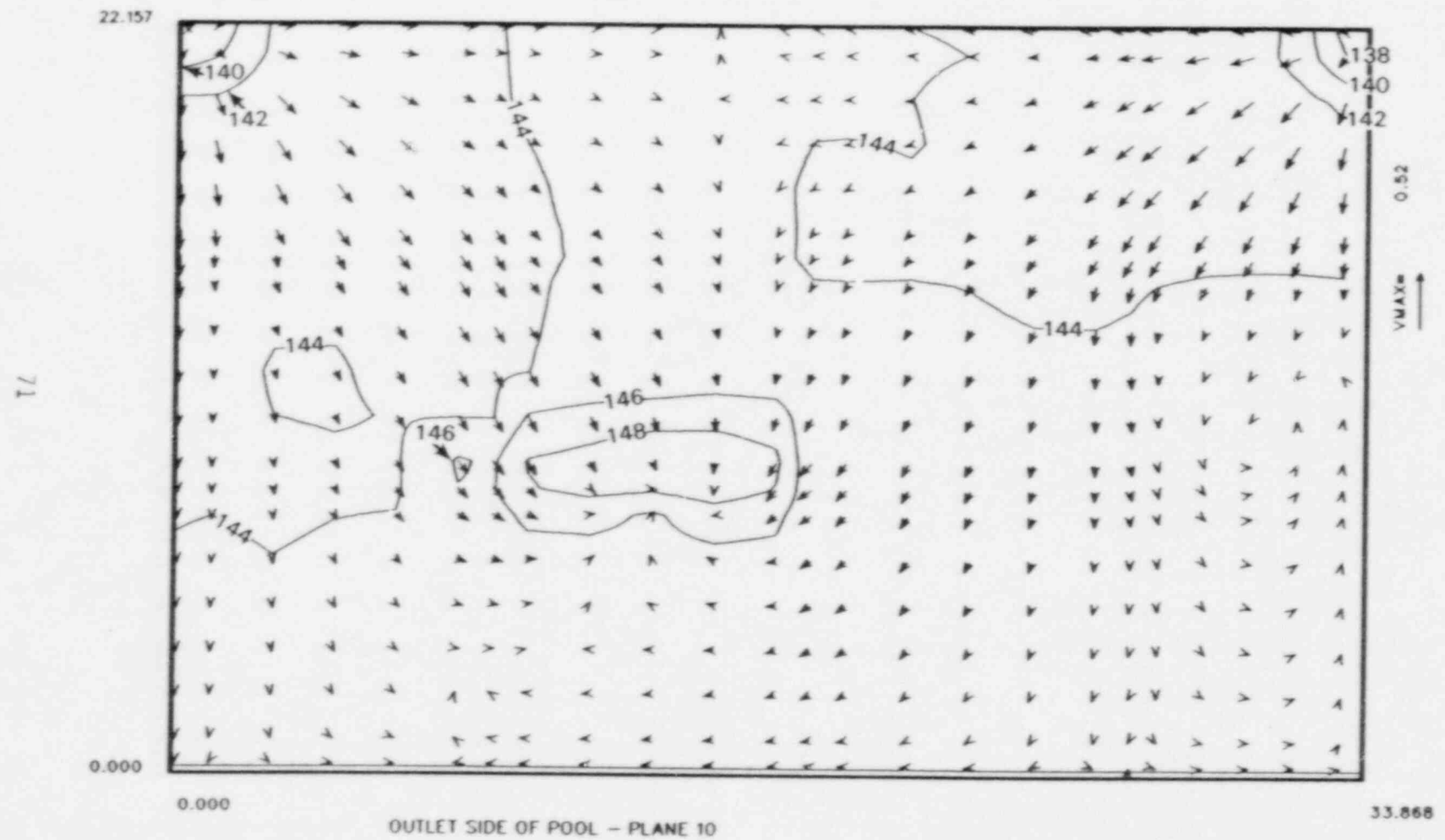


FIGURE 52. Temperature and Flow Distribution above the Fuel Bundles for Case Number 18. ($Q = 450 \text{ GPM}$, $T_{INLET} = 100^\circ\text{F}$, $P_L/P = 13.9$, inlet flow down, peak heat generation near center of pool)

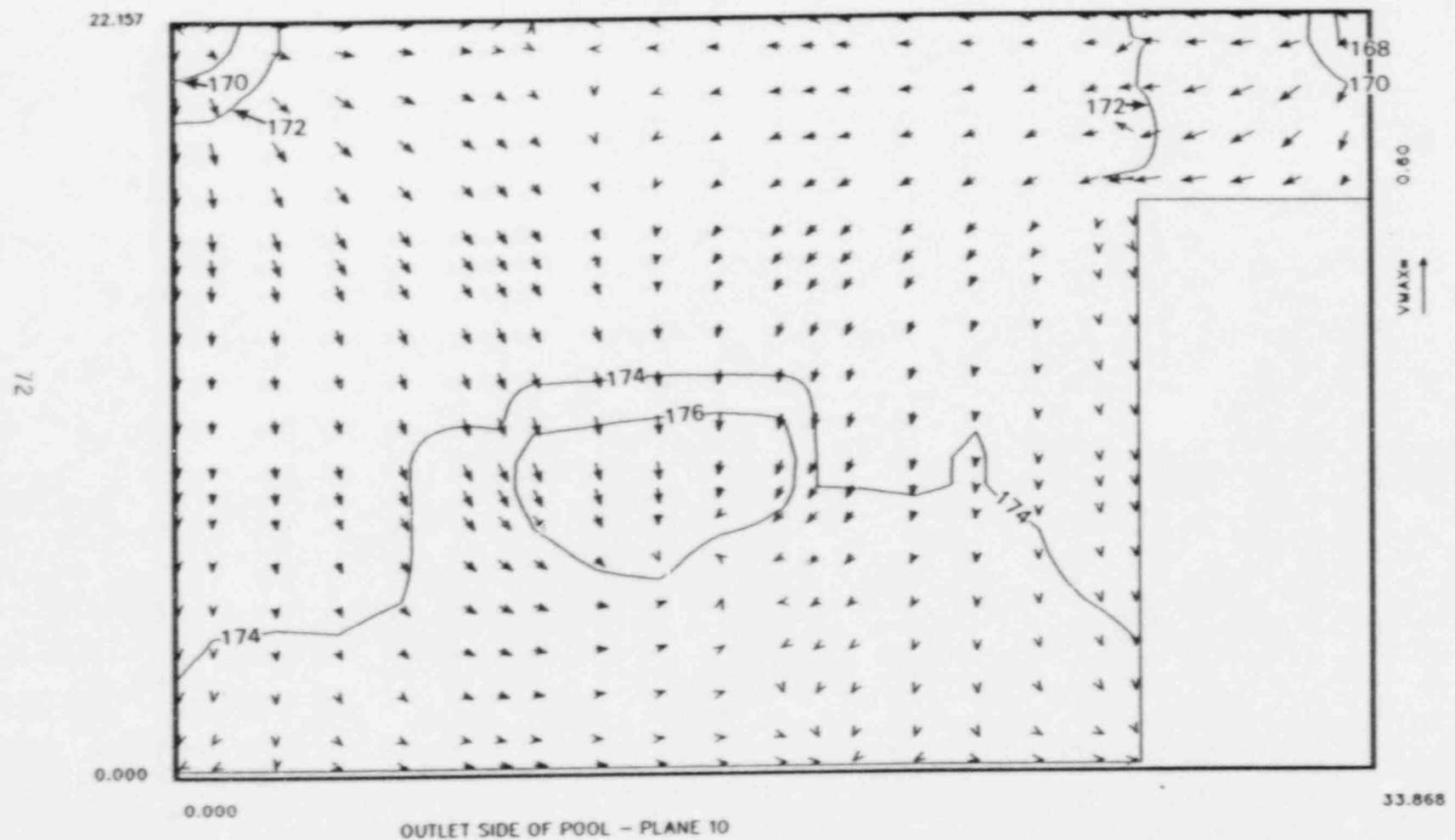


FIGURE 53. Temperature and Flow Distribution above the Fuel Bundles for Case Number 19. ($Q = 450 \text{ GPM}$,
 $T_{INLET} = 130^\circ\text{F}$, $P_t/P = 13.9$, inlet flow down, peak heat generation near center of pool, large
open flow region of cask area removed from model)

36.176

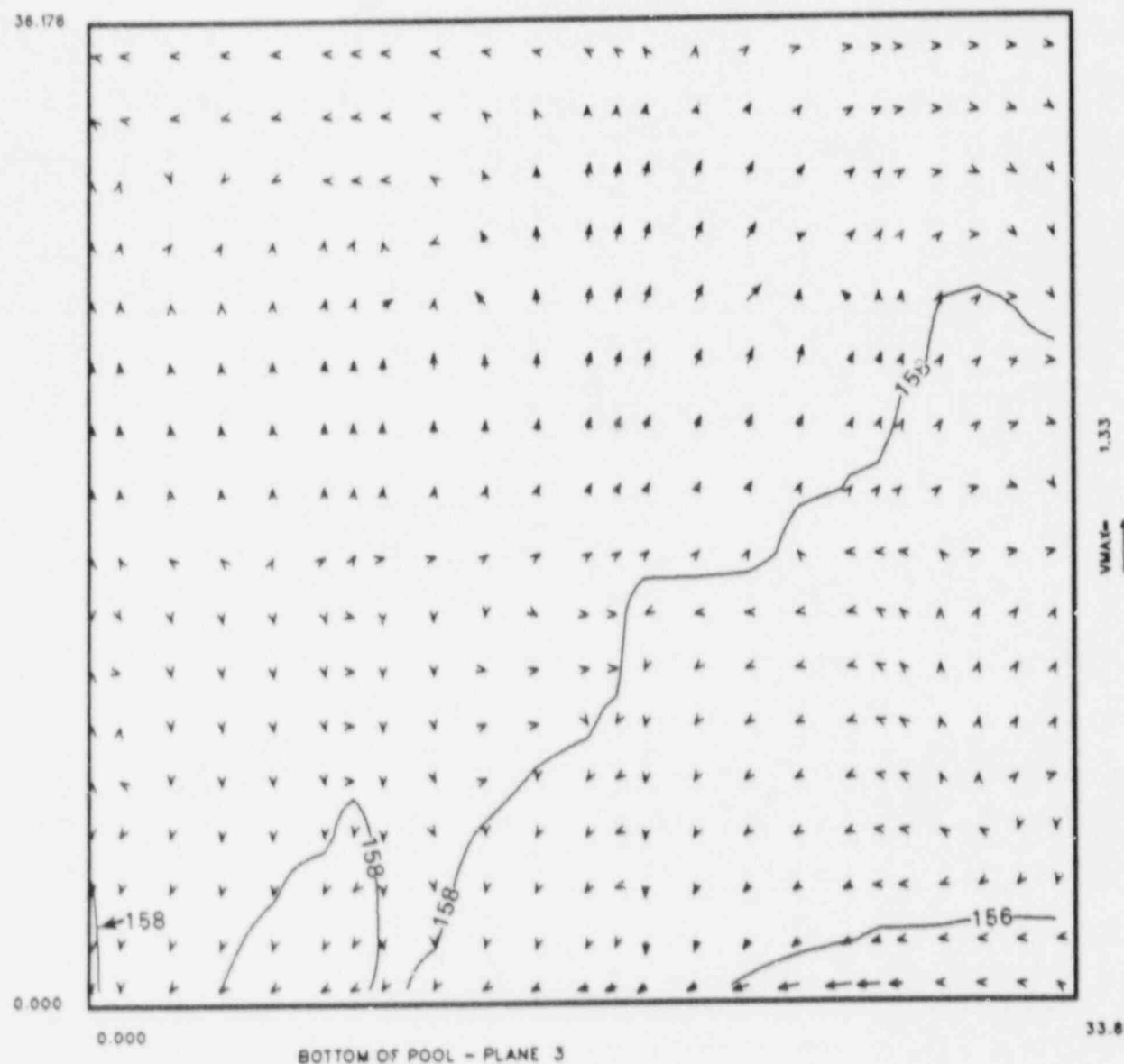
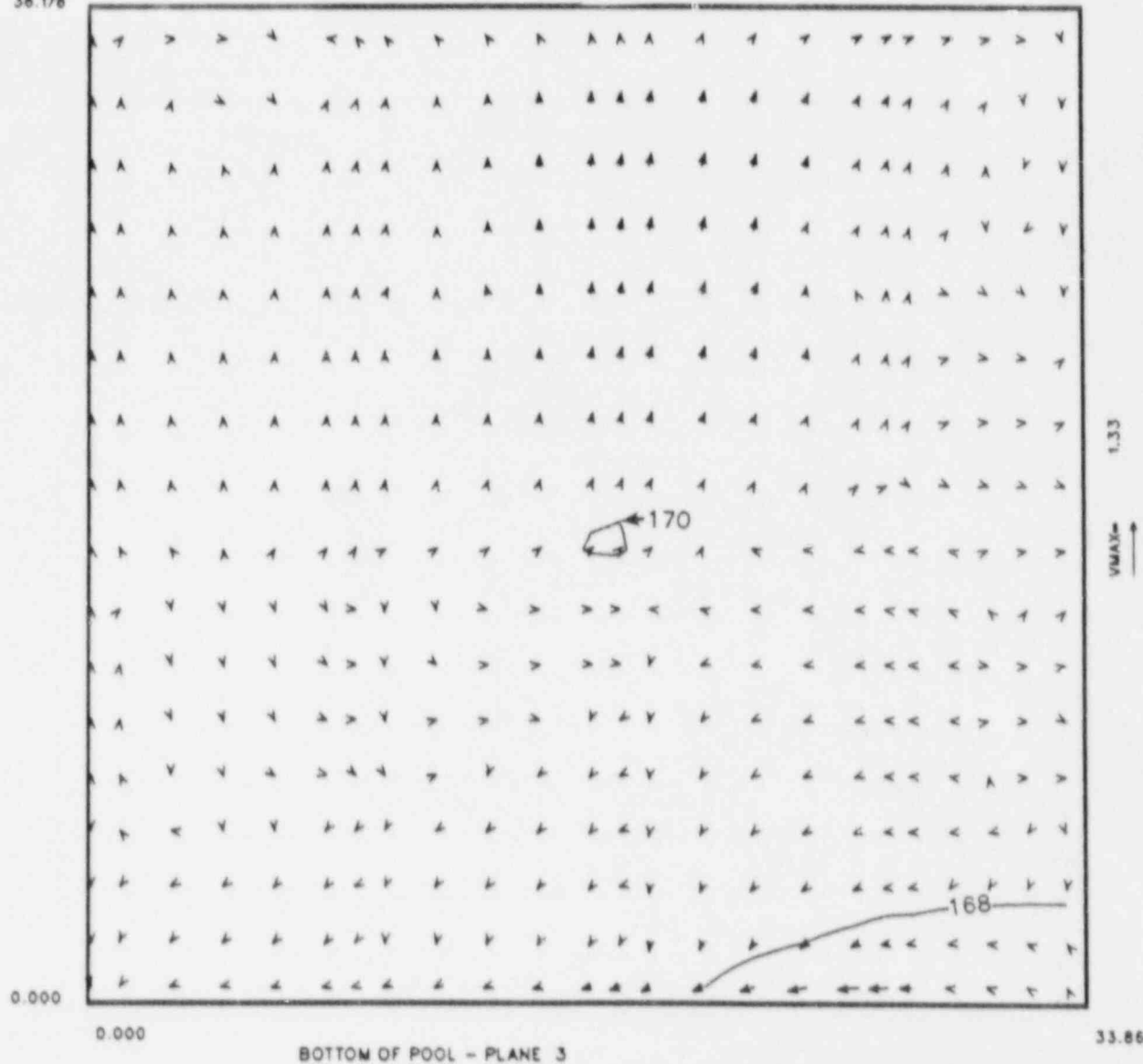


FIGURE 54. Temperature and Flow Distribution along the Front Wall of the Pool for Case Number 5. ($Q = 4187 \text{ GPM}$, $T_{INLET} = 150^\circ\text{F}$, $P_L/P = 1.4$, inlet flow down, peak heat generation near center of pool)

36.178



BOTTOM OF POOL - PLANE 3

FIGURE 55. Temperature and Flow Distribution along the Front Wall of the Pool for Case Number 11. ($Q = 1048 \text{ GPM}$, $T_{INLET} = 150^\circ\text{F}$, $P_L/\bar{P} = 1.4$, inlet flow down, peak heat generation under inlet)

38.178

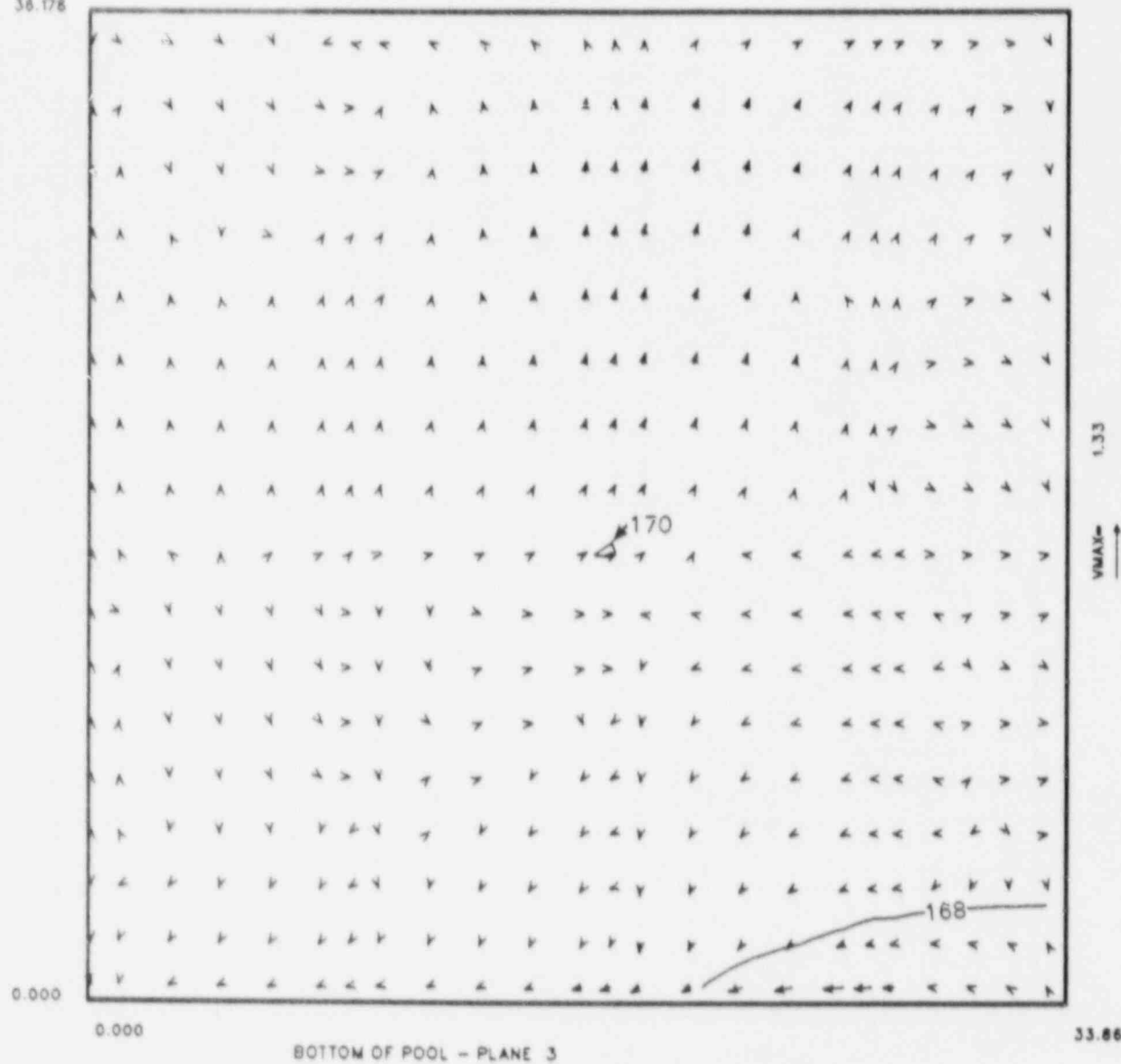


FIGURE 56. Temperature and Flow Distribution along the Front Wall of the Pool for Case Number 9. ($Q = 1048 \text{ GPM}$, $T_{INLET} = 150^\circ\text{F}$, $P_L/P = 1.4$, inlet flow down, peak heat generation near center of pool)

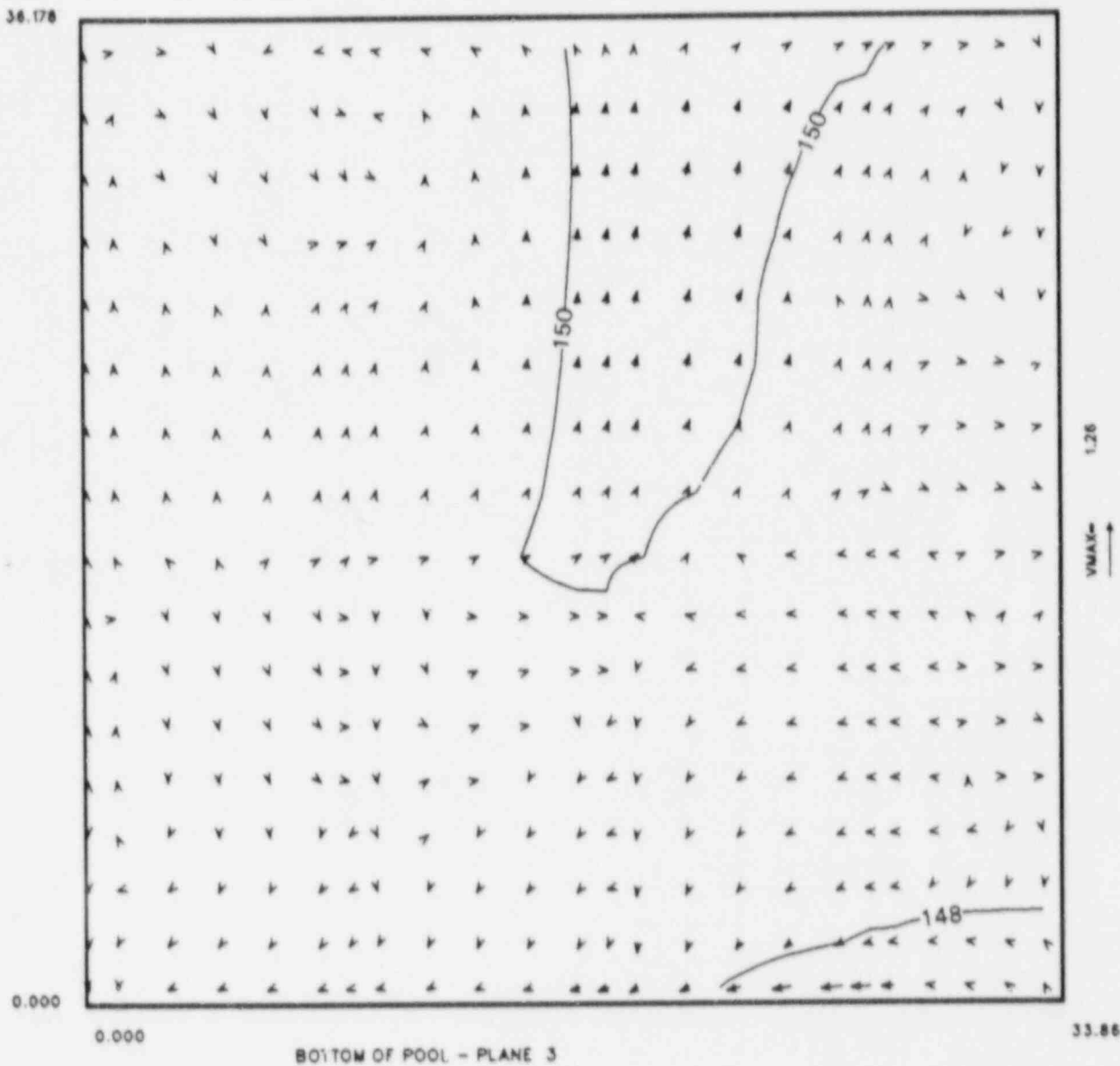


FIGURE 57. Temperature and Flow Distribution along the Front Wall of the Pool for Case Number 10. ($Q = 1048 \text{ GPM}$, $T_{INLET} = 130^\circ\text{F}$, $P_1/P = 1.4$, inlet flow down, peak heat generation near center of pool)

36.178

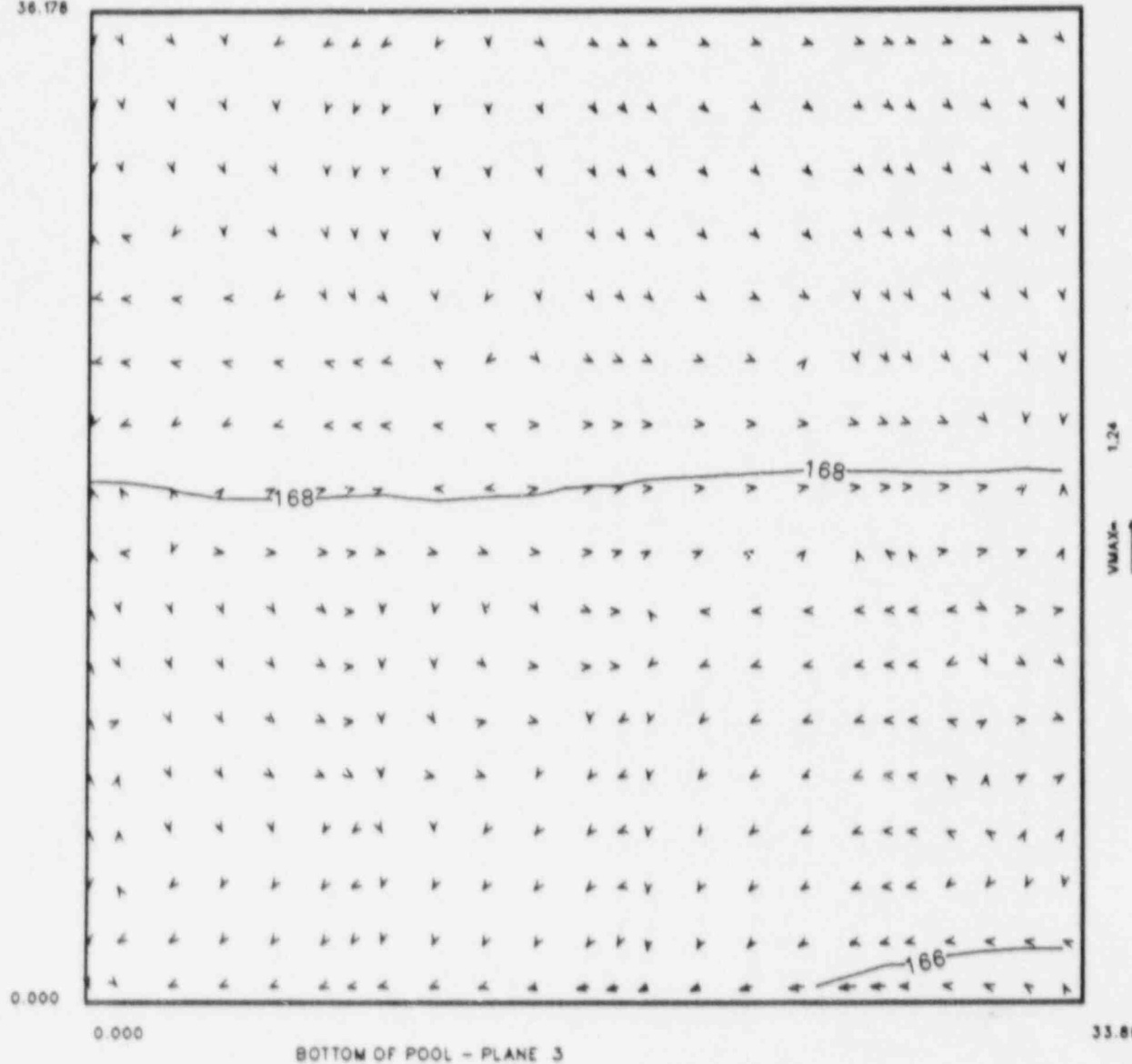


FIGURE 58. Temperature and Flow Distribution along the Front Wall of the Pool for Case Number 12. ($Q = 1048 \text{ GPM}$, $T_{INLET} = 150^\circ\text{F}$, $P_L/P = 13.9$, inlet flow down, peak heat generation near center of pool)

38.178

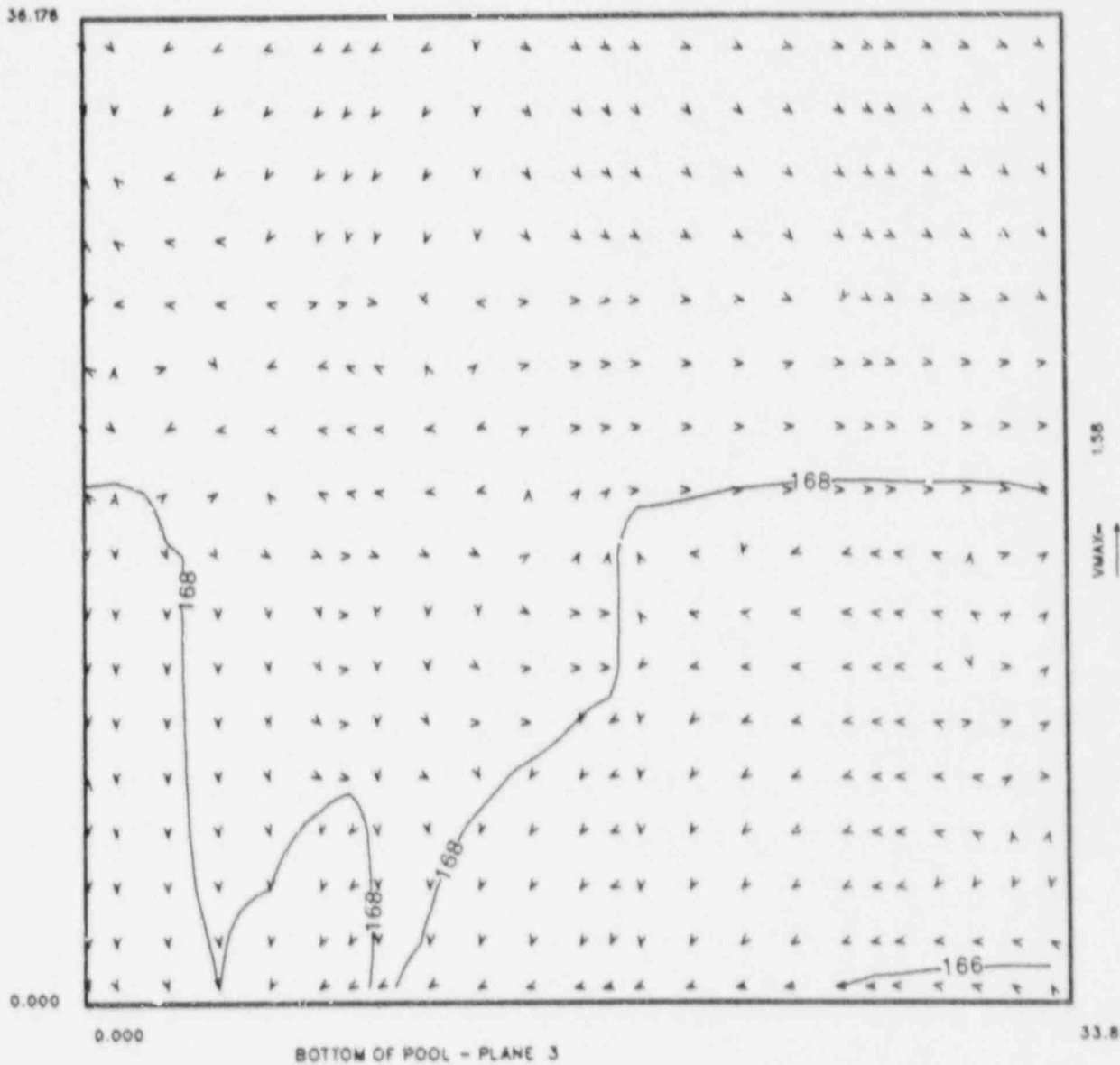


FIGURE 59. Temperature and Flow Distribution along the Front Wall of the Pool for Case Number 14. ($Q = 1048 \text{ GPM}$, $T_{INLET} = 150^\circ\text{F}$, $P_t/\bar{P} = 13.9$, inlet flow horizontal, peak heat generation near center of pool)

36.178

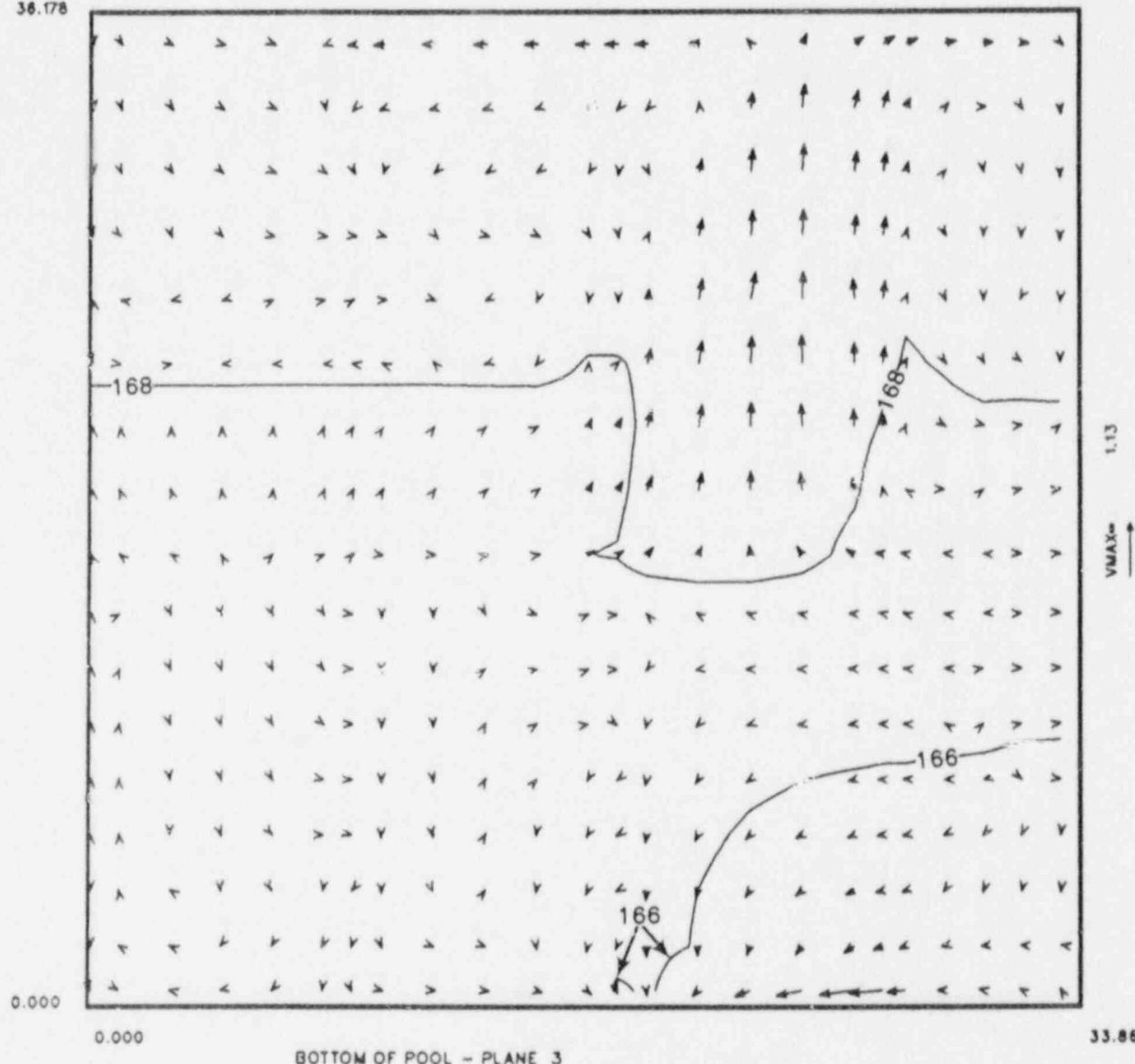


FIGURE 60. Temperature and Flow Distribution along the Front Wall of the Pool for Case Number 16. ($Q = 1048 \text{ GPM}$, $T_{INLET} = 150^\circ\text{F}$, $P_1/P = 13.9$, inlet flow down, peak heat generation near edge of pool)

36.178

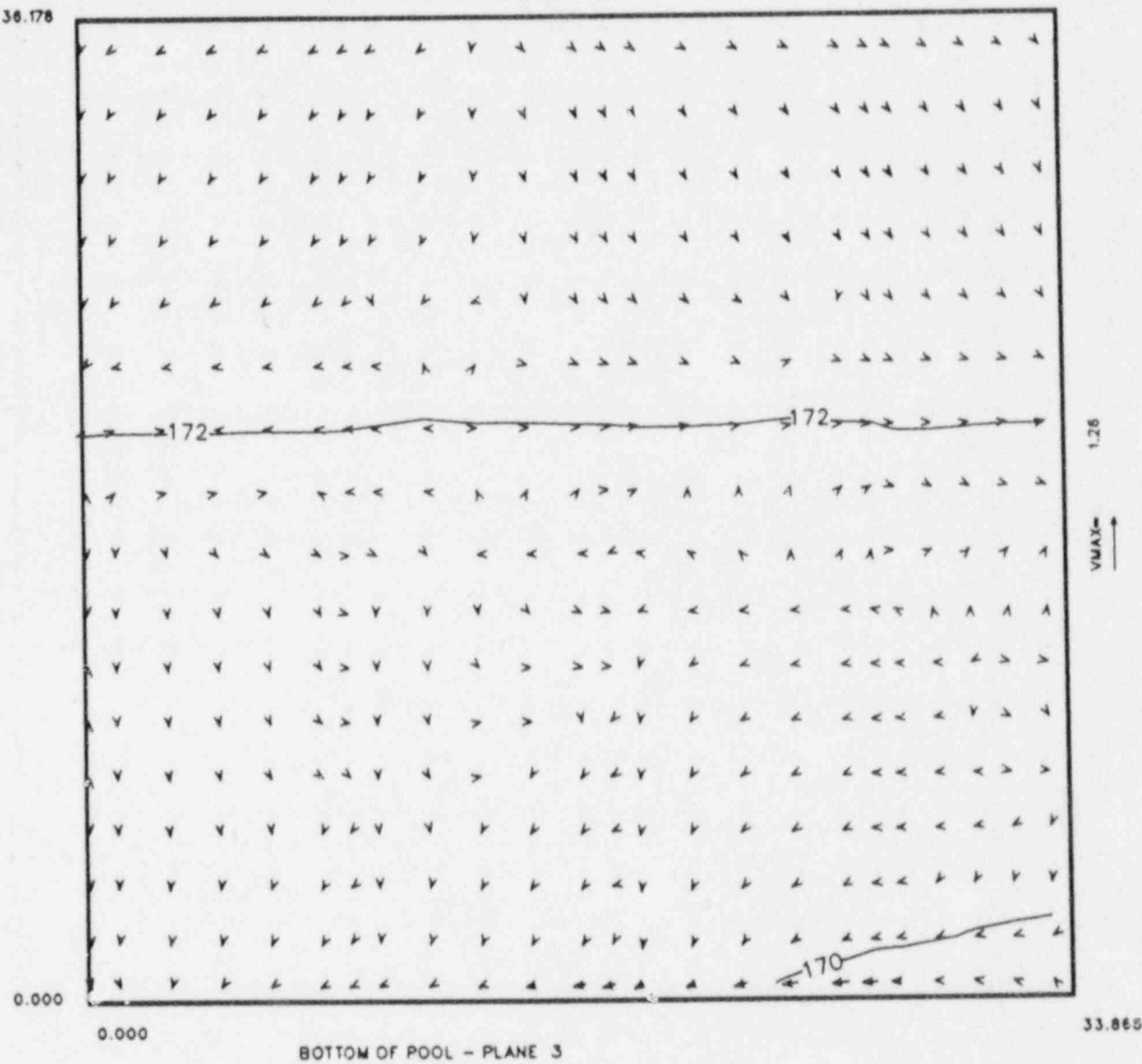


FIGURE 61. Temperature and Flow Distribution along the Front Wall of the Pool for Case Number 17. ($Q = 450 \text{ GPM}$, $T_{INLET} = 130^\circ\text{F}$, $P_1/\bar{P} = 13.9$, inlet flow down, peak heat generation near center of pool)

36.178

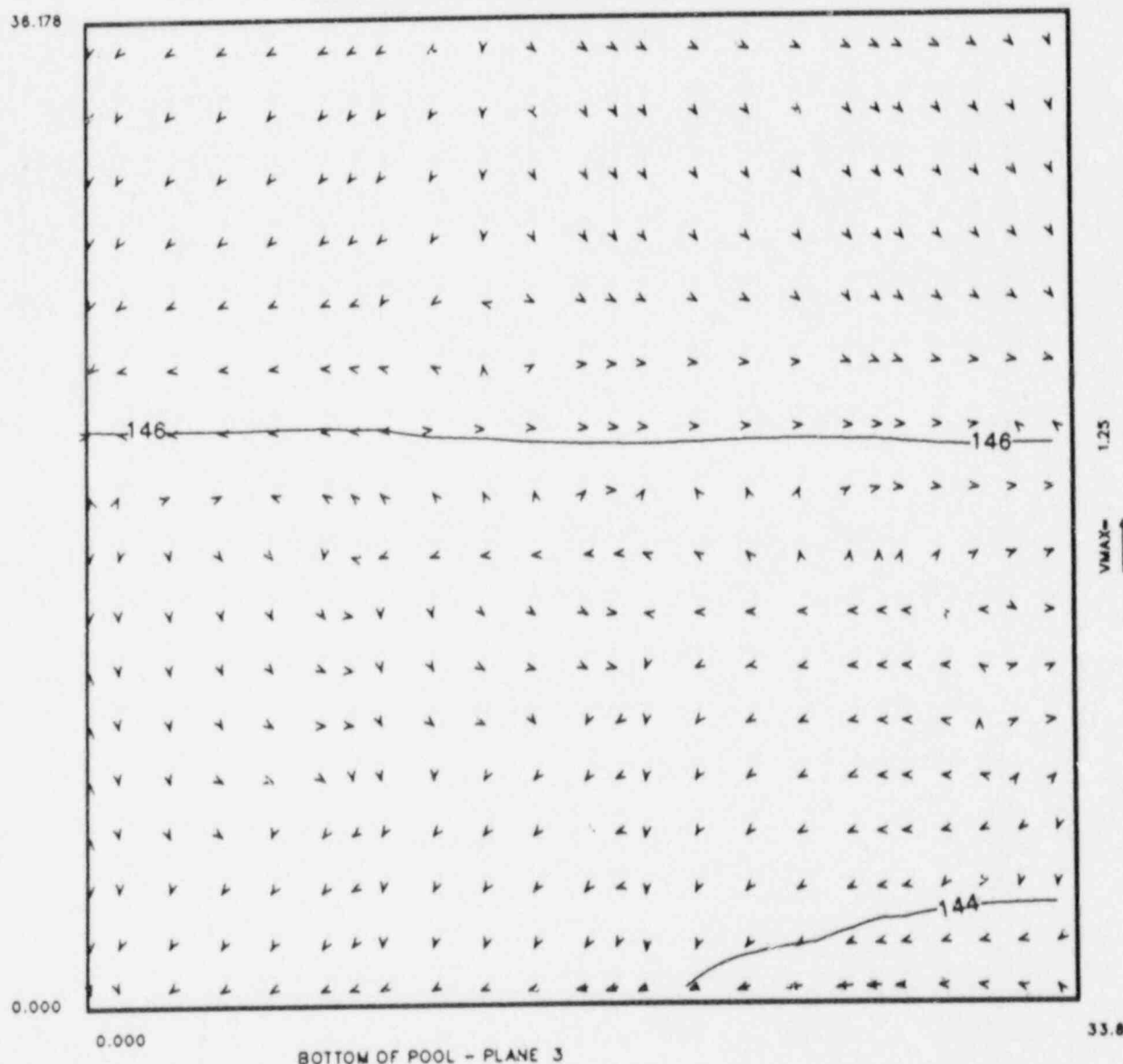
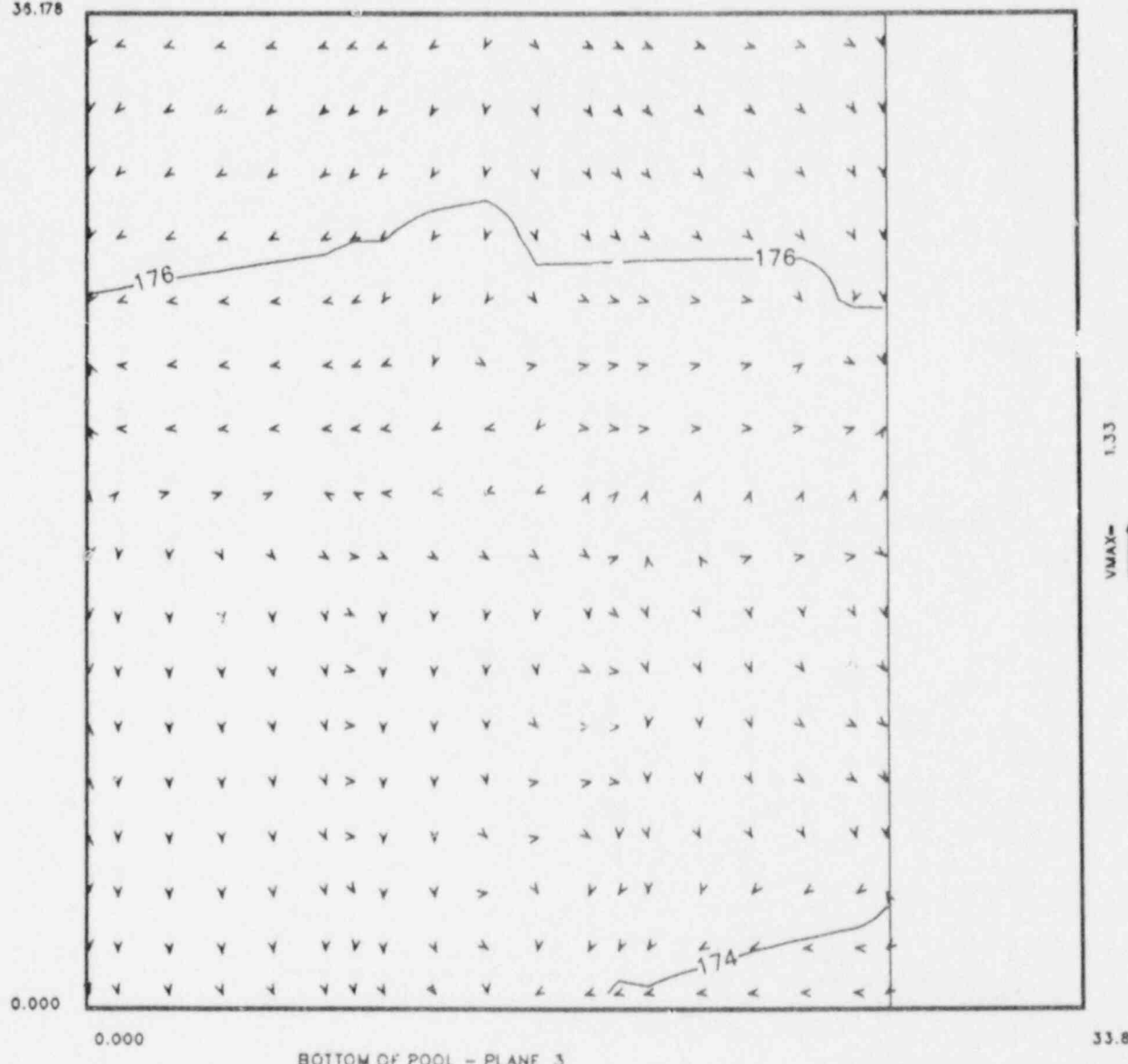


FIGURE 62. Temperature and Flow Distribution along the Front Wall of the Pool for Case Number 18. ($Q = 450 \text{ GPM}$, $T_{INLET} = 100^\circ\text{F}$, $P_t/P = 13.9$, inlet flow down, peak heat generation near center of pool)

35.178



BOTTOM OF POOL - PLANE 3

FIGURE 63. Temperature and Flow Distribution along the Front Wall of the Pool for Case Number 19. ($Q = 450$ GPM, $T_{INLET} = 130^{\circ}\text{F}$, $P_1/\bar{P} = 13.9$, inlet flow down, peak heat generation near center of pool, large open flow region of cask area removed from model)

36.178

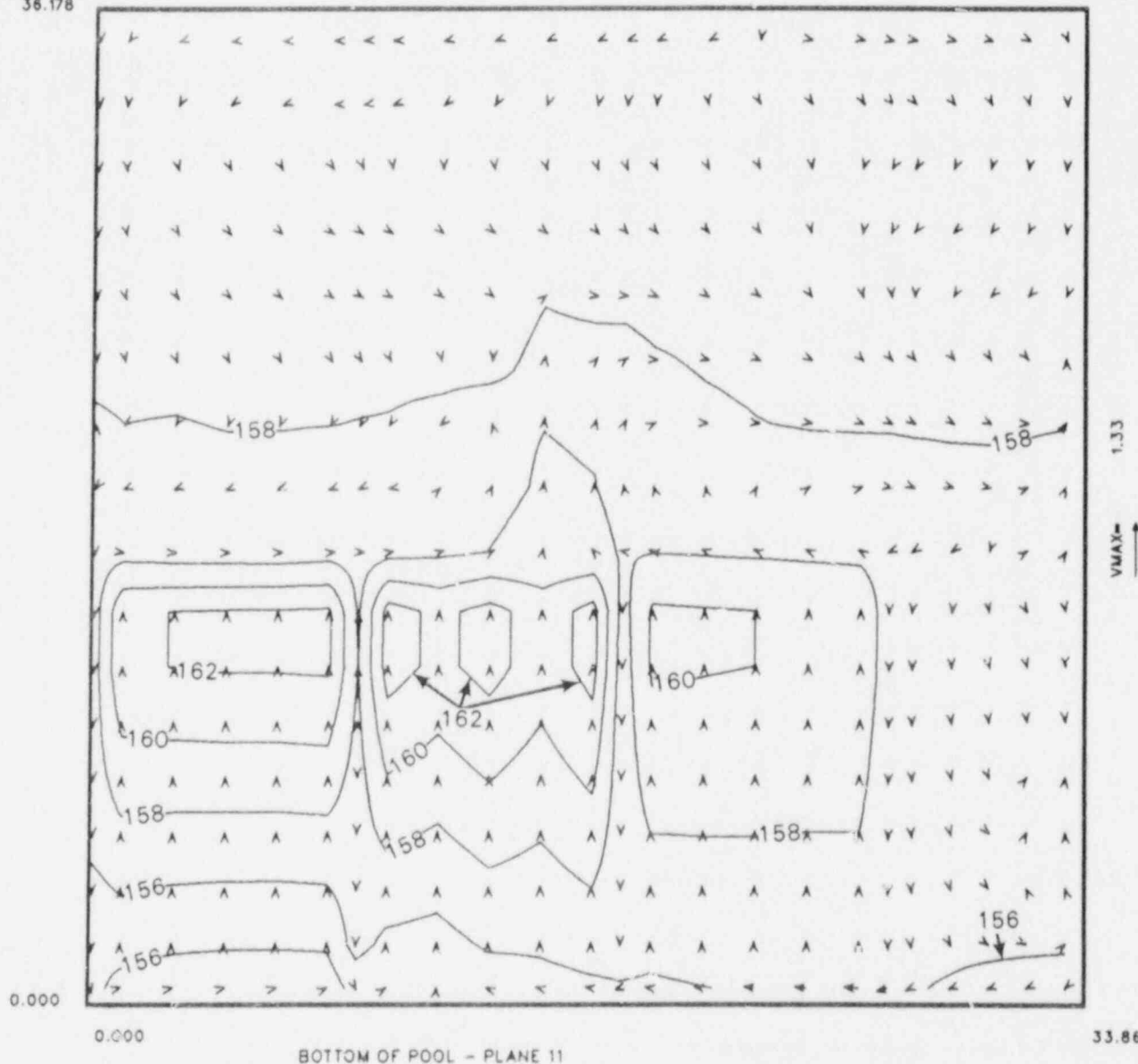


FIGURE 64. Temperature and Velocity Distribution in a Plane above the Leveling Pads for Case Number 5. ($Q = 4187 \text{ GPM}$, $T_{INLET} = 150^\circ\text{F}$, $P_t/P = 1.4$, inlet flow down, peak heat generation near center of pool)

36.178

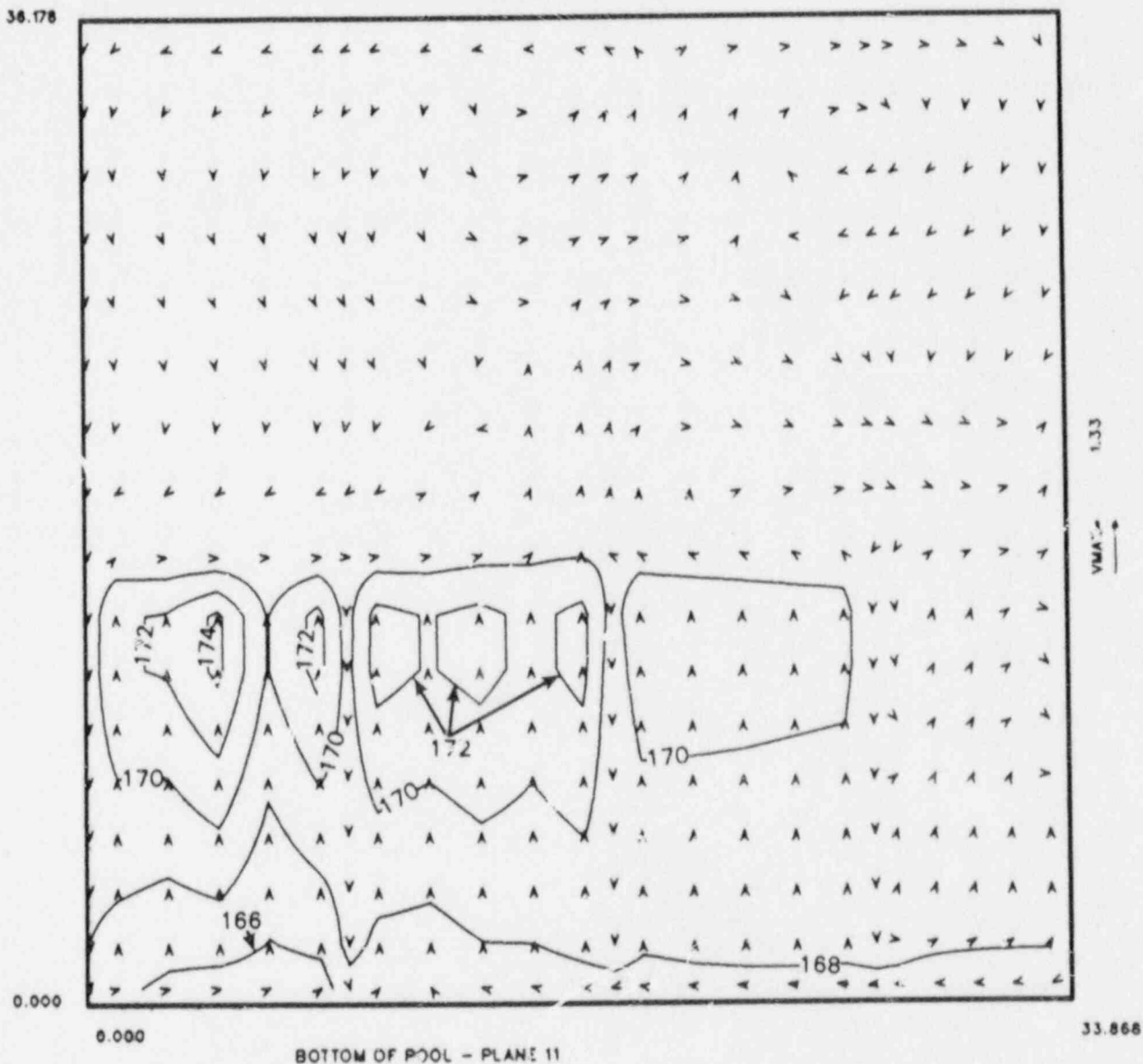


FIGURE 65. Temperature and Velocity Distribution in a Plane above the Leveling Pads for Case Number 9. ($Q = 1048 \text{ GPM}$, $T_{INLET} = 150^\circ\text{F}$, $P_e/P = 1.4$, inlet flow down, peak heat generation near center of pool)

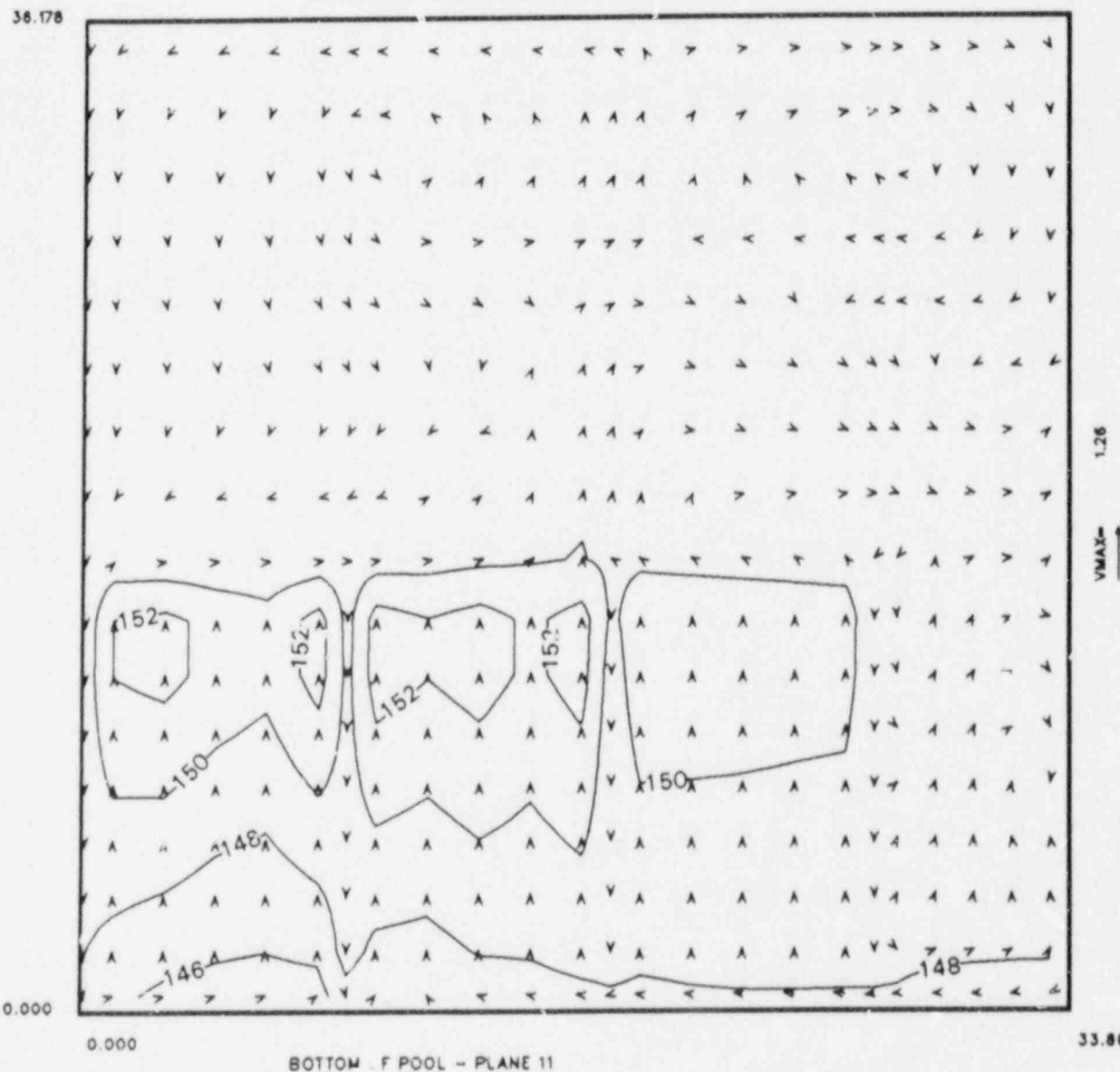


FIGURE 66. Temperature and Velocity Distribution in a Plane above the Leveling Pads for Case Number 10. ($Q = 1048 \text{ GPM}$, TINLET = 130°F , $P_f/P = 1.4$, inlet flow down, peak heat generation near center of pool)

36.078

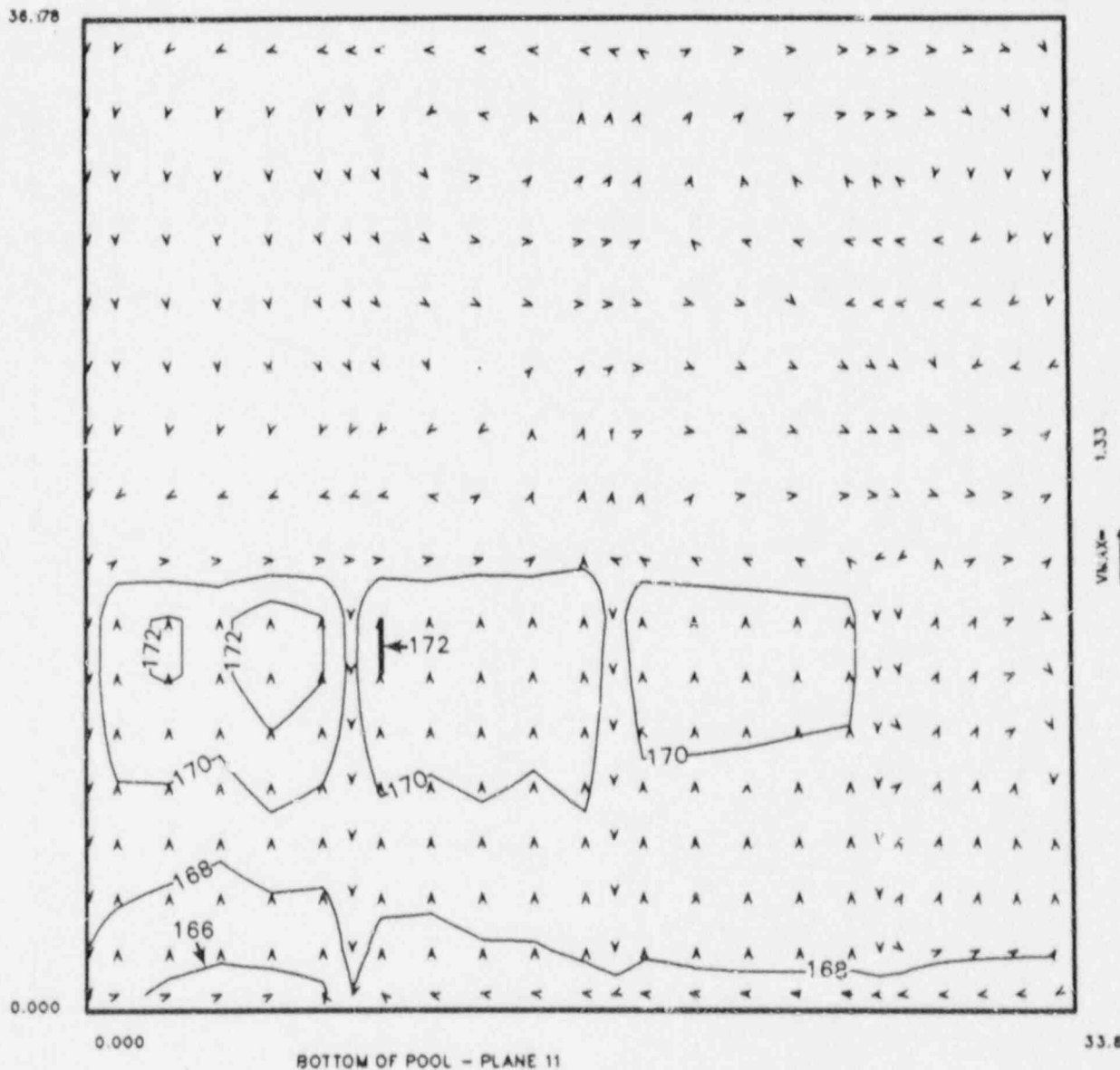


FIGURE 67. Temperature and Velocity Distribution in a Plane above the Leveling Pads for Case Number 11. ($Q = 1048 \text{ GPM}$, TINLET = 150°F , $P_L/P = 1.4$, inlet flow down, peak heat generation under inlet)

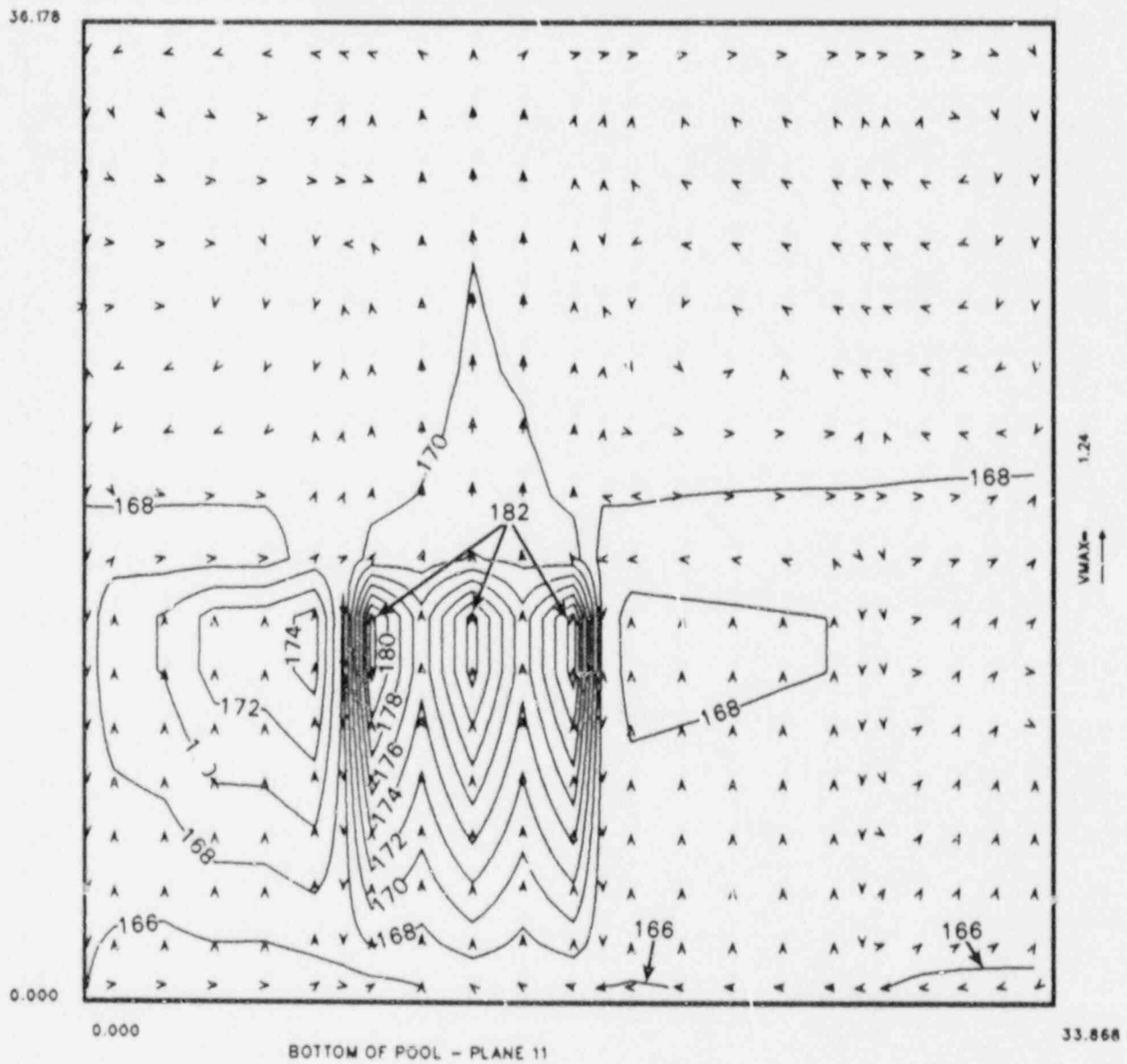


FIGURE 68. Temperature and Velocity Distribution in a Plane above the Leveling Pads for Case Number 12. ($Q = 1048 \text{ GPM}$, TINLET = 150°F , $P_t/P = 13.9$, inlet flow down, peak heat generation near center of pool)

38.178

0.000

1.58

VMAX

33.868

BOTTOM OF POOL - PLANE 11

FIGURE 69. Temperature and Velocity Distribution in a Plane above the Leveling Pads for Case Number 14. ($Q = 1048 \text{ GPM}$, TINLET = 150°F , $\dot{m}/\dot{P} = 13.9$, inlet flow horizontal, peak heat generation near center of pool)

36.178

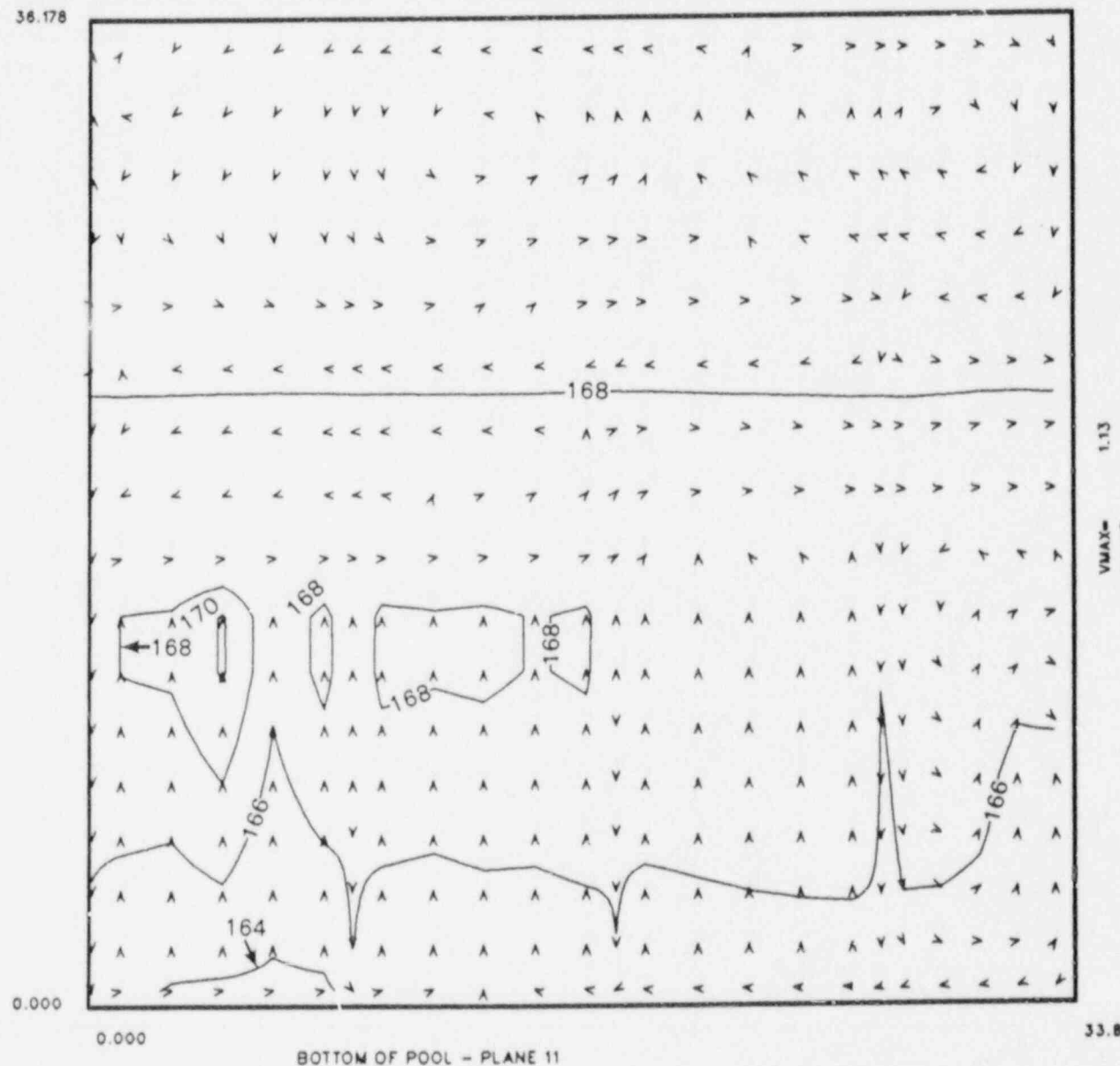


FIGURE 70. Temperature and Velocity Distribution in a Plane above the Leveling Pads for Case Number 16. ($Q = 1048 \text{ GPM}$, TINLET = 150°F , $P_1/P_0 = 13.9$, inlet flow down, peak heat generation near edge of pool)

38.178

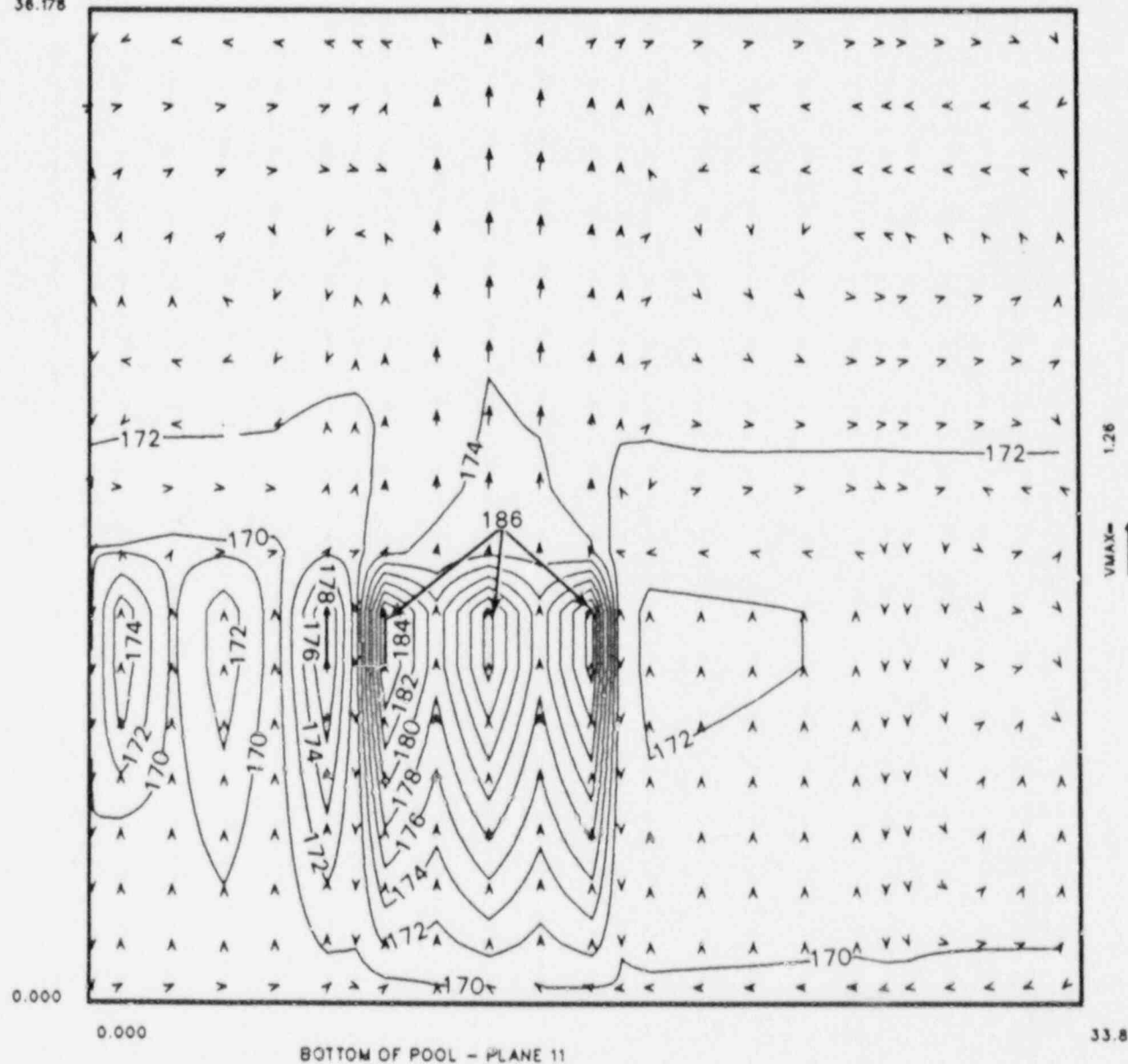


FIGURE 71. Temperature and Velocity Distribution in a Plane above the Leveling Pads for Case Number 17. ($Q = 450 \text{ GPM}$, TINLET = 130°F , $P_1/P_0 = 13.9$, inlet flow down, peak heat generation near center of pool)

36.178

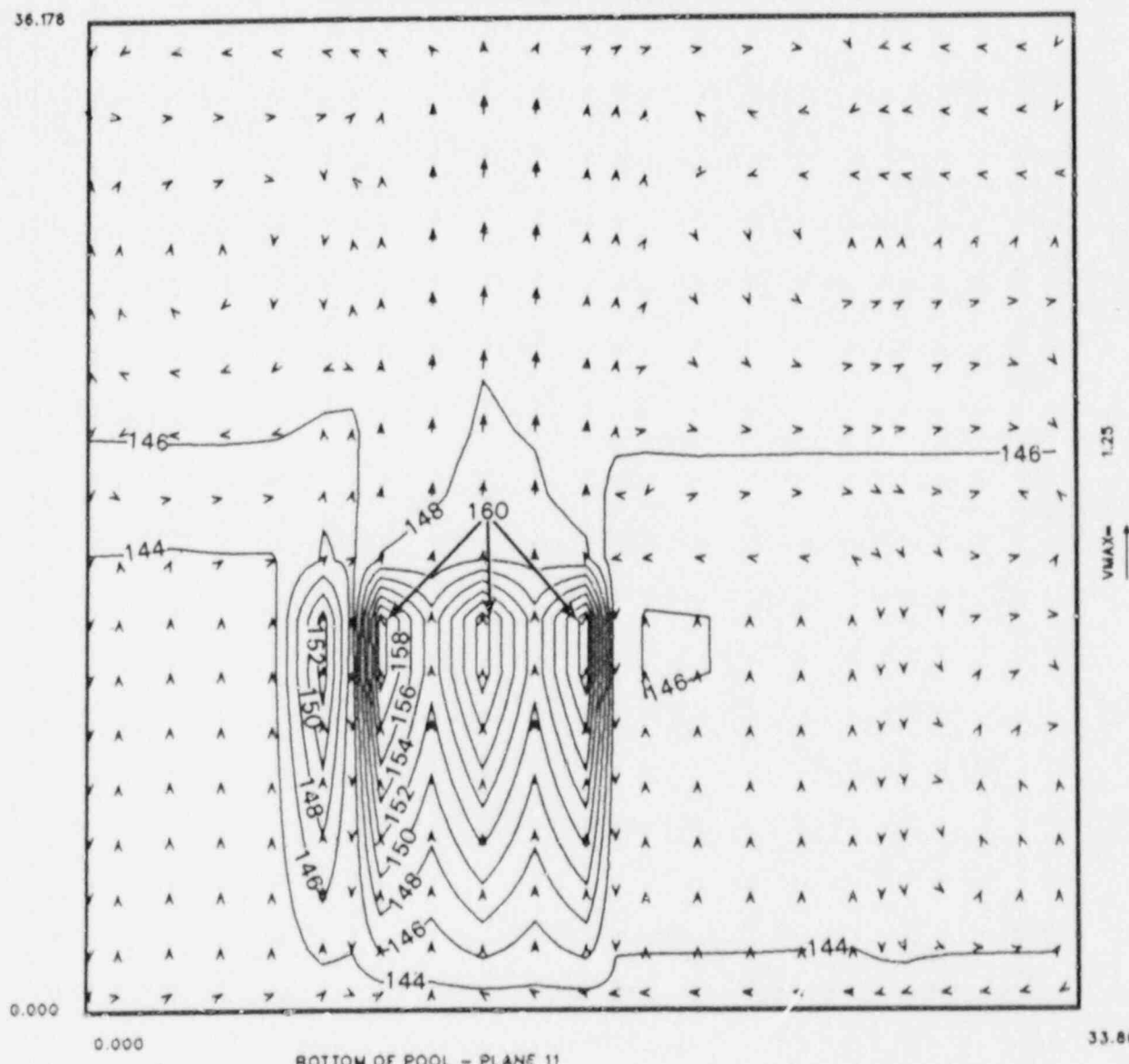


FIGURE 72. Temperature and Velocity Distribution in a Plane above the Leveling Pads for Case Number 18. ($Q = 450 \text{ GPM}$, TINLET = 100°F , $P_t/P = 13.9$, inlet flow down, peak heat generation near center of pool)

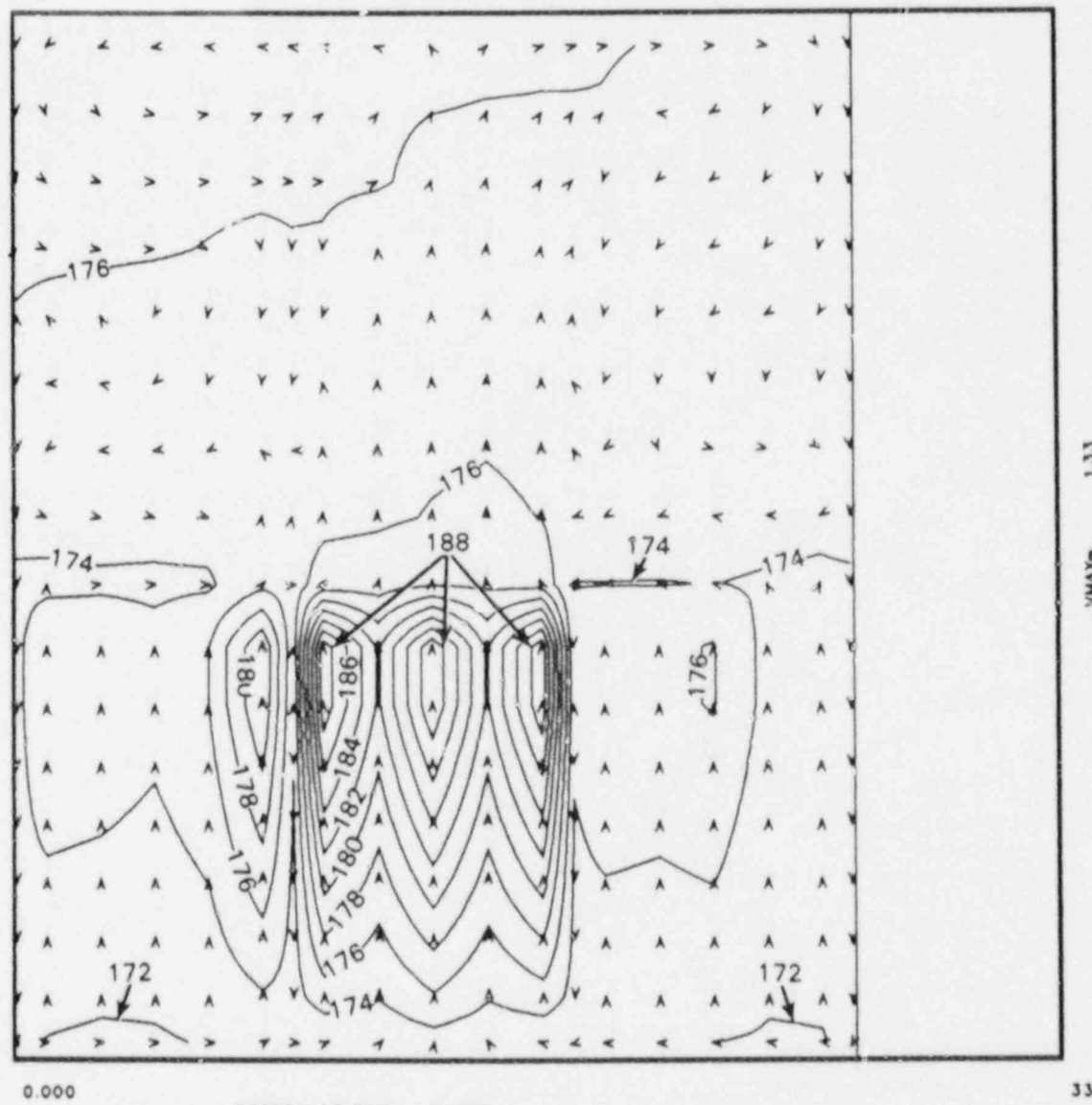
38.178

0.000

1.33

VMAXe

33.868



BOTTOM OF POOL - PLANE 11

FIGURE 73. Temperature and Velocity Distribution in a Plane above the Leveling Pads for Case Number 19. ($Q = 450 \text{ GPM}$, $T_{INLET} = 130^\circ\text{F}$, $P_t/P = 13.9$, inlet flow down, peak heat generation near center of pool, large open flow region of cask area removed from model)

CONCLUSIONS

The results presented in this report show that natural circulation is sufficient to ensure adequate cooling of the spent fuel, regardless of the loading pattern used or the orientation of the cooling system discharge nozzle. The licensee's analysis predicted a hot bundle temperature rise of 15° or 27% greater than that calculated by TEMPEST using a three-dimensional model and conservative bundle loss coefficients.

It is also concluded that the open flow region above the fuel will be well mixed and that there is sufficient flow area around the periphery and beneath the storage racks to ensure adequate cooling, regardless of the loading pattern used.

Locating the cooling system discharge nozzle in the region above the pool rather than below does not significantly degrade the pool cooling performance. However, locating the inlet above the fuel bundles does change the location of the maximum temperature rise, as it does not necessarily occur in the bundle with the highest heat generation rate. In addition, the incoming cold fluid tends to place a flow resistance cap over the bundles in the vicinity of the discharge nozzle, which competes with the buoyancy effects of the heated bundles below. This results in stable temperature oscillations of 8°F in some of the bundles near the discharge nozzle.

REFERENCE

Trent, D. S., L. L. Eyler and M. J. Budden. 1983. TEMPEST--A Three-Dimensional Time-Dependent Computer Program for Hydrothermal Analysis. Volume I: Numerical Methods and Input Instruction. PNL-4348, Pacific Northwest Laboratory, Richland, Washington.

APPENDIX A

INPUT FOR CASES 5, 9, 10, 11, 12, 14, 16, 17, 18, 19

APPENDIX A

INPUT FOR CASE 5

```

*
size,   26   19   23
time,  1.0   100          2200
prnt,    100   100    2   18   1
time,   .1   600          1700
prnt,                  2   18   1
rest,     1   1
pres,   200          1-8
post,
misc,
temp,

cont,read,tess,
cont,heat,pace,mont,dtim,
cont,save,
cont,rxio,besq,
cont,pore,
dbug,in t,prop,ttbl,mt p,nt p,size,data,
dbug,dcid,vp r,ap r,
aout,velz,vel ,vel ,temp,

      1   26   1   19   1   23   1   1
      0   1           2   25   2   18   3   22   1   1   all
      50          3   7   3   9   4   4   1   1   block
      50          9   10  3   9   4   4   1   1   block
      20          1           2   25   19  19   3   22   1   1   top
      0   1   0   0   25   25  14  14   21  21   1   1   inflo
      0   1   0   0   3   3   14  14   21  21   1   1   inflo
      0   1   2   1   25   25  14  14   21  21   1   1   inflo
      0   1   2   2   3   3   14  14   21  21   1   1   inflo
      40          1           10  10   14  14   2   2   1   1   outfl
      40          1           18  18   14  14   2   2   1   1   outfl
      1   49   1   3   19   3   9   4   22   4   4   cells
      50   51   1   3   19   3   9   3   3   4   4   edge
      50   51   0   3   25   3   9   22  22   4   4   edge
      1   51   50   2   2   3   9   3   21   4   4   side
      53   52   1   2   19   3   9   10  10   4   4   rstrip
      53   52   1   3   19   3   9   16  16   4   4   rstrip
      1   52   53   8   8   3   9   3   21   4   4   xstrip
      1   52   53   14  14   3   9   3   21   4   4   xstrip
      1   52   53   20  20   3   9   18  21   4   4   xstrip
      1   49   1   21  25   3   9   18  21   4   4   cells

```

1		21	25	3	9	17	17		4	cells
		2	2	3	9	10	10		4	in sect
		2	2	3	9	16	16		4	in sect
		8	8	3	9	10	10		4	in sect
		8	8	3	9	16	16		4	in sect
		14	14	3	9	10	10		4	in sect
		14	14	3	9	16	16		4	in sect
5		2	19	2	2	3	22		4	edge a k
2	4	3	3	19	2	2	4	21	4	l pleu k
2	6	3	9	9	2	2	11	11	4	foot k
2	6	3	9	9	2	2	15	15	4	foot k
2	6	3	11	11	2	2	11	11	4	foot k
2	6	3	11	11	2	2	15	15	4	foot k
2	6	3	13	13	2	2	11	11	4	foot k
2	6	3	13	13	2	2	15	15	4	foot k
2	4	3	21	25	2	2	18	21	4	1 pceuk
11	2	12	13	2	11	14	2	13	2	5 mont
11	5	12	13	5	11	14	5	13	2	5 mont
11	15	12	13	15	11	14	15	13	3	5 mont
20	3	19	20	3	20	20	3	21	1	5
9	5	21	11	5	9	6	5	13	1	5 mont
1	2	2.37	3	721.11	8	90	180	90		1
9	1321.11	14	14	2.75	15	1921.11			1	3in
20	20	2.75	21	2615.83					1	3in
1	2	14.5	3	9 24.	10	1927.96			1	4in
1	3	2.37	4	915.83	10	10	2.75		1	5in
11	1515.83	16	16	2.75	17	2115.83			1	5in
22	23	2.37							1	5in
150.			14.7	150.	50.	400.	26	1	2	1c1 6 h20
170.					1	26	1	19	1	23 9 allt
170.					1	26	9	19	1	23 9 upper
180.					3	19	3	8	4	21
150.					9	17	3	8	21	21 9 upit
150.					8	8	3	8	3	21 9
150.					14	14	3	8	3	21 9
150.					3	19	3	8	10	10 9
150.					3	19	3	8	16	16 9
170.					21	25	3	8	18	21 9
	1-9				2	25	2	18	3	22 r 9 all
2384.					3	19	3	8	4	21 r 9 heat1
2384.					21	25	3	8	18	21 r 9 heat2
3574.					7	13	3	8	11	15 r 9 hot1
1191.					9	10	3	8	21	21 r 9 hot2
1986.					18	18	3	8	21	21 r 9 heat4
794.7					11	17	3	9	21	21 r 9 heat5
596.					11	11	3	8	4	4 r 9 heat3
1-9					8	8	3	8	4	21 r 9 strip

1-9				14	14	3	8	4	21	r	9	strip	
1-9				3	19	3	8	10	10	r	9	strip	
1-9				3	19	3	8	16	16	r	9	strip	
0.	-1.07			-1.159132.					1	16		in sorce	
1.e+9	-1.07			-1.159132.					1	16		in sorce	
0.	-0.80			-.8649132.					2	16		in sorce	
1.e+9	-0.80			-.8649132.					2	16		in sorce	
0.	0.	30.	1.	1+9	1.				3	1	24	q-table	
-99999	2.								1	1	17	z-t wall	
.13	1.	.003	1.	.003	1.	.002	1.	.002	1.	49	53	17	friction
1.04	2.	.78	2.23	77	2.	1.6	2.	283.	2.	2	6	17	l plen
.695	1.0	.695	1.0			2	19	3	8	3	21	36	all pore
.695	.54	.695	.54			2	19	2	2	3	21	36	all pore
.232	1.0	.232	1.0			9	17	3	8	21	21	36	back pore
.602	1.0	.602	1.0			18	18	3	8	21	21	36	back pore
.174	1.0	.174	1.0			11	11	3	8	4	4	36	front pore
1.	1.	1.	1.0			2	19	2	8	3	3	36	strip p.
1.	1.	1.	1.0			2	19	2	8	10	36	strip p.	
1.	1.	1.	1.0			2	19	2	8	16	16	36	strip p.
1.	1.0	1.	1.			8	8	2	8	3	21	36	strip p.
1.	1.0	1.	1.			14	14	2	8	3	21	36	strip p.
.695	1.0	.695	1.0			21	25	3	8	18	21	36	c pore
1.	1.	1.	1.0			21	25	3	8	17	17	36	c pore
1.	1.	1.0	1.			20	20	2	8	18	21	36	c pore
.695	.54	.695	.54			21	25	2	2	18	21	36	c pore

INPUT FOR CASE 9

```

*
size,   26   19   23
cime,  1.0   100          2200
prnt,    100   100   2   18   1
time,   .1   600          1600
prnt,                2   18   1
rest,     1     1
pres,   200          1-8
post,
misc,                  1     1     1
temp,
seal,                      10.

```

```

cont,read,tess,
cont,heat,pace,mont,dtim,
cont,save,
cont,rxio,besq,
cont,pore,
dbug,in t,prop,ttbl,mt p,nt p,size,data,
dbug,dcid,vp r,ap r,
aout,velz,vel ,vel ,temp,

```

50			1	26	1	19	1	23		1	
0	1		2	25	2	18	3	22		1	all
50			3	7	3	9	4	4		1	block
50			9	10	3	9	4	4		1	block
20	1		2	25	19	19	3	22		1	top
0	1 0 0		25	25	14	14	21	21		1	inflo
0	1 0 0		3	3	14	14	21	21		1	inflo
0	1 2 1		25	25	14	14	21	21		1	inflo
0	1 2 2		3	3	14	14	21	21		1	inflo
40	1		10	10	14	14	2	2		1	outfl
40	1		18	18	14	14	2	2		1	outfl
1	49	1	3	19	3	9	4	22		4	cells
50	51	1	3	19	3	9	3	3		4	edge
50	51	0	3	25	3	9	22	22		4	edge
1	51	50	2	2	3	9	3	21		4	side
53	52	1	2	19	3	9	10	10		4	rstrip
53	52	1	3	19	3	9	16	16		4	rstrip
1	52	53	8	8	3	9	3	21		4	xstrip
1	52	53	14	14	3	9	3	21		4	xstrip
1	52	53	20	20	3	9	18	21		4	xstrip
1	49	1	21	25	3	9	18	21		4	cells
		1	21	25	3	9	17	17		4	cells
			2	2	3	9	10	10		4	in sect
			2	2	3	9	16	16		4	in sect

0.		-.267		-.2889132.			1	16	in sorce		
1.e+9		-.267		-.2889132.			1	16	in sorce		
0.		-0.20		-.2169132.			2	16	in sorce		
1.e+9		-0.20		-.2169132.			2	16	in sorce		
0.	0.	30.	1.	1e+9	1.		3	1	24	q-table	
-9999	2.					1	1		17	z-t wall	
.13	1.	.003	1.	.003	1.	.002	1.	.002	1.	friction	
1.04	2.	.78	2.23	.77	2.	1.6	2.	.283.	2.	1 plen	
.695	1.0	.695	1.0			2	19	3	8	21	all pore
.695	.54	.695	.54			2	19	2	2	21	all pore
.232	1.0	.232	1.0			9	17	3	8	21	back pore
.602	1.0	.602	1.0			18	18	3	8	21	back pore
.174	1.0	.174	1.0			11	11	3	8	4	front pore
1.	1.	1.	1.0			2	19	2	8	3	strip p.
1.	1.	1.	1.0			2	19	2	8	10	strip p.
1.	1.	1.	1.0			2	19	2	8	16	strip p.
1.	1.0	1.	1.			8	8	2	8	3	strip p.
1.	1.0	1.	1.			14	14	2	8	3	strip p.
.695	1.0	.695	1.0			21	25	3	8	18	c pore
1.	1.	1.	1.0			21	25	3	8	17	c pore
1.	1.	1.0	1.			20	20	2	8	18	: pore
.695	.54	.695	.54			21	25	2	2	18	: pore

INPUT FOR CASE 10

```
*tin=130., qtot=450gpm ,power=10.11 mbtu/hr
size, 26 19 23
time, 1.0 100 2200
prnt, 100 100 2 18 1
time, .1 600 1600
prnt, 2 18 1
rest, 1 1
pres, 200 1-8
post,
misc, 1 1 1
temp,
seal, 10.
```

```
cont,read,tess,
cont,heat,pace,mont,dtim,
cont,save,
cont,rxio,besq,
cont,pore,
dbug,in t,prop,ttbl,mt p,nt p,size,data,
dbug,dcid,vp r,ap r,
aout,velz,vel ,vel ,temp,
```

50			1	26	1	19	1	23	1	
0	1		2	25	2	18	3	22	1	all
50			3	7	3	9	4	4	1	block
50			9	10	3	9	4	4	1	block
20	1		2	25	19	19	3	22	1	top
0	1 0 0		25	25	14	14	21	21	1	inflo
0	1 0 0		3	3	14	14	21	21	1	inflo
0	1 2 1		25	25	14	14	21	21	1	inflo
0	1 2 2		3	3	14	14	21	21	1	inflo
40	1		10	10	14	14	2	2	1	outfl
40	1		18	18	14	14	2	2	1	outfl
1	49	1	3	19	3	9	4	22	4	cells
50	51	1	3	19	3	9	3	3	4	edge
50	51	0	3	25	3	9	22	22	4	edge
1	51	50	2	2	3	9	3	21	4	side
53	52	1	2	19	3	9	10	10	4	rstrip
53	52	1	3	19	3	9	16	16	4	rstrip
1	52	53	8	8	3	9	3	21	4	xstrip
1	52	53	14	14	3	9	3	21	4	xstrip
1	52	53	20	20	3	9	18	21	4	xstrip
1	49	1	21	25	3	9	18	21	4	cells
		1	21	25	3	9	17	17	4	cells
			2	2	3	9	10	10	4	in sect
			2	2	3	9	16	16	4	in sect

			8	8	3	9	10	10		4	in sect
			8	8	3	9	16	16		4	in sect
			14	14	3	9	10	10		4	in sect
			14	14	3	9	16	16		4	in sect
		5	2	19	2	2	3	22		4	edge a k
2	4	3	3	19	2	2	4	21		4	1 pleu k
2	6	3	9	9	2	2	11	11		4	foot k
2	6	3	9	9	2	2	15	15		4	foot k
2	6	3	11	11	2	2	11	11		4	foot k
2	6	3	11	11	2	2	15	15		4	foot k
2	6	3	13	13	2	2	11	11		4	foot k
2	6	3	13	13	2	2	15	15		4	foot k
2	4	3	21	25	2	2	18	21		4	1 pceuk
11	2	12	13	2	11	14	2	13	23	2	5 mont
11	5	12	13	5	11	14	5	13	23	5	5 mont
11	15	12	13	15	11	14	15	13	23	15	5 mont
20	3	19	20	3	20	20	3	21	20	3	5 mont
9	5	21	11	5	9	6	5	13	18	5	1 mont
						90	180	90			
1	2	2.37	3	721.11	8	8	2.75			1	1
9	1321.11	14	14	2.75	15	1921.11				1	3in
20	20	2.75	21	2615.83						1	3in
1	2	14.5	3	9 24.	10	1927.96				1	3in
1	3	2.37	4	915.83	10	10	2.75			1	4in
11	15	15.83	16	16	2.75	17	2115.83			1	5in
22	23	2.37								1	5in
			14.7	150.	50.	400.	26	1	2	1cl	6 h20
150.					1	26	1	19	1	23	9 allt
170.					1	26	9	19	1	23	9 upper
170.					3	19	3	8	4	21	9
180.					9	17	3	8	21	21	9 upit
150.					8	8	3	8	3	21	9
150.					14	14	3	8	3	21	9
150.					3	19	3	8	10	10	9
150.					3	19	3	8	16	16	9
170.					21	25	3	8	18	21	9
	1-9				2	25	2	18	3	22 r	9 all
1417.					3	19	3	8	4	21 r	9 heat1
1417.					21	25	3	8	18	21 r	9 heat2
2126.					7	13	3	8	11	15 r	9 hot1
708.3					9	10	3	8	21	21 r	9 hot2
1181.					18	18	3	8	21	21 r	9 heat4
472.6					11	17	3	9	21	21 r	9 heat5
354.4					11	11	3	8	4	4 r	9 heat3
1-9					8	8	3	8	4	21 r	9 strip
1-9					14	14	3	8	4	21 r	9 strip
1-9					3	19	3	8	10	10 r	9 strip
1-9					3	19	3	8	16	16 r	9 strip

0.		-.267		-.2887924.			1	16	in sorce				
1.e+9		-.267		-.2887924.			1	16	in sorce				
0.		-0.20		-.2167924.			2	16	in sorce				
1.e+9		-0.20		-.2167924.			2	16	in sorce				
0.	0.	30.	1.	1+9	1.		3	1	24	q-table			
-9999	2.					1	1		17	z-t wall			
.13	1.	.003	1.	.003	1.	.002	1.	.002	49	53	17	friction	
1.04	2.	.78	2.23	77	2.	1.6	2.	283.	2	6	17	l plen	
.695	1.0	.695	1.0			2	19	3	8	3	21	36	all pore
.695	.54	.695	.54			2	19	2	2	3	21	36	all pore
.232	1.0	.232	1.0			9	17	3	8	21	21	36	back pore
.602	1.0	.602	1.0			18	18	3	8	21	21	36	back pore
.174	1.0	.174	1.0			11	11	3	8	4	4	36	front pore
1.	1.	1.	1.0			2	19	2	8	3	3	36	strip p.
1.	1.	1.	1.0			2	19	2	8	10	10	36	strip p.
1.	1.	1.	1.0			2	19	2	8	16	16	36	strip p.
1.	1.0	1.	1.			8	8	2	8	3	21	36	strip p.
1.	1.0	1.	1.			14	14	2	8	3	21	36	strip p.
.695	1.0	.695	1.0			21	25	3	8	18	21	36	c pore
1.	1.	1.	1.0			21	25	3	8	17	17	36	c pore
1.	1.	1.0	1.			20	20	2	8	18	21	36	c pore
.695	.54	.695	.54			21	25	2	2	18	21	36	c pore

INPUT FOR CASE 11

```

* high power rods under inlet
size, 26 19 23
time, 1.0 100 2200
prnt, 100 100 2 18 1
time, .1 600 1600
prnt, 2 18 1
rest, 1 1
pres, 200 1-8
post,
misc, 1 1 1
temp,
seal, 10.
cont,read,tess,
cont,heat,pace,mont,dtim,
cont,save,
cont,rxio,besq,
cont,pore,
dbug,in t,prop,ttbl,mt p,nt p,size,data,
dbug,dcid,vp r,ap r,
aout,velz,vel ,vel ,temp,

```

50		1	26	1	19	1	23		1	
0	1		2	25	2	18	3	22	1	all
50			3	7	3	9	4	4	1	block
50			9	10	3	9	4	4	1	block
20	1		2	25	19	19	3	22	1	top
0	1 0 0		25	25	14	14	21	21	1	inflo
0	1 0 0		3	3	14	14	21	21	1	inflo
0	1 2 1		25	25	14	14	21	21	1	inflo
0	1 2 2		3	3	14	14	21	21	1	inflo
40	1		10	10	14	14	2	2	1	outfl
40	1		18	18	14	14	2	2	1	outfl
1	49	1	3	19	3	9	4	22	4	cells
50	51	1	3	19	3	9	3	3	4	edge
50	51	0	3	25	3	9	22	22	4	edge
1	51	50	2	2	3	9	3	21	4	side
53	52	1	2	19	3	9	10	10	4	rstrip
53	52	1	3	19	3	9	16	16	4	rstrip
1	52	53	8	8	3	9	3	21	4	xstrip
1	52	53	14	14	3	9	3	21	4	xstrip
1	52	53	20	20	3	9	18	21	4	xstrip
1	49	1	21	25	3	9	18	21	4	cells
		1	21	25	3	9	17	17	4	cells
			2	2	3	9	10	10	4	in sect
			2	2	3	9	16	16	4	in sect

	1-9				3	10	3	8	16	16	r	9	strip
0					.267	.2889132.				1	16		in sorce
1.e+9					-.267	-.2889132.				1	16		in sorce
0.					-0.20	-.2169132.				2	16		in sorce
1.e+9					-0.20	-.2169132.				2	16		in sorce
0.	0.	30.	1.	1+9	1.				3	1	24		q-table
-9999	2.								1	1	17		z-t wall
.13	1.	.003	1.	.003	1.	.002	1.	.002	49	53		17	friction
1.04	2.	.78	2.23	.77	2.	1.6	2.	283.	2	6		17	1 plen
.695	1.0	.695	1.0			2	19	3	8	3	21	36	all pore
.695	.54	.695	.54			2	19	2	2	3	21	36	all pore
.232	1.0	.232	1.0			9	17	3	8	21	21	36	back pore
.602	1.0	.602	1.0			18	18	3	8	21	21	36	back pore
.174	1.0	.174	1.0			11	11	3	8	4	4	36	front pore
1.	1.	1.	1.0			2	19	2	8	3	3	36	strip p.
1.	1.	1.	1.0			2	19	2	8	10	10	36	strip p.
1.	1.	1.	1.0			2	19	2	8	16	16	36	strip p.
1.	1.0	1.	1.			8	8	2	8	3	21	36	strip p.
1.	1.0	1.	1.			14	14	2	8	3	21	36	strip p.
.695	1.0	.695	1.0			21	25	3	8	18	21	36	c pore
1.	1.	1.	1.0			21	25	3	8	17	17	36	c pore
1.	1.	1.0	1.			20	20	2	8	18	21	36	c pore
.695	.54	.695	.54			21	25	2	2	18	21	36	c pore

INPUT FOR CASE 12

* assebΔmblies in hot discharge near center of pool. pr=13.9,ti=150f

size, 26 19 23
 time, 1.0 100 2200
 prnt, 100 100 2 18 1
 time, .1 600 1600 132
 prnt, 2 18 1
 rest, 1 1
 pres, 200 1-8
 post,
 misc,
 temp,
 seal,

10.

cont,read,tess,
 cont,heat,pace,mont,dtim,
 cont,save,
 cont,rxio,besq,
 cont,pore,
 dbug,in t,prop,ttbl,mt p,nt p,size,data,
 dbug,dcid,vp r,ap r,
 aout,velz,vel ,vel ,temp,

50		1	26	1	19	1	23	1	all
0	1		25	2	18	3	22	1	block
50			3	7	3	9	4	1	block
50			9	10	3	9	4	1	top
20	1		25	25	19	19	3	22	
0	1 0 0		25	25	14	14	21	21	inflo
0	1 0 0		3	3	14	14	21	21	inflo
0	1 2 1		25	25	14	14	21	21	inflo
0	1 2 2		3	3	14	14	21	21	inflo
40	1		10	10	14	14	2	2	outfl
40	1		18	18	14	14	2	2	outfl
1	49	1	3	19	3	9	4	22	cells
50	51	1	3	19	3	9	3	3	edge
50	51	0	3	25	3	9	22	22	edge
1	51	50	2	2	3	9	3	21	side
53	52	1	2	19	3	9	10	10	rstrip
53	52	1	3	19	3	9	16	16	rstrip
1	52	53	8	8	3	9	3	21	xstrip
1	52	53	14	14	3	9	3	21	xstrip
1	52	53	20	20	3	9	18	21	cells
1	49	1	21	25	3	9	18	21	cells
		1	21	25	3	9	17	17	in sect
			2	2	3	9	10	10	in sect
			2	2	3	9	16	16	

			8	8	3	9	10	10		4	in sect
			8	8	3	9	16	16		4	in sect
			14	14	3	9	10	10		4	in sect
			14	14	3	9	16	16		4	in sect
			2	19	2	2	3	22		4	edge a k
2	4	3	3	19	2	2	4	21		4	l pleuk
2	6	3	9	9	2	2	11	11		4	foot k
2	6	3	9	9	2	2	15	15		4	foot k
2	6	3	11	11	2	2	11	11		4	foot k
2	6	3	11	11	2	2	15	15		4	foot k
2	6	3	13	13	2	2	11	11		4	foot k
2	6	3	13	13	2	2	15	15		4	foot k
2	4	3	21	25	2	2	18	21		4	l pceuk
11	2	12	13	2	11	14	2	13	23	5	mont
11	5	12	13	5	11	14	5	13	23	5	mont
11	15	12	13	15	11	14	15	13	23	15	mont
20	3	19	20	3	20	20	3	21	20	3	22
9	5	21	11	5	9	6	5	13	18	5	1
										1	5
										5	mont

1	2	2.37	3	721.11	8	8	2.75	90	180	90		1
9	1321.11	14	14	2.75	15	1921.11					1	3in
20	20	2.75	21	2615.83							1	3in
1	2	14.5	3	9 24.	10	1927.96					1	3in
1	3	2.37	4	915.83	10	10	2.75				1	4in
11	1515.83	16	16	2.75	17	2115.83					1	5in
22	23	2.37									1	5in
											6	h20
150.				14.7	150.	50.	400.	26	1	2	1cl	
170.						1	26	1	19	1	23	9
170.						1	26	9	19	1	23	9
180.						3	19	3	8	4	21	9
150.						9	17	3	8	21	21	9
150.						8	8	3	8	3	21	9
150.						14	14	3	8	3	21	9
150.						3	19	3	8	10	10	9
150.						3	19	3	8	16	16	9
170.						21	25	3	8	18	21	9
	1-9					2	25	2	18	3	22	r
	535.7					3	19	3	8	4	21	r
	535.7					21	25	3	8	18	21	r
	803.8					7	13	3	8	11	15	r
	267.8					9	10	3	8	21	21	r
	446.5					18	18	3	8	21	21	r
	178.7					11	17	3	8	21	21	r
	211+2					7	13	3	8	11	11	r
	212+2					9	13	3	8	12	12	r
	134.0					11	11	3	8	4	4	r
	1-9					8	8	3	8	4	21	r
	1-9					14	14	3	8	4	21	r
											9	strip

					3	19	3	8	10	10	r	9	strip	
					3	19	3	8	16	16	r	9	strip	
1-9														
1-9														
0.			.267			.2889132.								
1.e+9			.267			.2889132.								
0.			-0.20			.2169132.								
1.e+9			-0.20			.2169132.								
0.	0.	30.	1.	1+9	1.					3	1	24	q-table	
-9999	2.									1	1	17	z-t wall	
.13	1.	.003	1.	.003	1.	.002	1.	.002	1.	49	53	17	friction	
1.04	2.	.78	2.23	.77	2.	1.6	2.	283.	2.	2	6	17	1 plen	
.695	1.0	.695	1.0				2	19	3	8	3	21	36 all pore	
.695	.54	.695	.54				2	19	2	2	3	21	36 all pore	
.232	1.0	.232	1.0				9	17	3	8	21	21	36 back pore	
.602	1.0	.602	1.0				18	18	3	8	21	21	36 back pore	
.174	1.0	.174	1.0				11	11	3	8	4	4	36 front pore	
1.	1.	1.	1.0				2	19	2	8	3	3	36 strip p.	
1.	1.	1.	1.0				2	19	2	8	10	10	36 strip p.	
1.	1.	1.	1.0				2	19	2	8	16	16	36 strip p.	
1.	1.0	1.	1.				8	8	2	8	3	21	36 strip p.	
1.	1.0	1.	1.				14	14	2	8	3	21	36 strip p.	
.695	1.0	.695	1.0				21	25	3	8	18	21	36 c pore	
1.	1.	1.	1.0				21	25	3	8	17	17	36 c pore	
1.	1.	1.0	1.				20	20	2	8	18	21	36 c pore	
.695	.54	.695	.54				21	25	2	2	18	21	36 c pore	

INPUT FOR CASE 14

* asse. in hot discharge near center of pool. pr=13.9,ti=150f, w/F.D.

size, 26 19 23
 time, 1.0 100 2200
 prnt, 100 100 2 18 1
 time, .1 600 1600 132
 prnt, 2 18 1
 rest, 1 1
 pres, 200 1-8
 post,
 misc, 1 1 1
 temp,
 seal, 10.

cont,read,tess,
 cont,heat,pace,mont,dtim,
 cont,save,
 cont,rxio,besq,
 cont,pore,
 dbug,in t,prop,ttbl,mt p,nt p,size,data,
 dbug,dcid,vp r,ap r,
 aout,velz,vel ,vel ,temp,

50		1	26	1	19	1	23	1	
0	1		2	25	2	18	3	22	1
50			3	7	3	9	4	4	1
50			9	10	3	9	4	4	1
20	1		2	25	19	19	3	22	1
0	1 0 0		25	25	14	14	21	21	1
0	1 0 0		3	3	14	14	21	21	1
0	1222 1		25	25	14	14	21	21	1
0	1122 2		3	3	14	14	21	21	1
40	1		10	10	14	14	2	2	1
40	1		18	18	14	14	2	2	1
1	49	1	3	19	3	9	4	22	4
50	51	1	3	19	3	9	3	3	4
50	51	0	3	25	3	9	22	22	4
1	51	50	2	2	3	9	3	21	4
53	52	1	2	19	3	9	10	10	4
53	52	1	3	19	3	9	16	16	4
1	52	53	8	8	3	9	3	21	4
1	52	53	14	14	3	9	3	21	4
1	52	53	20	20	3	9	18	21	4
1	49	1	21	25	3	9	18	21	4
		1	21	25	3	9	17	17	4
			2	2	3	9	10	10	4
			2	2	3	9	16	16	4

			8	8	3	9	10	10		4	in sect	
			8	8	3	9	16	16		4	in sect	
			14	14	3	9	10	10		4	in sect	
			14	14	3	9	16	16		4	in sect	
			5	2	19	2	2	3	22		4 edge a k	
2	4	3	3	3	19	2	2	4	21		4 l pleu k	
2	6	3	9	9	2	2	11	11			4 foot k	
2	6	3	9	9	2	2	15	15			4 foot k	
2	6	3	11	11	2	2	11	11			4 foot k	
2	6	3	11	11	2	2	15	15			4 foot k	
2	6	3	13	13	2	2	11	11			4 foot k	
2	6	3	13	13	2	2	15	15			4 foot k	
2	4	3	21	25	2	2	18	21			4 l pceuk	
11	2	12	13	2	11	14	2	13	23	2	13	4 mont
11	5	12	13	5	11	14	5	13	23	5	13	2 mont
11	15	12	13	15	11	14	15	13	23	15	13	3 mont
20	3	19	20	3	20	20	3	21	20	3	22	1 mont
9	5	21	11	5	9	6	5	13	18	5	2	1 mont
						90	180	90				1
1	2	2.37	3	721.11	8	8	2.75					3in
9	1321.11	14	14	2.75	15	1921.11						3in
20	20	2.75	21	2615.83								3in
1	2	14.5	3	9 24.	10	1927.96						4in
1	3	2.37	4	915.83	10	10	2.75					5in
11	1515.83	16	16	2.75	17	2115.83						5in
22	23	2.37		14.7 150.	50.	400.	26	1	2	1c1	6	h20
150.					1	26	1	19	1	23	9	allt
170.					1	26	9	19	1	23	9	upper
170.					3	19	3	8	4	21	9	
180.					9	17	3	8	21	21	9	upit
150.					8	8	3	8	3	21	9	
150.					14	14	3	8	3	21	9	
150.					3	19	3	8	10	10	9	
150.					3	19	3	8	15	16	9	
150.					21	25	3	8	18	21	9	
170.					2	25	2	18	3	22	r	all
1-9					3	19	3	8	4	21	r	heat1
535.7					21	25	3	8	18	21	r	heat2
535.7					7	13	3	8	11	15	r	hot1
803.8					9	10	3	8	21	21	r	hot2
267.8					18	18	3	8	21	21	r	heat4
446.5					11	17	3	8	21	21	r	heat5
178.7					7	13	3	8	11	11	r	hotd
211+2					9	13	3	8	12	12	r	hotd
212+2					11	11	3	8	4	4	r	heat3
134.0					8	8	3	8	4	21	r	strip
1-9					14	14	3	8	4	21	r	strip

					3	19	3	8	16	10	r	9	strip
					3	19	3	8	16	16	r	9	strip
0.	.068				-.063-	.2889132.				1	16		in sorce
1.e+9	.068				-.068-	.2889132.				1	16		in sorce
0.	-.080				-.080-	.2169132.				2	16		in sorce
1.e+9	-.080				-.080-	.2169132.				2	16		in sorce
0.	0.	30.	1.	1+9	1.					3	1	24	q-table
-9999	2.									1	1	17	z-t wall
.13	1.	.003	1.	.003	1.	.002	1.	.002	1.	49	53	17	friction
1.04	2.	.78	2.23	.77	2.	1.6	2.	.283.	2.	2	6	17	l plen
.695	1.0	.695	1.0			2	19	3	8	3	21	36	all pore
.695	.54	.695	.54			2	19	2	2	3	21	36	all pore
.232	1.0	.232	1.0			9	17	3	8	21	21	36	back pore
.602	1.0	.602	1.0			18	18	3	8	21	21	36	back pore
.174	1.0	.174	1.0			11	11	3	8	4	4	36	front pore
1.	1.	1.	1.0			2	19	2	8	3	3	36	strip p.
1.	1.	1.	1.0			2	19	2	8	10	10	36	strip p.
1.	1.	1.	1.0			2	19	2	8	16	16	36	strip p.
1.	1.0	1.	1.			8	8	2	8	3	21	36	strip p.
1.	1.0	1.	1.			14	14	2	8	3	21	36	strip p.
.695	1.0	.695	1.0			21	25	3	8	18	21	36	c pore
1.	1.	1.	1.0			21	25	3	8	17	17	36	c por.
1.	1.	1.0	1.			20	20	2	8	18	21	36	c
.695	.54	.695	.54			21	25	2	2	18	21	36	c pore

INPUT FOR CASE 16

* assebΔmblies in hot discharge near center of pool. pr=13.9,ti=150f
 size, 26 19 23
 time, 1.0 100 2200
 prnt, 100 100 2 18 1
 time, .1 60 1600 132
 prnt, 2 18 1
 rest, 1 1
 pres, 200 1-8
 post,
 misc, 1 1 1
 temp,
 seal, 10.

cont,read,tess,
 cont,heat,pace,mont,dtim,
 cont save,
 cont,rxiobesq,
 cont,pore,
 dbug,in t,prop,ttbl,mt p,nt p,size,data,
 dbug,dcid,vp r,ap r,
 aout,velz,vel ,ve? ,temp,

50		1	26	1	19	1	23	1	
0	1		25	2	18	3	22	1	all
50			3	7	3	9	4	4	block
50			9	10	3	9	4	4	block
20	1		2	25	19	19	3	22	1
0	1 0 0		25	25	14	14	21	21	top
0	1 0 0		3	3	14	14	21	21	inflo
0	1 2 1		25	25	14	14	21	21	inflo
0	1 2 2		3	3	14	14	21	21	inflo
40	1		10	10	14	14	2	2	outfl
40	1		18	18	14	14	2	2	outfl
1	49	1	3	19	3	9	4	22	cells
50	51	1	3	19	3	9	3	3	edge
50	51	0	3	25	?	9	22	22	edge
1	51	50	2	2	3	9	3	21	side
53	52	1	2	19	3	9	10	10	rstrip
53	52	1	3	19	3	9	16	16	rstrip
1	52	53	8	8	3	9	3	21	xstrip
1	52	53	14	14	3	9	3	21	xstrip
1	52	53	20	20	3	9	18	21	xstrip
1	49	1	21	25	3	9	18	21	cells
			21	25	3	9	17	17	cells
			2	2	3	9	10	10	in sect
			2	2	3	9	16	16	in sect

			8	8	3	9	10	10		4	in sect
			8	8	3	9	16	16		4	in sect
			14	14	3	9	10	10		4	in sect
			14	14	3	9	16	16		4	in sect
		5	2	19	2	2	3	22		4	edge a k
2	4	3	3	19	2	2	4	21		4	l pleuk
2	6	3	9	9	2	2	11	11		4	foot k
2	6	3	9	9	2	2	15	15		4	foot k
2	6	3	11	11	2	2	11	11		4	foot k
2	6	3	11	11	2	2	15	15		4	foot k
2	6	3	13	13	2	2	11	11		4	foot k
2	6	3	13	13	2	2	15	15		4	foot k
2	4	3	21	25	2	2	18	21		4	l pceuk
11	2	12	13	2	11	14	2	13	23	2	5 mont
11	5	12	13	5	11	14	5	13	23	5	5 mont
11	15	12	13	15	11	14	15	13	23	15	5 mont
20	3	19	20	3	20	20	3	21	20	3	5 mont
9	5	21	11	5	9	6	5	13	18	5	1 mont

1	2	2.37	3	721.11	8	8	2.75	90	180	90	1	1
9	1321.11	14	14	2.75	15	1921.11					1	3in
20	20	2.75	21	2615.83							1	3in
1	2	14.5	3	9	24.	10	1927.96				1	3in
1	3	2.37	4	915.83	10	10	2.75				1	4in
11	1515.83	16	16	2.75	17	2115.83					1	5in
22	23	2.37									1	5in
				14.7	150.	50.	400.	26	1	2	1c1	6 h20
150.						1	26	1	19	1	23	9 allt
170.						1	26	9	19	1	23	9 upper
170.						3	19	3	8	4	21	9
180.						9	17	3	8	21	21	9 upit
150.						8	8	3	8	3	21	9
150.						14	14	3	8	3	21	9
150.						3	19	3	8	10	10	9
150.						3	19	3	8	15	16	9
170.						21	25	3	8	18	21	9
1-9						2	25	2	18	3	22	r all
535.7						3	19	3	8	4	21	r heat1
535.7						21	25	3	8	18	21	r heat2
803.8						7	13	3	8	11	15	r hot1
267.8						9	10	3	8	21	21	r hot2
446.5						18	18	3	8	21	21	r heat4
178.7						11	17	3	8	21	21	r heat5
1-9						12	12	3	8	4	4	r cold
211+2						13	19	3	8	4	4	r hotd
1-9						13	13	3	8	5	5	r cold
211+2						15	19	3	8	5	5	r hotd
1-9						13	19	3	8	6	6	r cold

134.0		11	11	3	8	4	4	r	9	heat3
1-9		8	8	3	8	4	21	r	9	strip
1-9		14	14	3	8	4	21	r	9	strip
1-9		3	19	3	8	10	10	r	9	strip
1-9		3	19	3	8	16	16	r	9	strip
0.	-.267						1		16	in sorce
1.e+9	-.267						1		16	in sorce
0.	-0.20						2		16	in sorce
1.e+9	-0.20						2		16	in sorce
0.	0.	30.	1.	1+9	1.			3	1	q-table
-9999	2.					1	1		17	z-t wall
.13	1.	.003	1.	.003	1.	.002	1.	49	53	17
1.04	2.	.78	2.23	77	2.	1.6	2.	283.	2	friction
.695	1.0	.695	1.0		2	19	3	8	3	1 plen
.695	.54	.695	.54		2	19	2	2	3	all pore
.232	1.0	.232	1.0		9	17	3	8	21	all pore
.602	1.0	.602	1.0		18	18	3	8	21	back pore
.174	1.0	.174	1.0		11	11	3	8	4	back pore
1.	1.	1.	1.0		2	19	2	8	3	front pore
1.	1.	1.	1.0		2	19	2	8	10	strip p.
1.	1.	1.	1.0		2	19	2	8	16	strip p.
1.	1.0	1.	1.		8	8	2	8	3	strip p.
1.	1.0	1.	1.		14	14	2	8	3	strip p.
.695	1.0	.695	1.0		21	25	3	8	18	c pore
1.	1.	1.	1.0		21	25	3	8	17	c pore
1.	1.	1.0	1.		20	20	2	8	18	c pore
.695	.54	.695	.54		21	25	2	2	18	c pore
1.	1.	1.	1.0		15	19	3	8	6	cld pore
1.	1.	1.	1.0		13	13	3	8	5	cld pore
1.	1.	1.	1.0		12	12	3	8	4	cld pore

INPUT FOR CASE 17

```

*      assemblies in hot discharge near center of pool. pr=13.9,ti=130f
size,   26   19   23
time,   1.0  100          2200
prnt,    100  100   2   18   1
time,   .1   600          1600 132
prnt,                  2   18   1
rest,     1   1
pres,   200           1-8
post,
misc,
temp,
\$ 1,                      10.

cont,read,tess,
cont,heat,pace,mont,dtim,
cont,save,
cont,rxio,besq,
cont,pore,
dbug,in t,prop,ttbl,mt p,nt p,size,data,
dbug,dcid,vp r,ap r,
aout,velz,vel ,vel ,temp,

```

50		1	26	1	19	1	23		1	
0	1		2	25	2	18	3	22	1	all
50			3	7	3	9	4	4	1	block
50			9	10	3	9	4	4	1	block
20	1		2	25	19	19	3	22	1	top
0	1 0 0		25	25	14	14	21	21	1	inflo
0	1 0 0		3	3	14	14	21	21	1	inflo
0	1 2 1		25	25	14	14	21	21	1	inflo
0	1 2 2		3	3	14	14	21	21	1	inflo
40	1		10	10	14	14	2	2	1	outfl
40	1		18	18	14	14	2	2	1	outfl
1	49	1	3	19	3	9	4	22	4	cells
50	51	1	3	19	3	9	3	3	4	edge
50	51	0	3	25	3	9	22	22	4	edge
1	51	50	2	2	3	9	3	21	4	side
53	52	1	2	19	3	9	10	10	4	rstrip
53	52	1	3	19	3	9	16	16	4	rstrip
1	52	53	8	8	3	9	3	21	4	xstrip
1	52	53	14	14	3	9	3	21	4	xstrip
1	52	53	20	20	3	9	18	21	4	xstrip
1	49	1	21	25	3	9	18	21	4	cells
		1	21	25	3	9	17	17	4	cells
			2	2	3	9	10	10	4	in sect
			2	2	3	9	16	16	4	in sect

			8	8	3	9	10	10		4	in sect
			8	8	3	9	16	16		4	in sect
			14	14	3	9	10	10		4	in sect
			14	14	3	9	16	16		4	in sect
	5		2	19	2	2	3	22		4	edge a k
2	4	3	3	19	2	2	4	21		4	l pleuk
2	6	3	9	9	2	2	11	11		4	foot k
2	6	3	9	9	2	2	15	15		4	foot k
2	6	3	11	11	2	2	11	11		4	foot k
2	6	3	11	11	2	2	15	15		4	foot k
2	6	3	13	13	2	2	11	11		4	foot k
2	6	3	13	13	2	2	15	15		4	foot k
2	4	3	21	25	2	2	18	21		4	l pceuk
11	2	12	13	2	11	14	2	13	23	2	5 mont
11	5	12	13	5	11	14	5	13	23	5	5 mont
11	15	12	13	15	11	14	15	13	23	15	5 mont
20	3	19	20	3	20	20	3	21	20	3	22 1
9	5	21	11	5	9	6	5	13	18	5	2 1 5 mont
					90	180	90				1
1	2	2.37	3	721.11	8	8	2.75			1	3in
9	1321.11	14	14	2.75	15	1921.11				1	3in
20	20	2.75	21	2615.83						1	3in
1	2	14.5	3	9 24.	10	1927.96				1	4in
1	3	2.37	4	915.83	10	10	2.75			1	5in
11	1515.83	16	16	2.75	17	2115.83				1	5in
22	23	2.37		14.7	150.	50.	400.	26	1	2	1cl 6 h20
150.						1	26	1	19	1	23 9 allt
170.						1	26	9	19	1	23 9 upper
170.						3	19	3	8	4	21 9
180.						9	17	3	8	21	21 9 upit
150.						8	8	3	8	3	21 9
150.						14	14	3	8	3	21 9
150.						3	19	3	8	10	10 9
150.						3	19	3	8	16	16 9
170.						21	25	3	8	18	zi 9
1-9						2	25	2	18	3	22 r 9 all
535.7						3	19	3	8	4	21 r 9 heat1
535.7						21	25	3	8	18	21 r 9 heat2
803.8						7	13	3	8	11	15 r 9 hot1
267.8						9	10	3	8	21	21 r 9 hot2
446.5						18	18	3	8	21	21 r 9 heat4
178.7						11	17	3	8	21	21 r 9 heats5
211+2						7	13	3	8	11	11 r 9 hotd
212+2						9	13	3	8	12	12 r 9 hotd
134.0						11	11	3	8	4	4 r 9 heat3
1-9						8	8	3	8	4	21 r 9 strip
1-9						14	14	3	8	4	21 r 9 strip

1-9		3	19	3	8	10	10	r	9	strip			
1-9		3	19	3	8	16	16	r	9	strip			
0.	.267	-.1237924.									1	16	in sorce
1.e+9	.267	-.1237924.									1	16	in sorce
0.	-0.20	-.0937924.									2	16	in sorce
1.e+9	-0.20	-.0937924.									2	16	in sorce
0.	0.	30.	1.	1+9	1.				3	1	24	q-table	
-99999	2.						1	1			17	z-t wall	
.13	1.	.003	1.	.003	1.	.002	1.	.002	1.	49	53	17	friction
1.04	2.	.78	2.23	.77	2.	1.6	2.	.283.	2.	2	6	17	l plen
.695	1.0	.695	1.0			2	19	3	8	3	21	36	all pore
.695	.54	.695	.54			2	19	2	2	3	21	36	all pore
.232	1.0	.232	1.0			9	17	3	8	21	21	36	back pore
.602	1.0	.602	1.0			18	18	3	8	21	21	36	back pore
.174	1.0	.174	1.0			11	11	3	8	4	4	36	front pore
1.	1.	1.	1.0			2	19	2	8	3	3	36	strip p.
1.	1.	1.	1.0			2	19	2	8	10	10	36	strip p.
1.	1.	1.	1.0			2	19	2	8	16	16	36	strip p.
1.	1.0	1.	1.			8	8	2	8	3	21	36	strip p.
1.	1.0	1.	1.			14	14	2	8	3	21	36	strip p.
.695	1.0	.695	1.0			21	25	3	8	18	21	36	c pore
1.	1.	1.	1.0			21	25	3	8	17	17	36	c pore
1.	1.	1.0	1.			20	20	2	8	18	21	36	c pore
.695	.54	.695	.54			21	25	2	2	18	21	36	c pore

INPUT FOR CASE 18

* assemblies in hot discharge near center of pool. pr=13.9,ti=100f
 size, 26 19 23
 time, 1.0 100 2200
 prnt, 100 100 2 18 1
 time, .1 600 1600 132
 prnt, 2 18 1
 rest, 1 1
 pres, 200 1-8
 post,
 misc,
 temp,
 seal, 10.

 cont,read,tess,
 cont,heat,pace,mont,dtim,
 cont,save,
 cont,rxiobesq,
 cont,pore,
 dbug,in t,prop,ttbl,mt p,nt p,size,data,
 dbug,dcid,vp r,ap r,
 aout,velz,vel ,vel ,temp,

50		1	26	1	19	1	23	1	
0	1		2	25	2	18	3	22	1
50			3	7	3	9	4	4	1
50			9	10	3	9	4	4	1
20	1		2	25	19	19	3	22	1
0	1	0	0	25	25	14	14	21	21
0	1	0	0	3	3	14	14	21	21
0	1	2	1	25	25	14	14	21	21
0	1	2	2	3	3	14	14	21	21
40	1		10	10	14	14	2	2	1
40	1		18	18	14	14	2	2	1
1	49	1	3	19	3	9	4	22	4
50	51	1	3	19	3	9	3	3	4
50	51	0	3	25	3	9	22	22	4
1	51	50	2	2	3	9	3	21	4
53	52	1	2	19	3	9	10	10	4
53	52	1	3	19	3	9	16	16	4
1	52	53	8	8	3	9	3	21	4
1	52	53	14	14	3	9	3	21	4
1	52	53	20	20	3	9	18	21	4
1	49	1	21	25	3	9	18	21	4
		1	21	25	3	9	17	17	4
			2	2	3	9	10	10	4
			2	2	3	9	16	16	4

			8	8	3	9	10	10		4	in sect
			8	8	3	9	16	16		4	in sect
			14	14	3	9	10	10		4	in sect
			14	14	3	9	16	16		4	in sect
	5		2	19	2	2	3	22		4	edge a k
2	4	3	3	19	2	2	4	21		4	l pleu k
2	6	3	9	9	2	2	11	11		4	foot k
2	6	3	9	9	2	2	15	15		4	foot k
2	6	3	11	11	2	2	11	11		4	foot k
2	6	3	11	11	2	2	15	15		4	foot k
2	6	3	13	13	2	2	11	11		4	foot k
2	6	3	13	13	2	2	15	15		4	foot k
2	4	3	21	25	2	2	18	21		4	l pceuk
11	2	12	13	2	11	14	2	13	23	2	5 mont
11	5	12	13	5	11	14	5	13	23	5	5 mont
11	15	12	13	15	11	14	15	13	23	15	5 mont
20	3	19	20	3	20	20	3	21	20	3	5
9	5	21	11	5	9	6	5	13	18	5	2
					90	180	90				1
1	2	2.37	3	721.11	8	8	2.75			1	3in
9	1321.11	14	14	2.75	15	1921.11				1	3in
20	20	2.75	21	2615.83						1	3in
1	2	14.5	3	9 24.	10	1927.96				1	4in
1	3	2.37	4	915.83	10	10	2.75			1	5in
11	1515.83	16	16	2.75	17	2115.83				1	5in
22	23	2.37			14.7	150.	50.	400.	26	1	2
							1	26	1	19	1
							1	26	9	19	1
							3	19	3	8	4
							9	17	3	8	21
							8	8	3	8	21
							14	14	3	8	3
							3	19	3	8	10
							3	19	3	8	16
							21	25	3	8	18
							2	25	2	18	3
							3	19	3	8	4
							21	25	3	8	18
							7	13	3	8	11
							9	10	3	8	21
							18	18	3	8	21
							11	17	3	8	21
							7	13	3	8	11
							9	13	3	8	12
							11	11	3	8	4
							8	8	3	8	4
							14	14	3	8	4
										21	r 9 strip
										21	r 9 strip

1-9		3	19	3	8	10	10	r	9	strip		
1-9		3	19	3	8	16	16	r	9	strip		
0.	.267	-.1236175.								1	16	in sorce
1.e+9	.267	-.1236175.								1	16	in sorce
0.	-0.20	-.0936175.								2	16	in sorce
1.e+9	-0.20	-.0936175.								2	16	in sorce
0.	0.	30.	1.	1+9	1.			3	1	24	q-table	
-9999	2.						1	1		17	z-t wall	
.13	1.	.003	1.	.003	1.	.002	1.	.002	1.	49	53	friction
1.04	2.	.78	2.23	77	2.	1.6	2.	.283	2.	2	6	1 plen
.695	1.0	.695	1.0			2	19	3	8	3	21	all pore
.695	.54	.695	.54			2	19	2	2	3	21	all pore
.232	1.0	.232	1.0			9	17	3	8	21	21	back pore
.602	1.0	.602	1.0			18	18	3	8	21	21	back pore
.174	1.0	.174	1.0			11	11	3	8	4	4	front pore
1.	1.	1.	1.0			2	19	2	8	3	3	strip p.
1.	1.	1.	1.0			2	19	2	8	10	10	strip p.
1.	1.	1.	1.0			2	19	2	8	16	16	strip p.
1.	1.0	1.	1.			8	8	2	8	3	21	strip p.
1.	1.0	1.	1.			14	14	2	8	3	21	strip p.
.695	1.0	.695	1.0			21	25	3	8	18	21	c pore
1.	1.	1.	1.0			21	25	3	8	17	17	c pore
1.	1.	1.0	1.			20	20	2	8	18	21	c pore
.695	.54	.695	.54			21	25	2	2	18	21	c pore

INPUT FOR CASE 19

* asse. in hot discharge near c.o.p.. pr=13.9,ti=130f (no cask area)
 size, 26 19 23
 time, 1.0 100 2200
 prnt, 100 100 2 18 1
 time, .1 600 1600 132
 prnt, 2 18 1
 rest, 1 1
 pres, 200 1-8
 post,
 misc, 1 1 1
 temp,
 seal, 10.

cont,read,tess,
 cont,heat,pace,mont,dtim,
 cont,save,
 cont,rxio,besq,
 cont,pore,
 dbug,in t,prop,ttbl,mt p,nt p,size,data,
 dbug,dcid,vp r,ap r,
 aout,velz,vel ,vel ,temp,

50			1	26	1	19	1	23		1	
0	1		2	25	2	18	3	22		1	all
50			3	7	3	9	4	4		1	block
50			9	10	3	9	4	4		1	block
20	1		2	25	19	19	3	22		1	top
0	1 0 0		25	25	14	14	21	21		1	inflo
0	1 0 0		3	3	14	14	21	21		1	inflow
0	1 2 1		25	25	14	14	21	21		1	inflo
0	1 2 2		3	3	14	14	21	21		1	inflo
40	1		10	10	14	14	2	2		1	outfl
40	1		18	18	14	14	2	2		1	outfl
50			21	25	1	19	1	17		1	imag
1	49 1		3	19	3	9	4	22		4	cells
50	51 1		3	19	3	9	3	3		4	edge
50	51 0		3	25	3	9	22	22		4	edge
1	51 50		2	2	3	9	3	21		4	side
53	52 1		2	19	3	9	10	10		4	rstrip
53	52 1		3	19	3	9	16	16		4	rstrip
1	52 53		8	8	3	9	3	21		4	xstrip
1	52 53		14	14	3	9	3	21		4	xstrip
1	52 53		20	20	3	9	18	21		4	xstrip
1	49 1		21	25	3	9	18	21		4	cells
			1	21	25	3	9	17		4	cells
				2	2	3	9	10		4	in sect

			2	2	3	9	16	16		4	in sect			
			8	8	3	9	10	10		4	in sect			
			8	8	3	9	16	16		4	in sect			
			14	14	3	9	10	10		4	in sect			
			14	14	3	9	16	16		4	in sect			
2	5		2	19	2	2	3	22		4	edge a k			
2	4	3	3	19	2	2	4	21		4	l pleu k			
2	6	3	9	9	2	2	11	11		4	foot k			
2	6	3	9	9	2	2	15	15		4	foot k			
2	6	3	11	11	2	2	11	11		4	foot k			
2	6	3	11	11	2	2	15	15		4	foot k			
2	6	3	13	13	2	2	11	11		4	foot k			
2	6	3	13	13	2	2	15	15		4	foot k			
2	4	3	21	25	2	2	18	21		4	l pceuk			
11	2	12	13	2	11	14	2	13	23	2	13	4	mont	
11	5	12	13	5	11	14	5	13	23	5	13	2	mont	
11	15	12	13	15	11	14	15	13	23	15	13	3	mont	
20	3	19	20	3	20	20	3	21	20	3	22	1	5	
9	9	13	6	9	21	24	9	18	6	9	13	1	5	mont
1	2	2.37	3	721.11	8	8	2.75	90	180	90		1	1	
9	1321.11	14	14	2.75	15	1921.11						1	3in	
20	20	2.75	21	2615.83								1	3in	
1	2	14.5	3	9	24.	10	1927.96					1	4in	
1	3	2.37	4	915.83	10	10	2.75					1	5in	
11	1515.83	16	16	2.75	17	2115.83						1	5in	
22	23	2.37										1	5in	
150.			14.7	150.	50.	400.	26	1	2	1c1	6	h20		
170.					1	26	1	19	1	23	9	allt		
170.					1	26	9	19	1	23	9	upper		
180.					3	19	3	8	4	21	9			
150.					9	17	3	8	21	21	9	upit		
150.					8	8	3	8	3	21	9			
150.					14	14	3	8	3	21	9			
150.					3	19	3	8	10	10	9			
150.					3	19	3	8	16	16	9			
170.					21	25	3	8	18	21	9			
1-9					2	25	2	18	3	22	r	all		
535.7					3	19	3	8	4	21	r	heat1		
535.7					21	25	3	8	18	21	r	heat2		
803.8					7	13	3	8	11	15	r	hot1		
267.8					9	10	3	8	21	2i	r	hot2		
446.5					18	18	3	8	21	21	r	heat4		
178.7					11	17	3	8	21	21	r	heat5		
211+2					7	13	3	8	11	11	r	hotd		
212+2					9	13	3	8	12	12	r	hotd		
134.0					11	11	3	8	4	4	r	heat3		
1-9					8	8	3	8	4	21	r	strip		

DISTRIBUTION

No. of
Copies

OFFSITE

20 NRC
J. N. Ridgely
Rm. 428, Phillips Building
Washington, D.C. 20555

ONSITE

9 Pacific Northwest Laboratory

C. W. Stewart
C. L. Wheeler
Publishing Coordination (2)
Technical Report Files (5)

NRC FORM 336 (2-84) NRCM 1102 3201-3202		U.S. NUCLEAR REGULATORY COMMISSION	
BIBLIOGRAPHIC DATA SHEET			
SEE INSTRUCTIONS ON THE REVERSE		1. REPORT NUMBER (Assigned by TIPR - D.V.M. No. 5048)	
2. TITLE AND SUBTITLE		NUREG/CR-5048 PNL-6388	
REVIEW OF THE NATURAL CIRCULATION EFFECT IN THE VERMONT YANKEE SPENT-FUEL POOL		3. LEAVE BLANK	
4. DATE REPORT COMPLETED		4. DATE REPORT ISSUED	
MONTH YEAR		MONTH YEAR	
December 1987		January 1988	
5. AUTHOR(S)		PROJECT/TASK WORK UNIT NUMBER	
C.L. Wheeler		6. FIN OR GRANT NUMBER	
7. PERFORMING ORGANIZATION NAME AND MAILING ADDRESS (Include Zip Code)		FIN Number I2003	
Fluid and Thermal Engineering Section Engineering Physics Department Pacific Northwest Laboratory Post Office Box Number 999 Richland, Washington 99352		11a. TYPE OF REPORT	
10. SPONSORING ORGANIZATION NAME AND MAILING ADDRESS (Include Zip Code)		Final	
Division of Engineering & Systems Technology Office of Nuclear Reactor Regulation Nuclear Regulatory Commission Washington, D.C. 20555		11b. PERIOD COVERED (Inclusive dates)	
12. SUPPLEMENTARY NOTES		12/86 to 12/87	
Report is in support of staff review of proposed re-racking of SFP under TAC # 61351 on Docket Number 50-271		13. ABSTRACT (200 words or less)	
A 7,429-node, three-dimensional computer model of the Vermont Yankee spent-fuel pool was set up and run using the porous media model of the TEMPEST computer code. The results of this analysis show that natural circulation is sufficient to ensure adequate cooling, regardless of the loading pattern used or the orientation of the cooling system discharge nozzle.		14. DOCUMENT ANALYSIS / KEYWORDS/DESCRIPTIONS	
Spent-Fuel Pool, Spent-Fuel Storage, Spent-Fuel Racks, Natural Circulation, TEMPEST, Re-rack, Spent-Fuel Pool Cooling System		15. AVAILABILITY STATEMENT	
		unlimited	
16. SECURITY CLASSIFICATION		(This page)	
		unclassified	
17. NUMBER OF PAGES		(This report)	
		unclassified	
18. PRICE			

UNITED STATES
NUCLEAR REGULATORY COMMISSION
WASHINGTON, D.C. 20555

SPECIAL FOURTH CLASS RATE

POSTAGE & FEES PAID
USNRC

PERMIT No. G 67

OFFICIAL BUSINESS
PENALTY FOR PRIVATE USE, \$300

120555078877 1 1AN1RJ
US NRC-OARM-ADM
DIV OF PUB SVCS
POLICY & PUB MGT BR-PDR NUREG
W-537 DC 20555
WASHINGTON